MARMARA UNIVERSITY

FACULTY OF ENGINEERING

Response Analysis of Magnetostrictive Material Under Varying Magnetic Field on Rotating Members

Vedatcan ÇETİNKAYA

GRADUATION PROJECT REPORT

Department Of Mechanical Engineering

Thesis Supervisor

Res. Ast. Dr. ÖMER HALUK BAYRAKTAR

Thesis Co-Supervisor

Res. Ast. HÜSEYİN YALTIRIK

ISTANBUL, 2023

MARMARA UNIVERSITY

FACULTY OF ENGINEERING

Response Analysis of Magnetostrictive Material Under Varying Magnetic Field on Rotating Members

by

Vedatcan Çetinkaya

February 2023, Istanbul

SUBMITTED TO THE DEPARTMENT OF MECHANICAL ENGINEERING IN PARTIAL FULFILLMENT OF THE REQUIREMENTS FOR THE DEGREE OF BACHELOR OF SCIENCE AT

MARMARA UNIVERSITY

Signature of Author(s)..VEDATCAN ÇETİNKAYA.....

Department of Mechanical Engineering

Certified By..Dr. Haluk Sayraktar.....

Project Supervisor, Department of Mechanical Engineering

Accepted by.....Prof. Dr. Bülent Ekici.....

Head of the Department of Mechanical Engineering

ACKNOWLEDGEMENT

First of all, I would like to thank my Co-Supervisor HÜSEYİN YALTIRIK and my supervisor Ömer Haluk BAYRAKTAR, for the valuable guidance and advice on preparing this thesis and giving me moral and material support.

Secondly, I would like to thank Yunus EFE, engineer of Kurçelik A.Ş., who helped us with the parts to be produced in this thesis.

Finally, and most importantly, I would like to thank my family members Sedat ÇETİNKAYA and Hatice ÇETİNKAYA for their financial and moral support in this thesis.

February 2023 Vedatcan ÇETİNKAYA

Contents

ABSTRACT

Magnetostrictive materials develop an expansion response under magnetic fields. In this thesis, it is aimed to observe the effects of different sets of varying magnetic fields on a magnetostrictive material, created with permanent magnets of different geometric shape, size, configuration and distances. In particular, a firm relationship between a rotating members angular position and the expansion of the magnetostrictive material under alternating magnetic fields is attempted for possible commercial use.

The experimental setup was designed in Cad environment and the components of the assembly were either purchased from the internet or manufactured on lathes and CNC machines. The rotation direction and speed of the stepper motor were controlled by Arduino. Orientation of the rotating members were measured by a Vernier rotary motion sensor. The expansion response of the magnetostrictive material is measured by a force sensor, which then is converted by NI data acquisition components and collected by LabView program.

SYMBOLS

Fe : Iron

Ni : Nickel

Co : Cobalt

Ppm :Parts per million

σ : Stress

ε : Strain

H : Magnetic field

M : Magnetization of the material.

V : Voltage

A : Amper

Kg : Kilogram

Cm : Centimetre

Mm : Millimetre

LIST OF FIGURES

LIST OF TABLES

1. INTRODUCTION

1.1. Description of Magnetostrictive Material

Magnetostrictive materials are a class of smart materials that can convert energy between the magnetic and elastic states. For this reason, magnetostrictive materials and devices based on these materials are often referred to as transducers. Due to the bidirectional nature of this energy exchange, magnetostrictive materials can be employed for both actuation and sensing. Alloys based on the transition metals iron, nickel, and cobalt in combination with certain rare-earth elements are currently employed in actuator and sensor systems in a broad range of industrial, biomedical, and defense applications. Because magnetostriction is an inherent property of ferromagnetic materials, it does not degrade over time as do some poled piezoelectric substances. In addition, newer magnetostrictive materials provide strains, forces, energy densities, and coupling coefficients that compete favourably with more established technologies such as those based on piezoelectricity. As evidenced by the ever-increasing number of patented magnetostrictive systems, transducer designers are finding new opportunities to employ magnetostrictive materials in a wide variety of applications ranging from stand-alone transducers to complex smart structure systems.

A number of design and modelling issues, however, complicate the implementation of magnetostrictive materials in certain applications in which other smart material technologies are currently favored. For instance, due to the required solenoid and related magnetic circuit components, magnetostrictive transducers are usually larger and bulkier than their piezoelectric or electrostrictive counterparts. Hence, they are employed primarily in applications that require high strains and forces but where weight is not an issue. One additional consideration is that the most technologically advanced magnetostrictive materials are costly to manufacture. Advanced crystalline materials are manufactured by employing sophisticated crystal growth techniques that produce directional solidification along the drive axis of the transducer material. The manufacturing process also includes precision machining of laminations, final diameters, and parallel ends of cut-to-length drivers, as well as thorough quality assurance and performance evaluation throughout the process. These technological and cost-related

problems have been mitigated to some extent through the advent of new manufacturing techniques that have enabled more capable magnetostrictive materials in various forms, including amorphous or crystalline thin films, magnetostrictive particle-aligned polymer matrix composite structures, and sintered powder compacts suitable for mass production of small irregular shapes. From the perspective of modelling and control, magnetostrictive materials exhibit nonlinear effects and hysteretic phenomena to a degree which other smart materials, for instance electrostrictive compounds, do not. These effects are particularly exacerbated at the moderate to high drive level regimes in which magnetostrictive materials are most attractive. These issues have been addressed through recent modelling techniques, and as new applications are developed, model accuracy and completeness will almost surely follow.

The term magnetostriction is a synonym for magnetically induced strain, and it refers to the change in physical dimensions exhibited by most magnetic materials when their magnetization changes. Magnetization, defined as the volume density of atomic magnetic moments, changes as a result of the reorientation of magnetic moments in a material. This reorientation can be brought about by applying either magnetic fields, heat or stresses. The linear magnetostriction $\Delta L/L$ that results from applying a longitudinal magnetic field on a sample of length L, illustrated in Fig. 1, is the most commonly employed attribute of the magnetostrictive principle in actuator applications.

Though most ferromagnetic materials exhibit linear magnetostriction, only a small number of compounds that contain rare-earth elements provide “giant” magnetostrictions in excess of $1000 \times 10{-}6$. These large magnetostrictions are a direct consequence of the strong magneto mechanical coupling that arises from the dependence of magnetic moment orientation on interatomic spacing. When a magnetic field is applied to a magnetostrictive material, the magnetic moments rotate to the direction of the field and produce deformations in the crystal lattice and strains in the bulk material. Referring again to Fig. 1 which pertains to a material that has positive magnetostriction, note that the sample elongates irrespective of the direction of rotation of the magnetic moments. A symmetrical magnetostriction curve is obtained when the field is cycled, as depicted in Fig. 1b,c. If stress is applied instead, the material deformations lead to magnetic moment reorientation and a subsequent change in the magnetization M. This magnetization change can be detected through the voltage induced in a sensing solenoid wrapped around the

sample, which provides a mechanism for sensing. In applications, either one sensing solenoid or a plurality of them arranged along the length of the driver can be placed inside of the driving coil. Alternatively, it is possible to employ only one solenoid to drive the magnetostrictive material and sense its magnetization changes. This configuration exhibits the major disadvantage that additional signal processing hardware is required to extract the sensing voltage from the driving signal. [1]

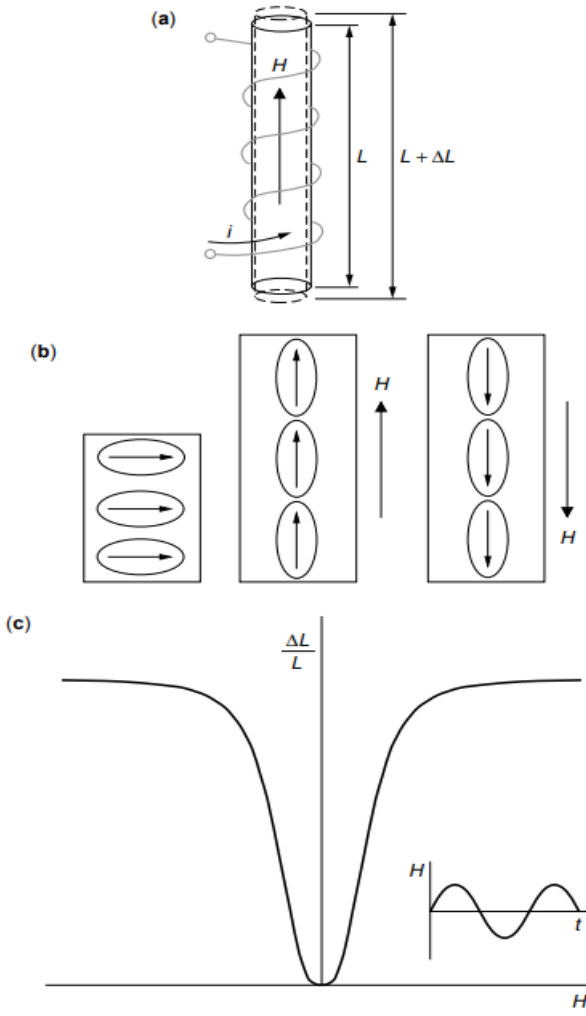

Figure 1 Joule magnetostriction produced by a magnetic field H. [1]

There are many magnetostrictive materials. In Table 1, the magnetoelastic values of these materials are given.

Material	$\frac{3}{2}\lambda_s(\times 10^{-6})$	ρ (g/cm^3)	B_s (T)	T_c(°C)	E (GPa)	k
Fe	–14 (8)	7.88 (14)	2.15 (14)	770 (14)	285 (14)	
Ni	–50 (14)	8.9 (14)	0.61 (14)	358 (14)	210 (1)	0.31 (8)
Co	–93 (14)	8.9 (14)	1.79 (14)	1120 (14)	210 (1)	
50% Co–50% Fe	87 (2)	8.25 (8)	2.45 (76)	500 (14)		0.35 (8)
50% Ni–50% Fe	19 (2)		1.60 (76)	500 (14)		
$TbFe_2$	2630 (8)	9.1 (14)	1.1 (2)	423 (8)		0.35 (8)
Tb	3000 (–196°C) (36)	8.33 (14)		–48 (13)	55.7 (1)	
Dy	6000 (–196°C) (36)	8.56 (14)		–184 (1)	61.4 (1)	
Terfenol-D	1620 (8)	9.25	1.0	380 (76)	110 (77)	0.77 (78)
$Tb_{0.6}Dy_{0.4}$	6000 (–196°C) (36)					
Metglas 2605SC	60 (36)	7.32 (2)	1.65 (76)	370 (2)	25–200 (2)	0.92 (1)

Table 1 Magnetoelastic Properties of Some Magnetostrictive Materials [1]

1.2 Magnetic Field

The magnetic field is an event that occurs as a result of the movement of electric charges. Negatively charged electrons in atoms, which are the smallest part of a material, move in orbit around the nucleus, as well as make a rotational motion around their own axis. If electrically charged particles are in motion, a change occurs in the environment. This change, which occurs as a magnetic force in the environment where the current carrying magnet is located, is called the magnetic field. The magnetic field is a vector quantity. It is denoted by the symbol H and its unit is Ampere/m. [2]

The magnetic field in any medium is represented by lines of force or magnetic flux lines. Lines of force form a closed loop. As we can see in the figure, the magnetic field representations with lines of force are shown in the solenoid with an air core and an iron core. The lines of force exit the N pole and enter the S pole and pass through the solenoid, forming a closed path.

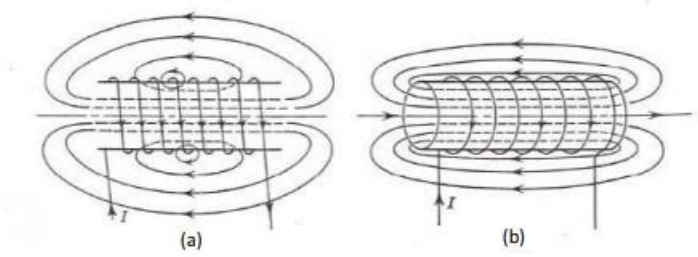

Figure 2 a) Air core solenoid b) Magnetic field in iron core solenoid material. [3]

The magnetic force connection acting on the charge q moving with velocity v in the magnetic field H.

$$F_H = qvxH \tag{1.1}$$

given in this way. The magnetic force is perpendicular to both the particle's velocity and the field. The magnitude of the magnetic force.

$$F_H = |q|vH \sin\theta \tag{1.2}$$

given in this way.

1.2.1 Magnetic flux

Magnetic field lines are considered to run from the N pole to the S pole in the scientific community. As we will see in Figure 3, magnetic field lines are formed when we pour iron powder on the ends of the magnet. The magnetic field intensity is higher in regions where magnetic field lines are dense.

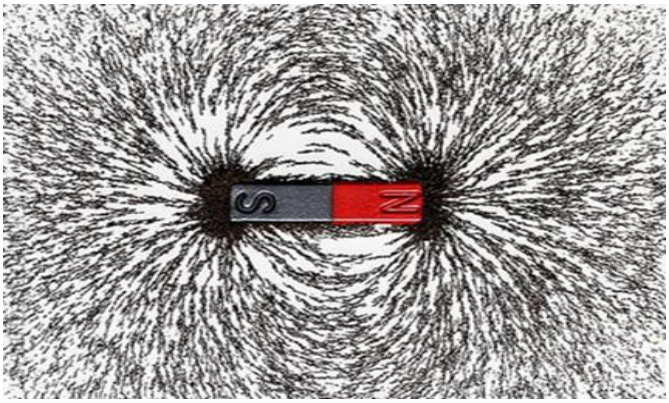

Figure 3 Experimental representation of magnetic field strength[17]

1.3. Magnets

Magnets are materials that create magnetic fields in general. While it attracts some metals such as iron, nickel, cobalt, it does not affect some metals and non-metals such as copper, aluminium and plastic. We can give natural magnets, artificial magnets and electromagnetic magnets as examples of magnet types.

1.3.1 Natural magnets

Natural magnets are generally magnet types that can maintain their magnetic fields after being magnetized. We define natural magnets as magnets that occur in nature and are found as stones. If we give an example of natural magnets, we can give an example of magnet stone.

1.3.2 Artificial magnets

Artificial magnets are generally non-magnetic materials, but later magnetized materials can be called artificial magnets. Most magnets we use in our daily lives are evaluated in this category. Artificial magnets behave like magnets when they are in a magnetic field, but they are magnets that lose their magnetic identity when they leave the magnetic field.

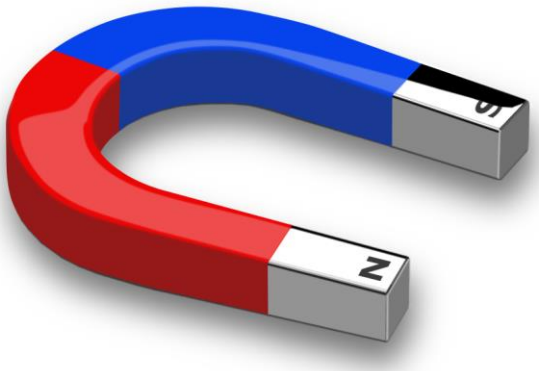

Figure 4 General magnet representation

1.3.3. Electromagnet

Magnetic materials that can show the properties of the magnet with the effect of electric current are called electromagnets. Electromagnets are formed by wrapping insulated thin cables in iron material and passing current through the cables. If we want to fully characterize electromagnets, they are types of magnets that act as magnets when electric current passes through them.

1.3.4 Neodymium magnets

Neodymium magnet is a type of magnet with strong attraction force covered with steel of the earth magnet. Because the neodymium element is difficult to pronounce by people, it is also called neodymium magnet, rare earth magnet, neodymium magnet, neodymium magnet. [4]

In this experiment, we used neodymium magnets and these magnets have very high attractive forces. However, Neodymium magnets lose their magnetic field effects at temperatures above 85°C. Neodymium magnets are fragile by nature. As a result of rapid fusion, they can be broken by impact. The general view of the neodymium magnet to be used in the experiment is given in figure 5.

Figure 5 General structure of neodymium magnets [4]

1.4 Stepper Motors

A stepper motor is a device that converts electrical energy into rotational motion. When the electrical energy is received, the rotor and the shaft connected to it start to rotate in constant angular units. Stepper motors are connected to a driver with very high-speed switching, and as an example, we can give the TB6600 driver board as an example. This driver receives input pulses from an encoder or PLC. For each input pulse received, the motor advances one step. Stepper motors are referred to by the number of steps per motor revolution. For example, a 200-step stepper motor makes 200

steps in one complete revolution (revolution). In this case the angle of a step is 360/200 = 1.8 degrees

Stepping accuracy is further increased when stepper motors operate in half-step mode. For example, a stepper motor of 200 steps/revolution makes 400 steps per revolution in half-step mode. This means a step angle of 0.9 degrees, which is more precise than 1.8 degrees.

1.4.1 Structure of stepper motors

The stator of the stepper motor usually has eight poles. Their polarity is changed with the help of electronic switches. As a result of the switching, the average south and north poles of the stator are rotated. The south pole of the rotor is aligned with the north pole of the stator. The magnetism of the rotor can be created by a permanent magnet or external excitation methods. Meanwhile, a permanent magnet will form. The average stator field rotates by means of its steps (steps), and the rotor follows it among similar (steps) steps. Small teeth are made on the rotor and stator to achieve better selectivity. These teeth should not come into contact with each other. [5]

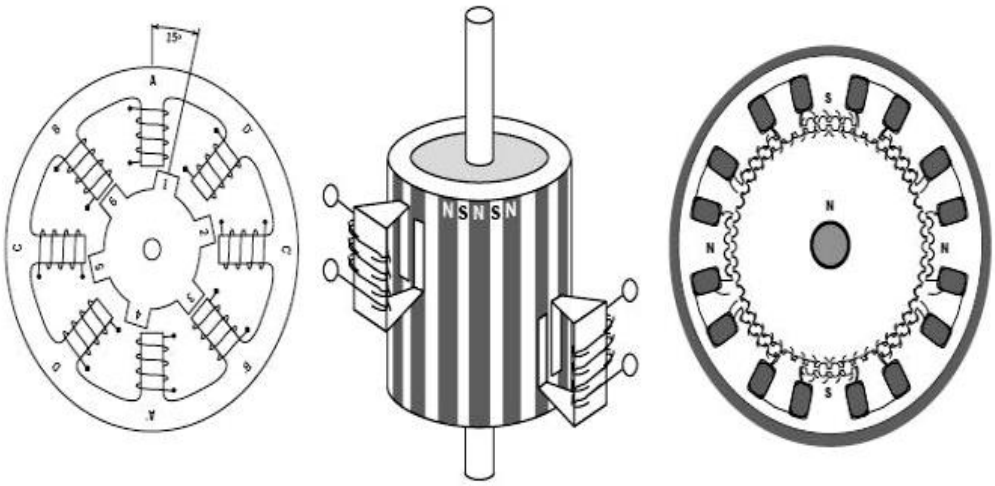

Figure 6 Stepper motor structures [6]

1.4.2 Working principle of stepper motor.

When the input pulse is applied to the stepper motor, it rotates a certain amount and stops. This amount of rotation is limited to a certain angle according to the structure

of the engine. The rotation of the rotor in the stepper motor changes depending on the number of pulses applied to the input. With a single pulse given to the input, the rotor moves one step and stops. When more pulses are applied, it moves as many steps as the number of pulses.

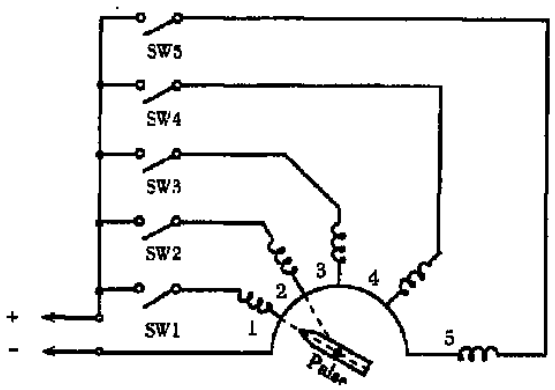

Figure 7 Principal diagram of stepper motor [6]

1.5 TB6600 Stepper Motor Driver

This is a professional two-phase stepper motor driver. It supports speed and direction control. You can set its micro step and output current with 6 DIP switch. There are7kindsof micro steps (1, 2 / A, 2 / B, 4, 8, 16, 32) and 8 kinds of current control (0.5A, 1A, 1.5A, 2A, 2.5A, 2.8A, 3.0A, 3.5A) in all. And all signal terminals adopt high-speed optocoupler isolation, enhancing its anti-high-frequency interference ability.

Features:

- Support 8 kinds of current control.
- Support 7 kinds of micro steps adjustable.
- The interfaces adopt high-speed optocoupler isolation.
- Automatic semi-flow to reduce heat.
- large area heat sink.
- Anti-high-frequency interference ability.
- Input anti-reverse protection.
- Overheat, over current and short circuit protection.

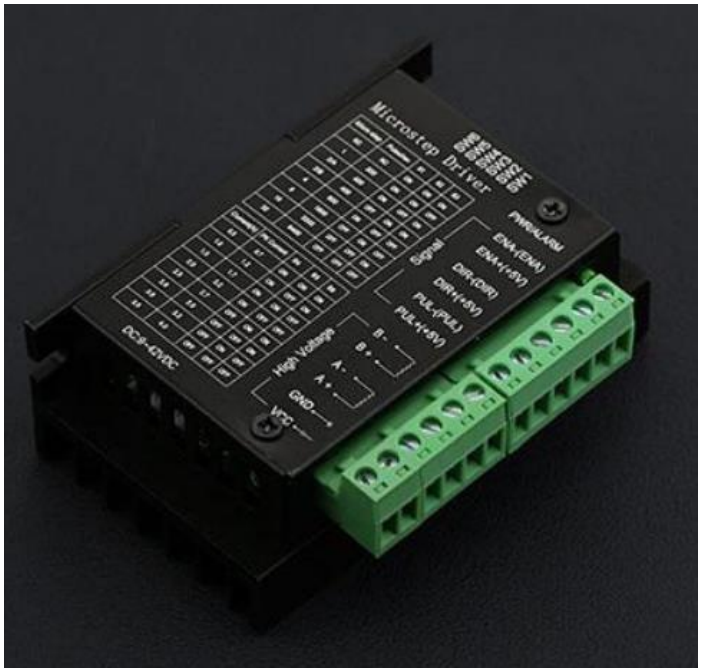

Figure 8 TB6600 Stepper Motor Driver [7]

1.6 Computer Aided Design Programs.

3D drawing programs that enable drawings by computer support are used in every sector where drawing, design and assembly are together. Thanks to the drawing programs that are actively used in architecture, construction, mechanics, electricity and even in the furniture industry, drawings can be completed quickly and practically compared to traditional methods. If we give an example of these programs, AutoCAD, SolidWorks and Catia are the pioneers of these programs.

1.6.1 SolidWorks

SolidWorks, which is mostly a 3D drawing-oriented computer program, is the most widely used computer-aided design program in engineering. While making three-dimensional modelling with SolidWorks, various strength analysis can be performed by selecting the material type to be made of that model. With this aspect, SolidWorks is frequently used in engineering branches such as machinery and construction. In this thesis, the solid student version was used.

1.6.2 LabVIEW

LabVIEW is a graphical programming language used by many engineers and scientists around the world. LabVIEW is a program for combining many small programs using object-oriented programs that you can prepare and make flow diagrams with small graphical icons and cables. Rather than text-based languages, it is easier to use and offers a more visual platform for developing algorithms. [8]

1.7 Vernier Rotary Motion Sensor

The Vernier Rotary Motion Sensor is a bidirectional angle sensor designed to measure rotational or linear position, velocity and acceleration. It is used for a variety of investigations, including measurement of rotational inertia and verification of the conservation of angular momentum. Vernier rotary motion sensors consist of a total of four components. These ; Rotary Motion Sensor, Thumb screw, 3-stage pulley and mounting screw, O-ring.

Figure 9 Vernier Rotary Motion Sensor [9]

1.8 Sensor DAQ

The SensorDAQ® interface provides connectivity between Vernier or custom sensors and a Windows computer running LabVIEW software. More than 50 Vernier sensors are available for use with the SensorDAQ. The SensorDAQ package contains the following equipment: SensorDAQ interface, USB cable, User's Manual, Vernier Voltage Probe.

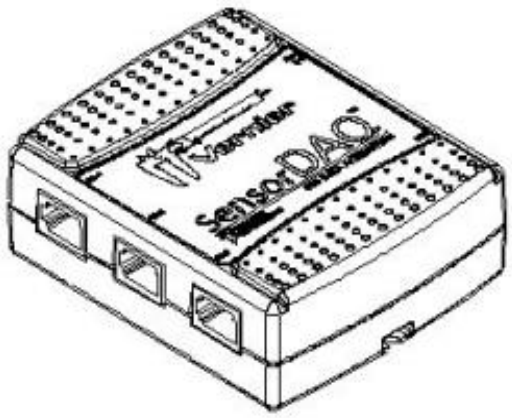

Figure 10 Vernier SensorDAQ [10]

1.9 PCB Piezotronics Force Sensor(Model 208C01)

PCB force sensors incorporate a built-in MOSFET microelectronic amplifier. This serves to convert the high impedance charge output into a low impedance voltage signal for analysis or recording. PCB sensors, are powered from a separate constant current source, operate over long ordinary coaxial or ribbon cable without signal degradation. The low impedance voltage signal is not affected by triboelectric cable noise or environmental contaminants.

Power to operate PCB sensors is generally in the form of a low cost, 24-27 VDC, 2-20 mA constant current supply. Figure 1 schematically illustrates a typical PCB sensor system. PCB offers a number of AC or battery-powered, single or multichannel power/signal conditioners, with or without gain capabilities for use with force sensors. In addition, many data acquisition systems now incorporate constant current power for directly powering PCB sensors. Because static calibration or quasi-static short-term response lasting up to a few seconds is often required, PCB manufactures signal conditioners that provide DC coupling.

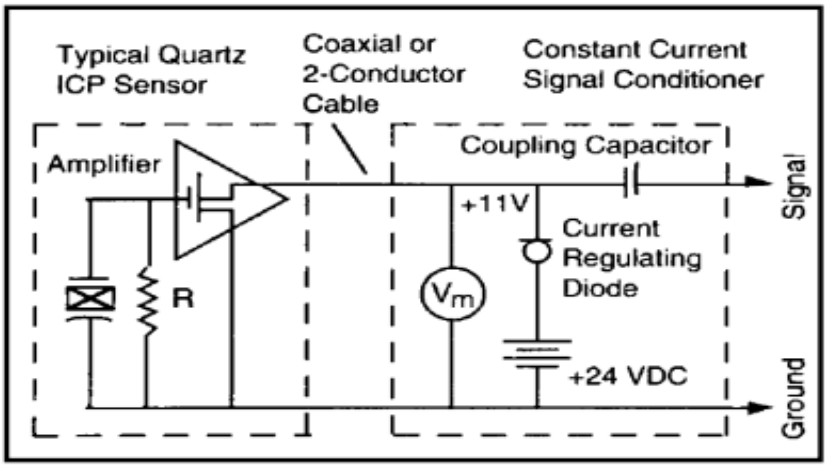

Figure 11 PCB Sensor System Schematic [11]

1.10 NI 9234 Input Module

The NI 9234 Sound and Vibration Input Module has four analog input channels and is designed to perform precise measurements from IEPE sensors. The dynamic range of this module is 102 dB. The input channels sample at rates as fast as 51.2 kS/s. The NI 9234 has four BNC connectors that provide connections to four simultaneously sampled analog input channels.

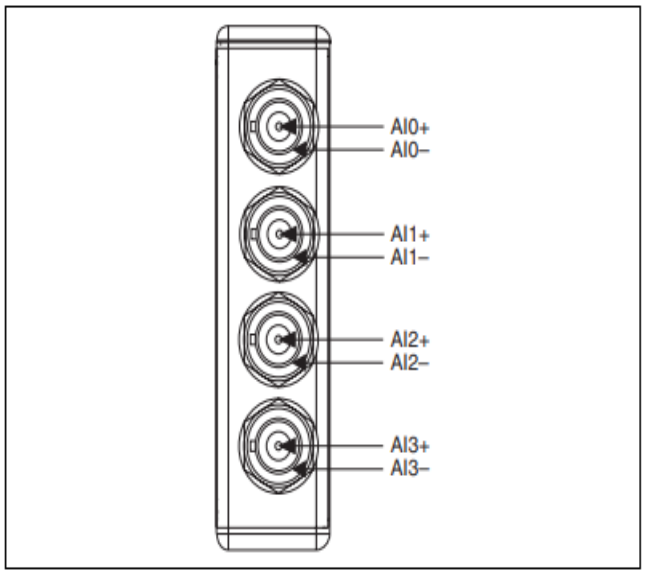

Figure 12 NI 9234 Connector Assignments [12]

2. MATERIAL AND METHOD

Our thesis is an applied thesis study. For this, we first started our studies by investigating the properties of the magnetostrictive material that we will use in our thesis. Then, we aimed to prepare our experimental setup with materials that will not be affected by the magnetic field, and we concluded our thesis by taking our experimental results.

2.1 Magnetostrictive Material

Magnetostrictive materials are materials that can convert energy between magnetic and elastic states. Therefore, magnetostrictive materials and devices based on these materials are often called transducers. Due to the bidirectional nature of this energy exchange, magnetostrictive materials can be used for both actuation and sensing. Alloys based on iron, nickel and cobalt, which are transition metals in combination with some rare earth elements, are currently used in actuator and sensor systems in a wide variety of industrial, biomedical and defence applications. [13] In this experiment, we used magnetostrictive material, which is an alloy containing 60 percent iron and 40 percent nickel. The magnetostrictive material used for this thesis is given in Fig 13.

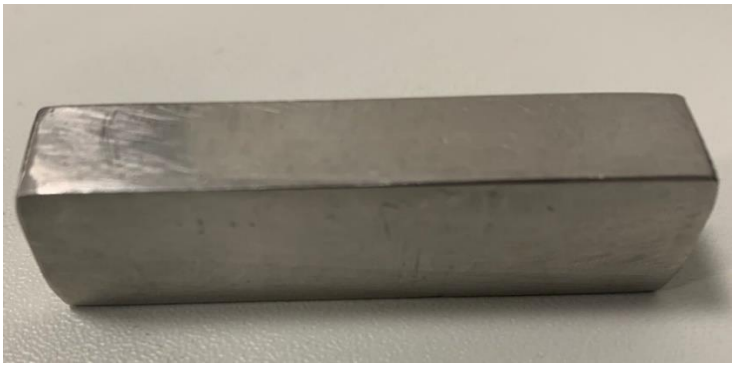

Figure 13 Magnetostrictive material used in the thesis.

2.2 Design

In the previous experiment, a DC motor and fixed objects were preferred. In order to develop our thesis, we wanted to create a design that requires movement in three axes and we continued our work in this direction. For this design, we prepared a motion design for both the engine part and the part to which our material is attached, using the SolidWorks program. By dividing the movement in these three axes, we used the two

axes (x, y) movement to the motor side, and the part to which our material is attached for the movement in the other axis (z).

2.2.1 Sigma profiles

Sigma profiles, also known as industrial aluminium profiles, provide an easy and versatile mounting opportunity thanks to their channelled structure. However, it is an ideal method for applications that require movement in three axes like mine. If we talk about the general usage areas of Sigma profiles, we can give examples of areas such as cabinet, table, conveyor and CNC.

In this study, we used the sigma profile shown in figure 14. to provide movement in three axes. We bought three of these sigma profiles in 150x30x30 dimensions. We used two parts on the floor surface and mounted the other part on the upper part of the two sigma profiles and provided movement in two axes.

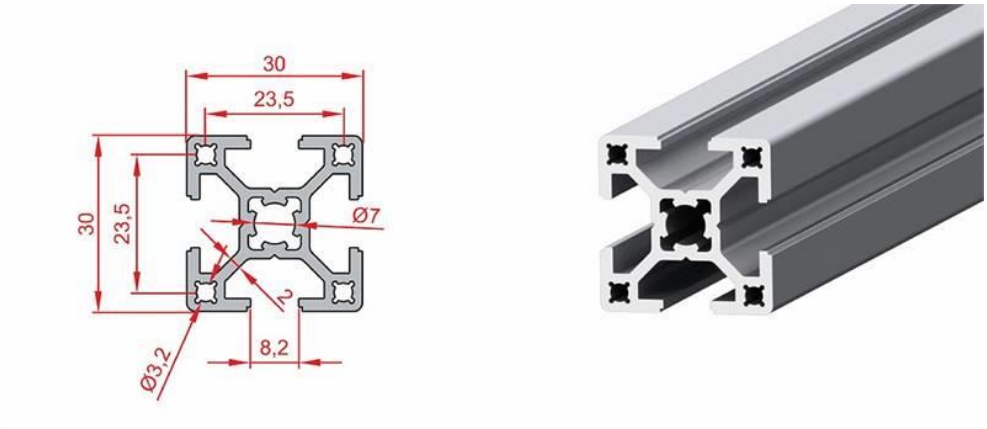

Figure 14 Technical drawing of the Sigma profile [14]

2.2.2 T nut

T nuts are one of the main detachable fasteners used with bolts. Basically, it is a simple piece with a tapped (screwed) hole in the middle and we used it to provide interchannel movement in this thesis. The t nut we use in Figure 15. is a T nut with a 5m hole.

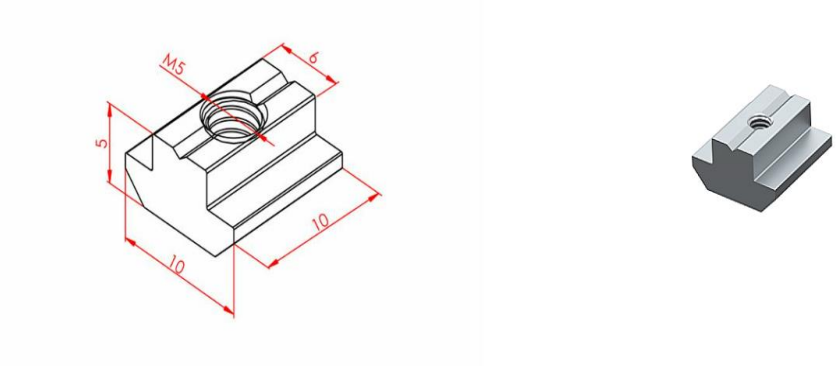

Figure 15 Technical drawing of T nut [14]

2.2.3 Fasteners

We can define fasteners as elements used to connect elements in a system or machine. They can be rivets, pins, springs, bolts, nuts, screws, solder, etc. We can give examples of parts. The fasteners we see in Figure 16. are the fasteners we use to fix the sigma profiles.

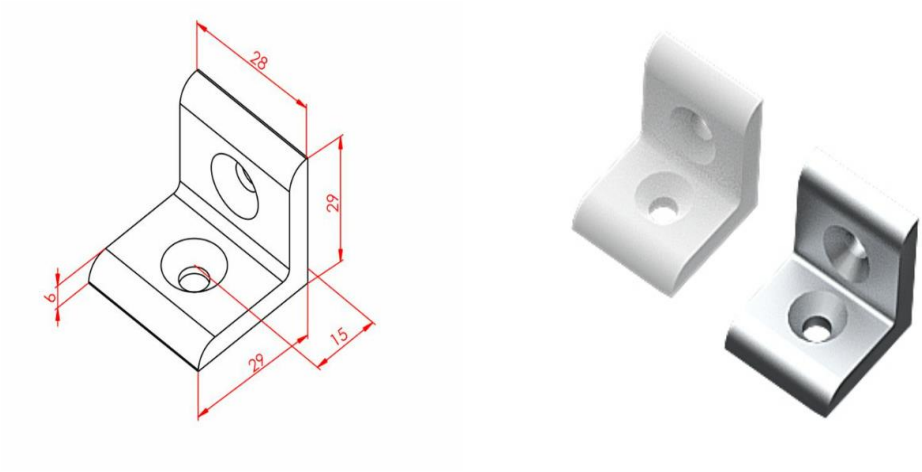

Figure 16 Technical Drawing of fasteners [14]

2.2.4 Stepper motor

Stepper motors are electromechanical devices that convert electrical energy into physical energy with rotational motion, as we have explained before. These motors are step-by-step motors. If we want to give a little more detail, they are permanent magnet pole motors that produce analog rotational motion output against the pulse signals applied to their inputs and provide this rotational movement step by step and with very precise control.

In this thesis, we used the nema 17 engine as we will see in figure 17. This motor has a 1.8° step angle, can rotate 200 steps per revolution, and has both unipolar and bipolar features. Our stepper motor, which can rotate in both directions, works with 4V and 1.2A per phase. However, it has a stopping torque of 3.2 kg-cm.

Figure 17 Nema 17 stepper motor [15]

2.2.5 Actuator

Actuators are generally electrical equipment that allows us to use the motors more effectively by changing the speed and frequency of asynchronous, servo and stepper motors.

In this thesis, we used the tb6600 actuator shown in figure 18. This actuator can work between 9-40V. However, it is a sensitive actuator that allows our stepper motor to take 6400 steps when requested to be used.

Figure 18 Tb6600 Actuator [15]

2.2.6 Arduino

Arduino is an open-source electronic programming platform that offers easy-to-use software and hardware. In this thesis, we worked with Arduino uno, which is compatible with our nema 17 stepper motor and tb6600 actuator shown in figure 19.

Figure 19 Arduino uno [15]

The wiring diagram for these three components (stepper motor, Tb6600 actuator and Arduino) is shown in figure 20.

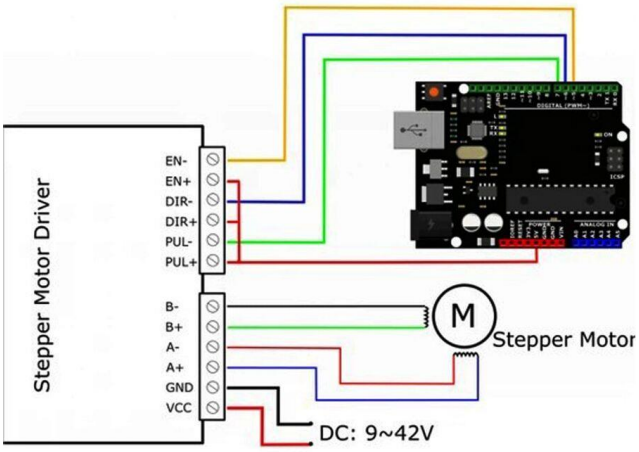

Figure 20 Wiring diagram for stepper motor, TB6600 actuator and Arduino [16]

2.3 Discs

Discs are parts that are generally used in engine blocks and produced to be attached to the engine shaft. In this thesis, we started our work on the discs by choosing the material first. The main logic of our disks was that they did not create magnetic fields. For this reason, we wanted to use polyamide material in our disc designs. Because these materials are hard plastic materials that are not affected by the magnetic field.

2.3.1 Square and circular disc design

We started by designing a square magnet of 25x25x5 lengths so that we could tell the difference with other results that had been tested before in this disk design. On the other hand, we wanted to create 20 circular magnet designs with a diameter of 5mm by developing a design that can create a magnetic field around the magnetostrictive material and examine the movement of circular discs, and we created the design shown in figure 21.

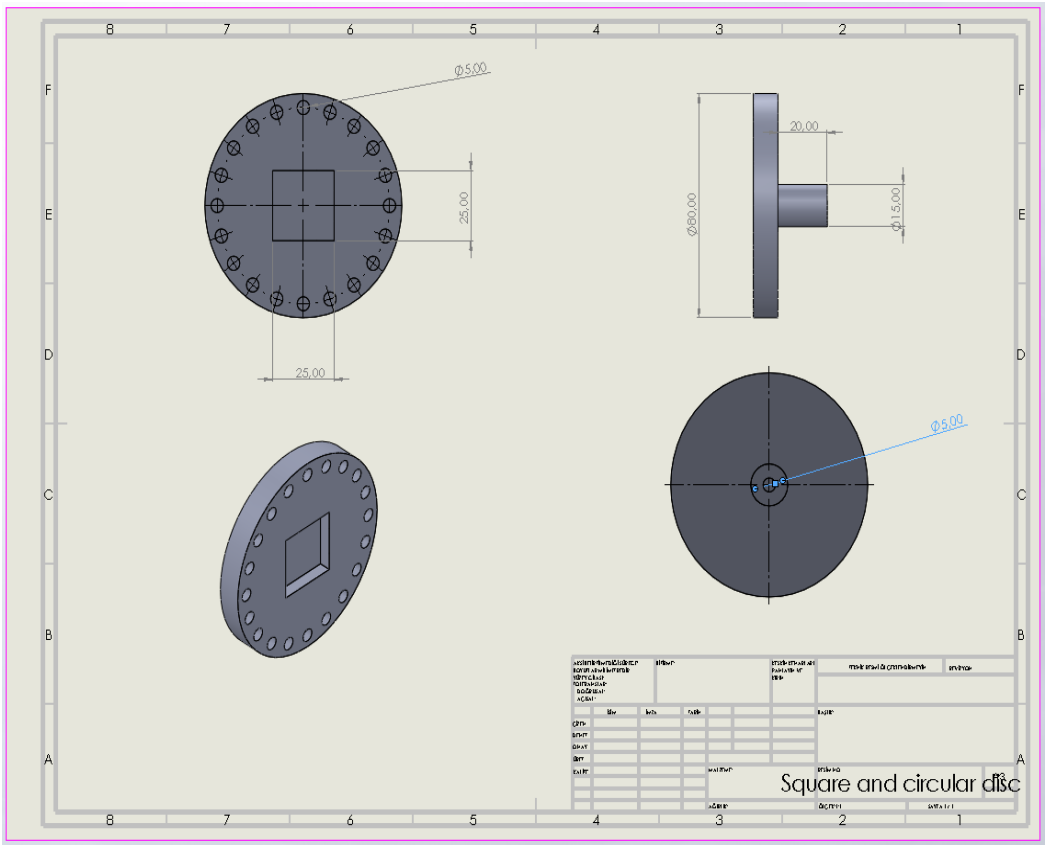

Figure 21 Technical drawing of square and circular disc

2.3.2 Two Square and Two Rectangular Disc designs

In this design, we designed two 25x25x5 square magnets and two 40x10x5 rectangular magnets. In order to understand the difference of the previous one with a single square magnet, we aimed to examine the change that will occur in the material by increasing the number of magnets. The purpose of our rectangular magnets is to understand the difference in rectangular magnets as opposed to square magnets, we created the design shown in figure 22.

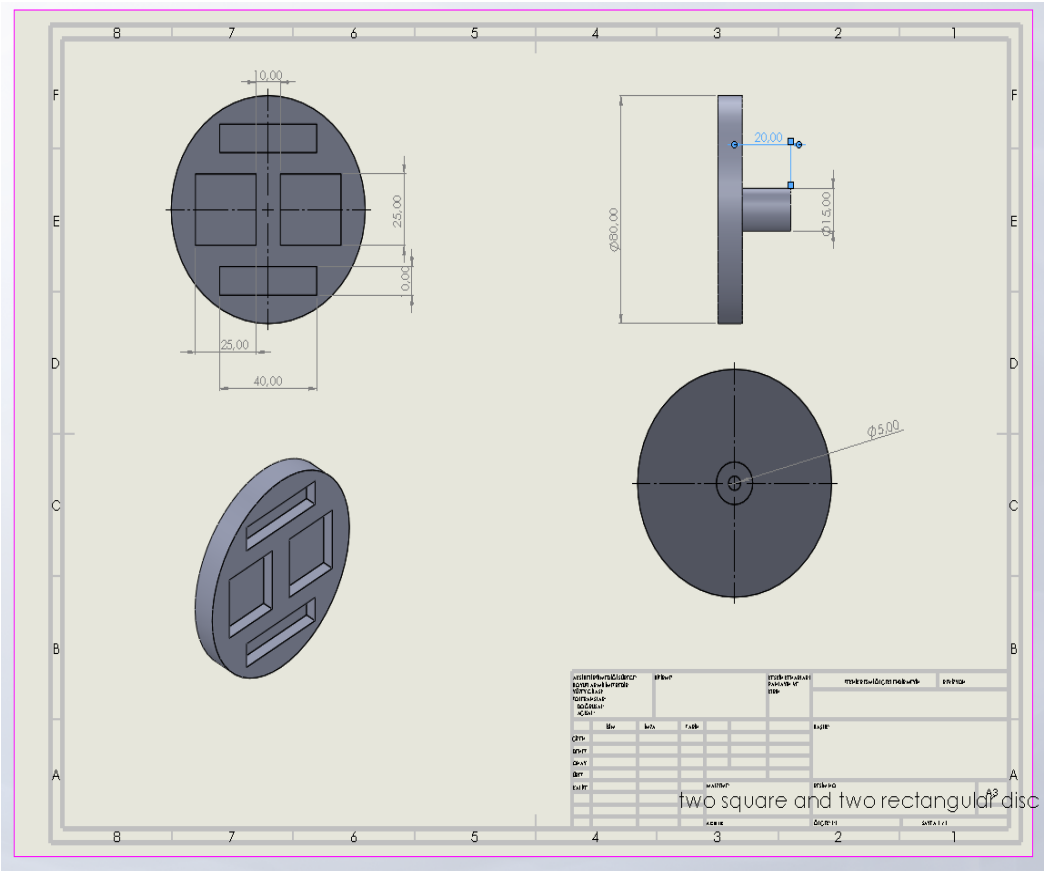

Figure 22 Technical drawing of two square and two rectangular discs

2.3.3 Rectangles disc

In this design, we used one 40x10x5 rectangular magnet and four 20x10x5 rectangular magnets. In this design, we aimed to see the differences between the other results by using rectangular magnets of different sizes and increasing the number of magnets. As a result, we created the design shown in figure 23.

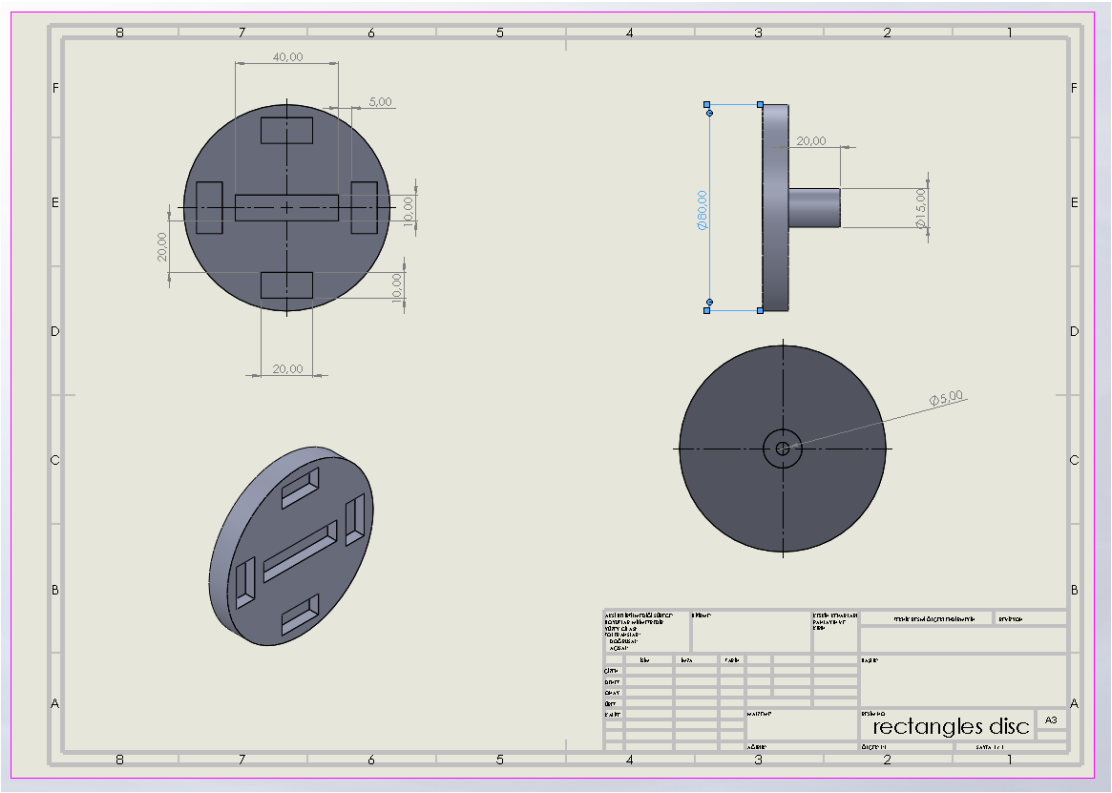

Figure 23 Technical Drawing of five rectangular disks of different sizes

The produced versions of the discs shown in these technical drawings are also shown in the figure24.

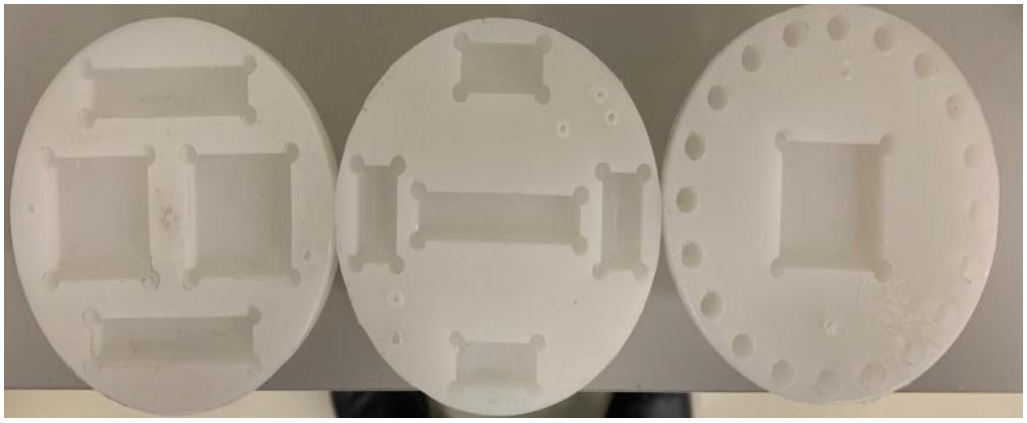

Figure 24 Manufactured versions of the discs whose technical drawings are given.

In order to be ready to get results, we first complete the assembly of our polyamide material, which we use to prevent our four sigma profiles from being affected by the magnetic field. We mount this assembly on two floors and one on top of these two profiles in an inverted position. We use my fasteners and bolts for this assembly. After fixing our

parts, we use our t-nuts for the movement of the engine part. Then, we complete the assembly of our material, which we will fix our engine block, with the help of a t nut.

For the apartment where we will connect our material, we first complete the assembly of the last remaining sigma profile vertically to the middle of our discs. However, we complete our movement in three axes (x, y, z).

We connect the Arduino USB cable to our computer by completing the stepper motor, Arduino and actuator tb6600 connections as shown in figure 20 before. We transfer the software we prepared for our stepper motor to our Arduino and make our motor ready. The Arduino codes used for the stepper motor are given in figure 25.

Stepper motor.ino

```
1   void setup() {
2     pinMode(2, OUTPUT);
3     pinMode(3, OUTPUT);
4     digitalWrite(2, HIGH) ;
5
6   }
7
8
9   void loop() {
10    digitalWrite(3, LOW);
11    digitalWrite(3, HIGH);
12    delayMicroseconds(100000) ;
13
14  }
15
16
```

Figure 25 Arduino codes

We use a rotary motion sensor to get the angle information and we fix it to our table with clamps as shown in figure 31 and connect the two discs with a tape. With the rotation of our disk, our sensor also starts to rotate, and in this way, we receive the angle information from our disk.

We used the PCB piezotronics 208C01 force sensor, which is connected to our material, to measure the force that will affect our material. We used the LabVIEW program to get these two computer-aided data. We collected the data by plugging both of our sensors into our computer with a USB cable like Arduino.

The LabVIEW program was used to simultaneously measure the angle information and the force information generated during the experiment. The block diagram of this program is given in figure 26.

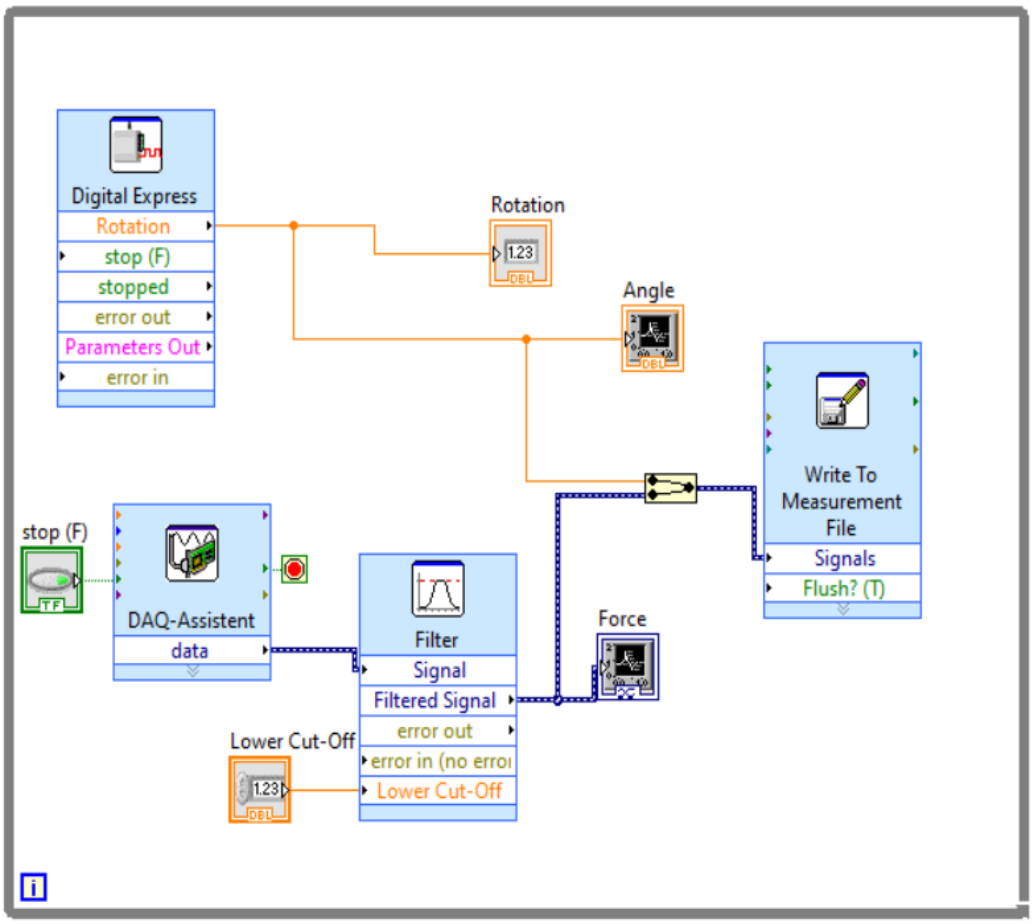

Figure 26 LabVİEW blog diagram

In the blog diagram given in Figure 26, it is connected to our rotary motion sensor with a digital express daq card. With this, as our stepper motor rotates, angle information is obtained with the help of the sensor. PCB piezotronics 208C01 force sensor, which is used to measure the force applied to the magnetostrictive material as a result of the magnetic field generated when the stepper motor rotates, is connected with our other DAQ-Assistent sensor seen in the blog diagram. We connected these two components to rotation and force to transfer them to our front panel. By connecting these two connections to each other, we directed the test results to the excel data in order to transfer them to us simultaneously. Digital express and DAQ-Assistent properties screens are given in figures 27 and 28.

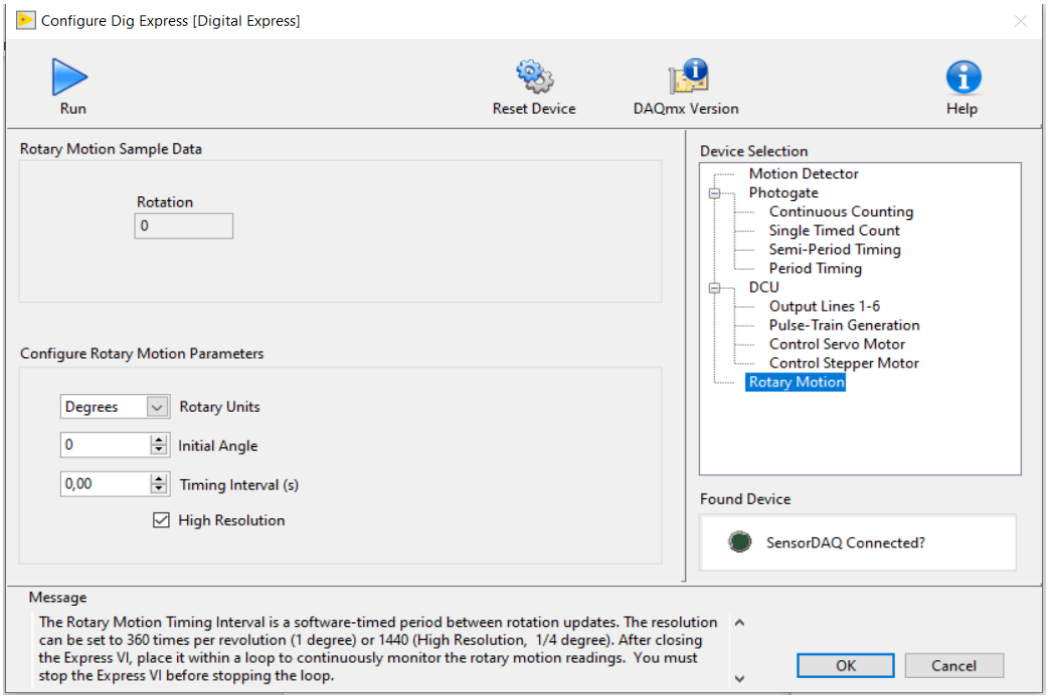

Figure 27 Digital express properties screen

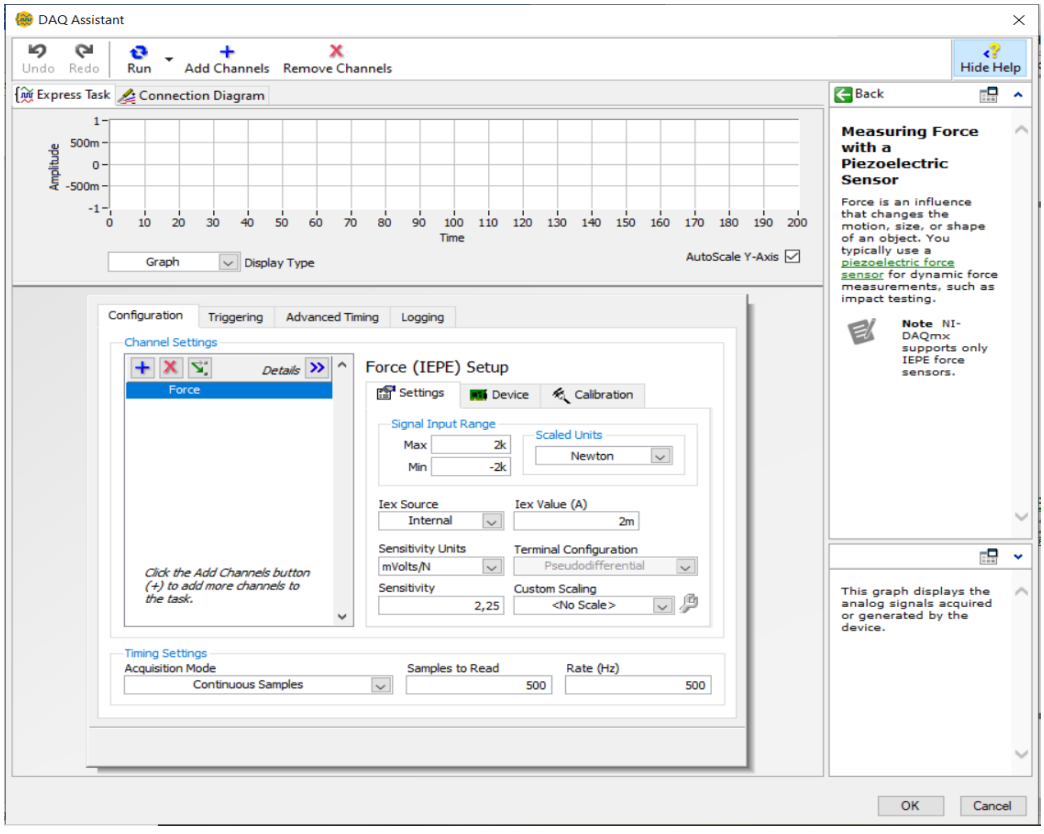

Figure 28 DAQ- Assistent properties screen

The front panel screen used for the test results is given in figures 29 and 30. The screen used for the screen angle measurement seen in Figure 29 is the screen where the screen force measurements seen in Figure 30 are followed.

Figure 29 Angle front panel screen

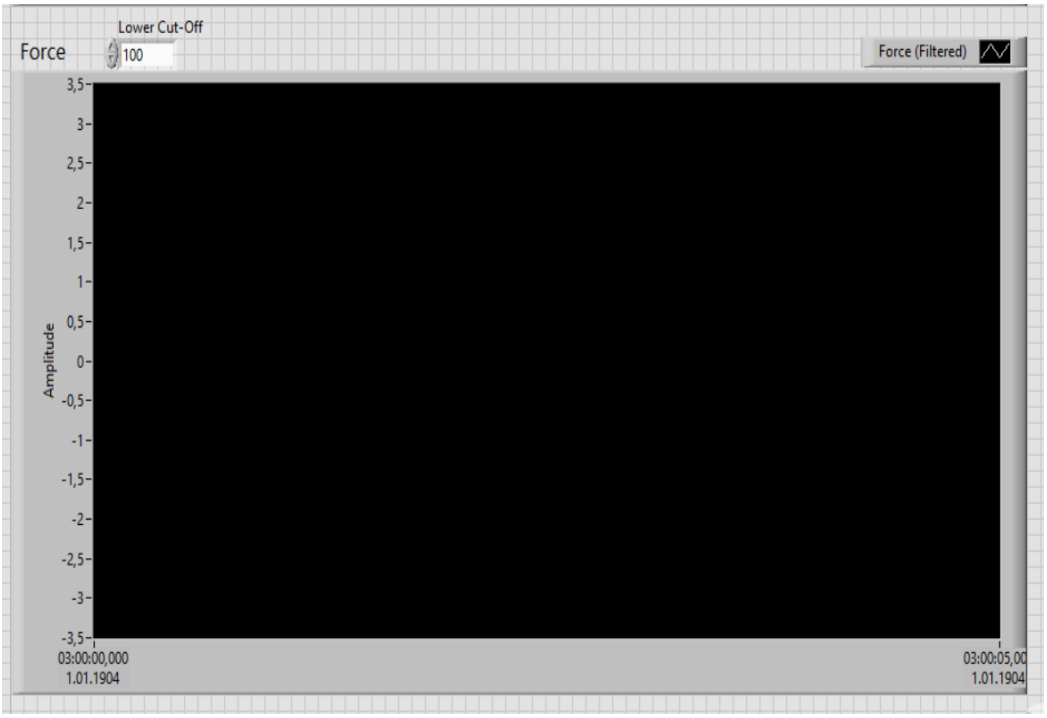

Figure 30 Force front panel screen

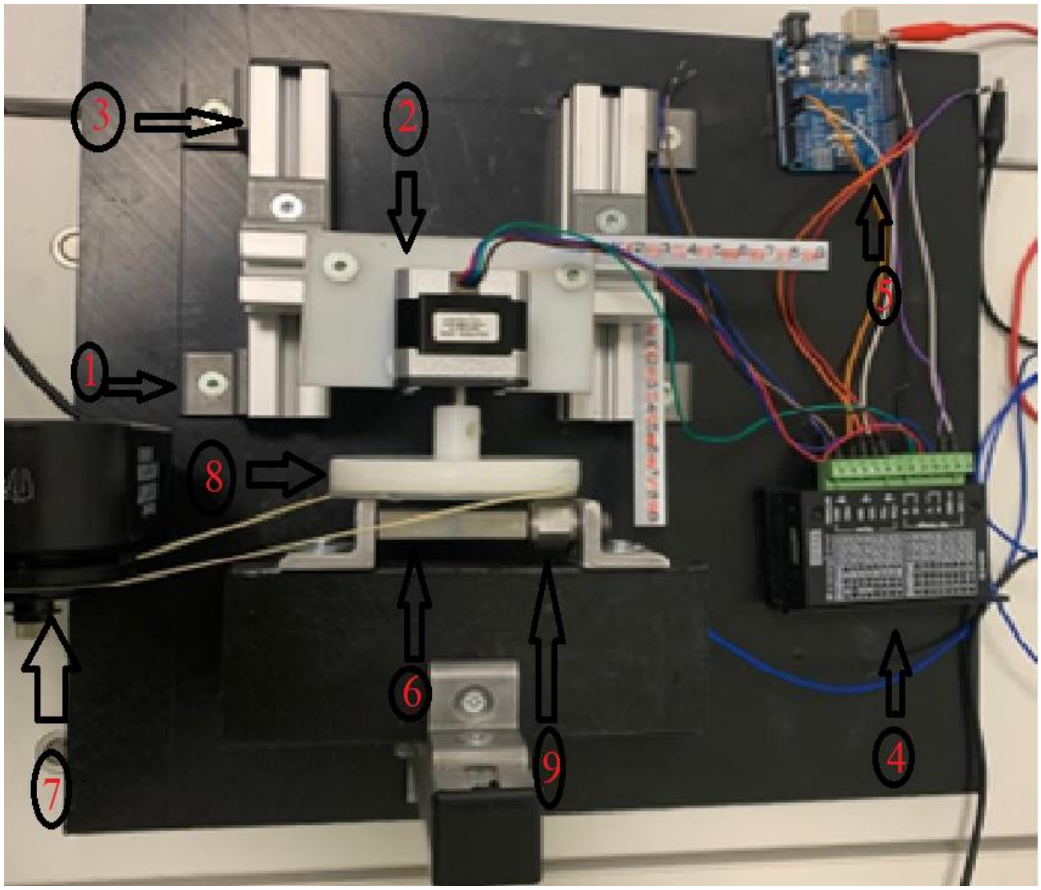

Figure 31 The experimental setup

All materials used for the preparation of the experimental setup are given in figure 31. These materials;

1. Fasteners
2. Stepper motor
3. Sigma profile
4. TB6600 driver
5. Arduino uno
6. Magnetostrictive material
7. Vernier rotary motion sensor
8. Disc
9. 208C01 force sensor

3. RESULTS AND DISCUSSION

Four positions were used in the experimental setup. For these positions, we considered the points where the midpoint of our disc and the midpoints of our material contact each other as x=0 y=0 z=0 points. All measuring positions are given in figures 21,22,23 and 24.However, we used a constant speed in our experimental work. We got our experimental results as 100000ms waiting time between our step-by-step steps. On the other hand, we aimed to see the difference between them better by moving our disc both clockwise and counter clockwise. The figure of our disk in different positions is given below. The graphs with the measurement results were filtered at every 10 degrees and prepared.

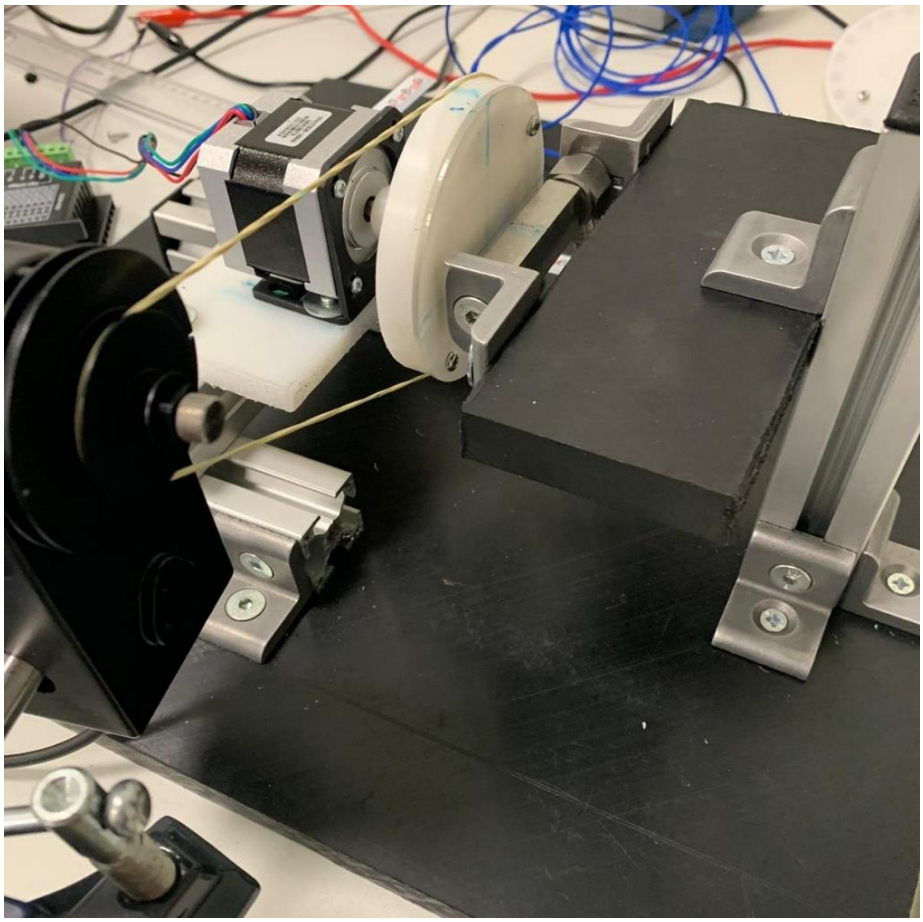

Figure 32 Position 1 x=-7mm y=0 z=0

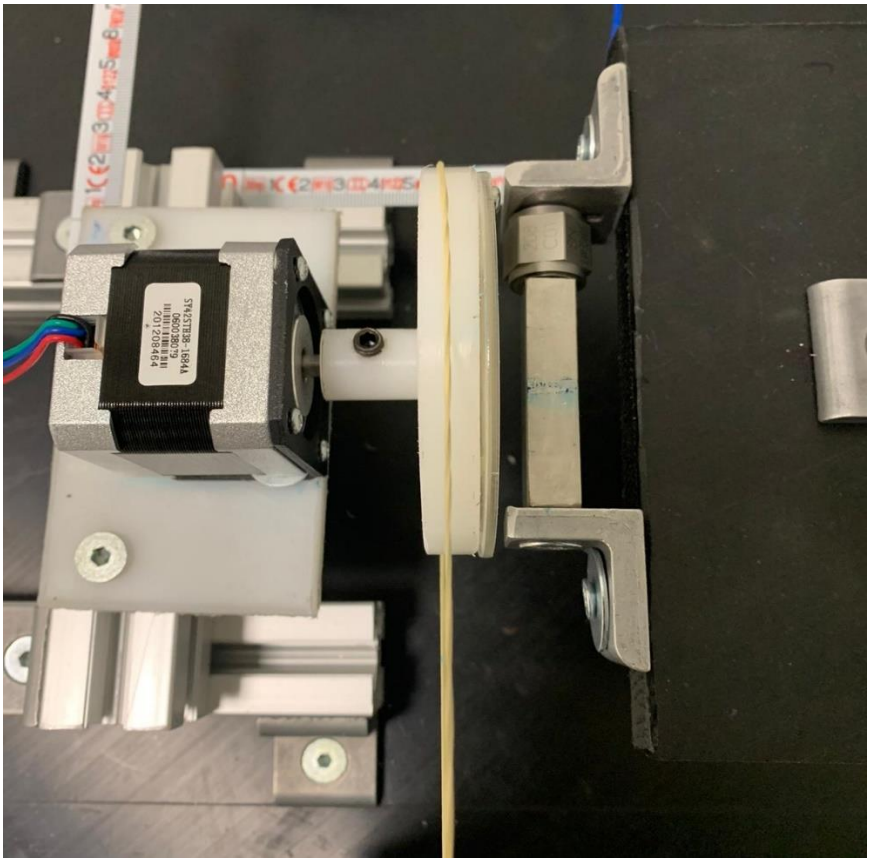

Figure 33 Position 2 x=-7mm y=+5mm z=0

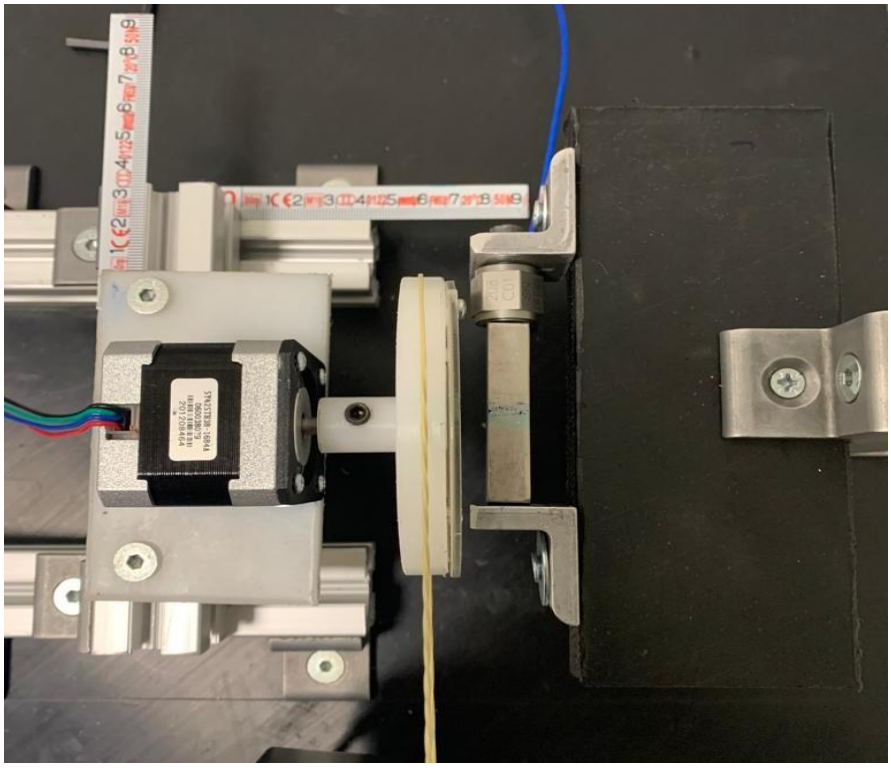

Figure 34 Position 3 x=-7mm y=-5mm z=0

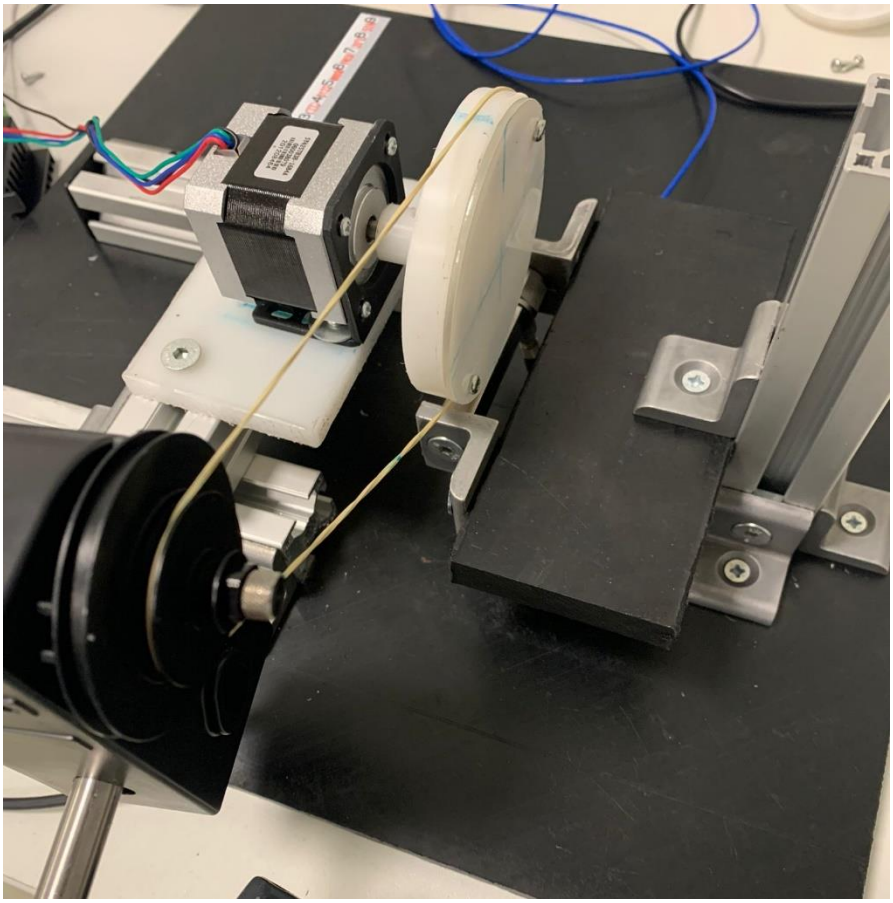

Figure 35 Position 4 x=+7.5mm y=0mm z=-42

3.1 Position 1 x=-7mm y=0 z=0 (clockwise)

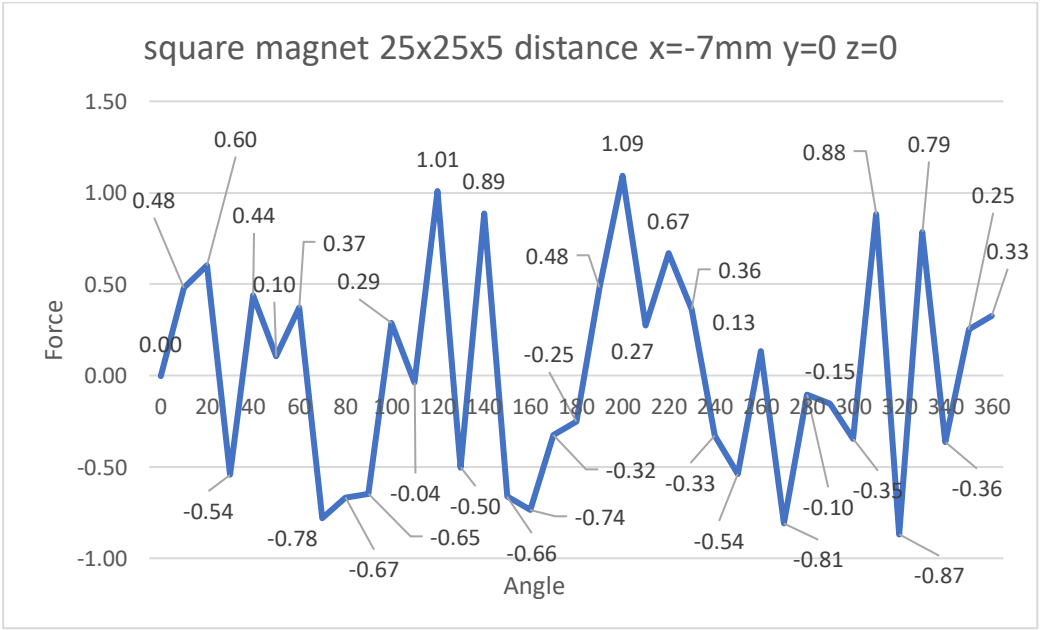

Figure 36 Force-angle graph of square magnet Position 1 x=-7mm y=0 z=0 (clockwise)

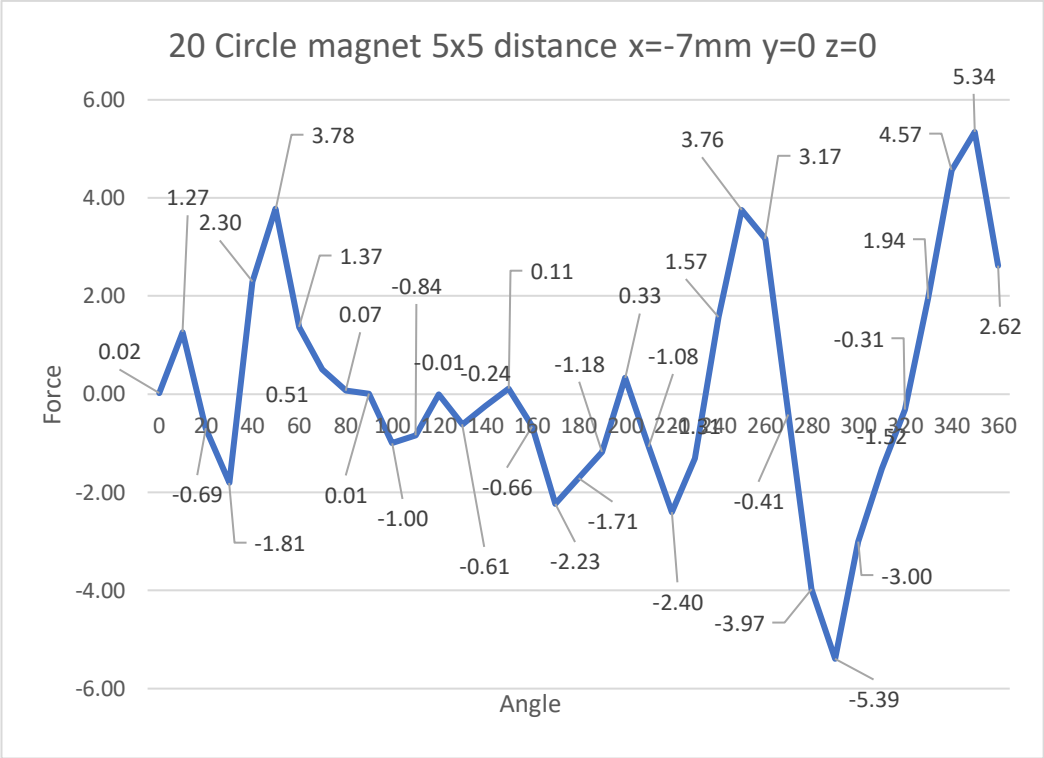

Figure 37 Force-angle graph of 20 circle magnet Position 1 x=-7mm y=0 z=0 (clockwise)

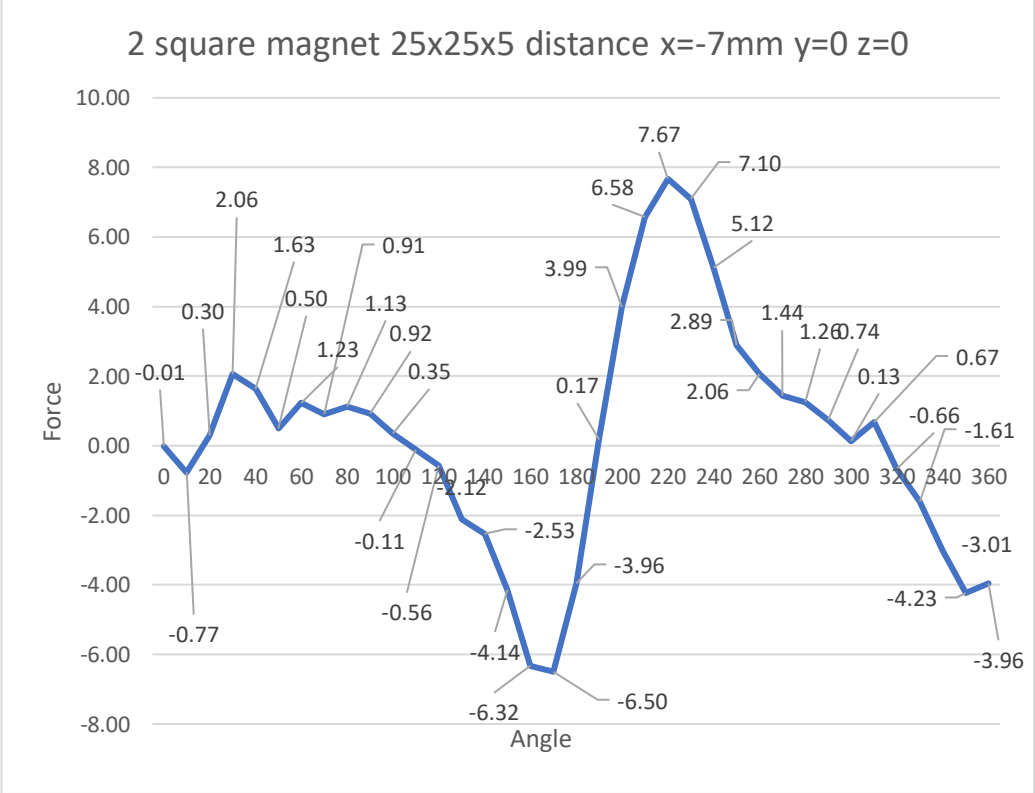

Figure 38 Force-angle graph of 2 square magnet Position 1 x=-7mm y=0 z=0 (clockwise)

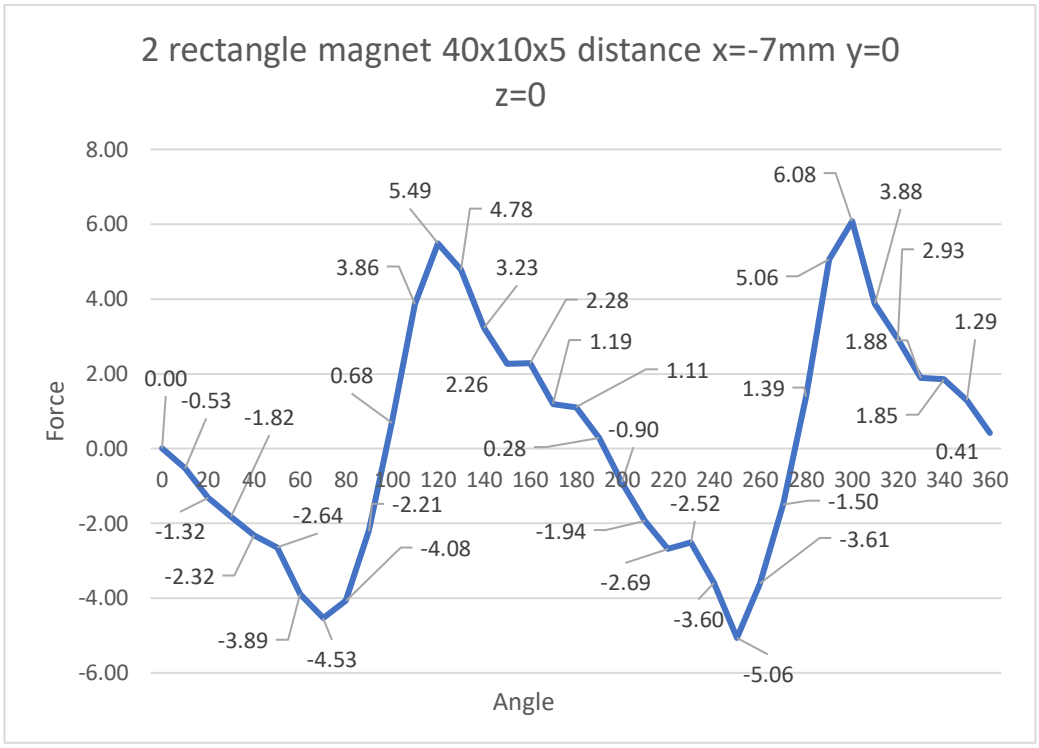

Figure 39 Force-angle graph of 2 rectangle magnet Position 1 x=-7mm y=0 z=0 (clockwise)

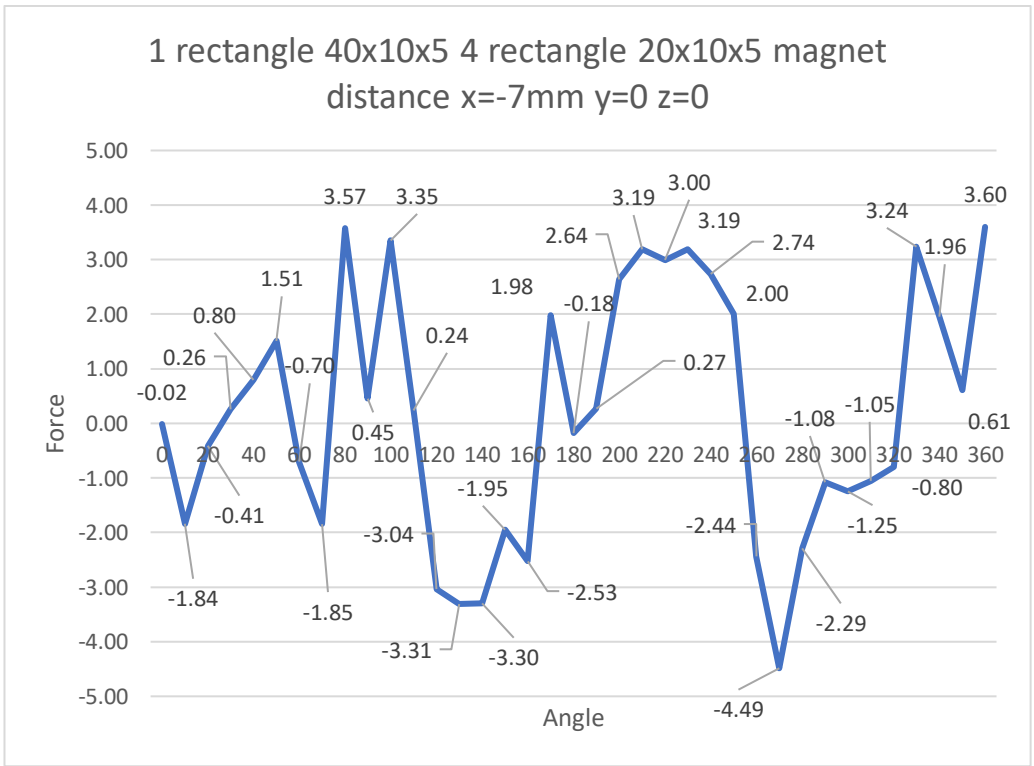

Figure 40 Force-angle graph of 5 rectangle magnet Position 1 x=-7mm y=0 z=0 (clockwise)

3.2 Position 1 x=-7mm y=0 z=0 (counter clockwise)

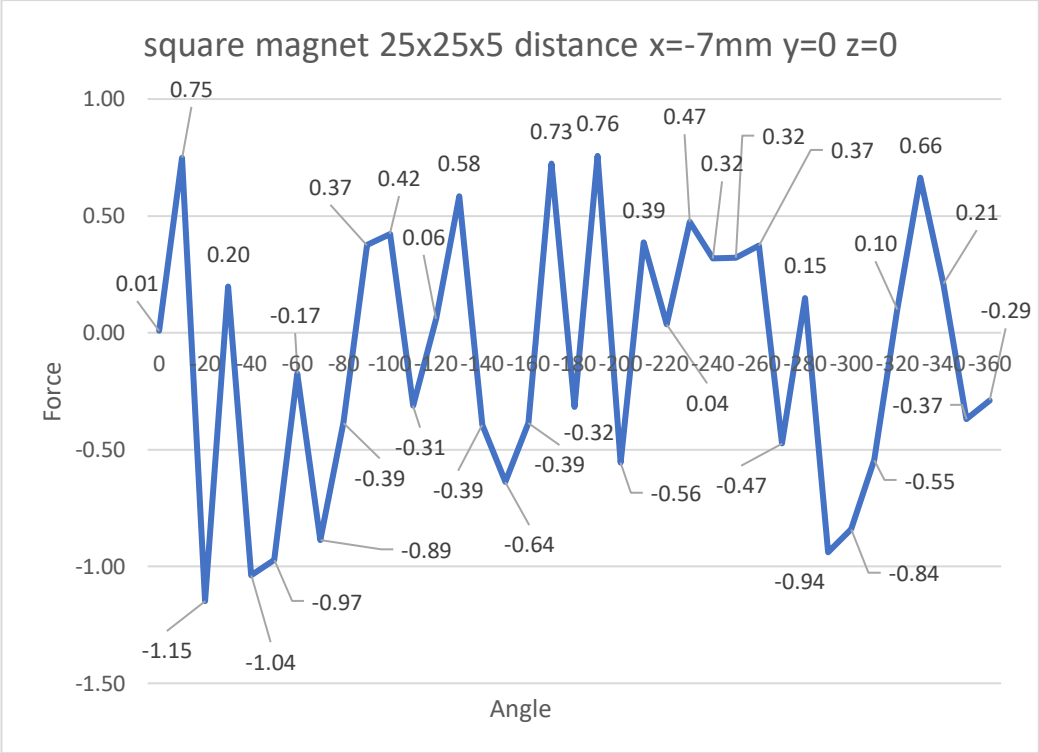

Figure 41 Force-angle graph of square magnet Position 1 x=-7mm y=0 z=0 (counter clockwise)

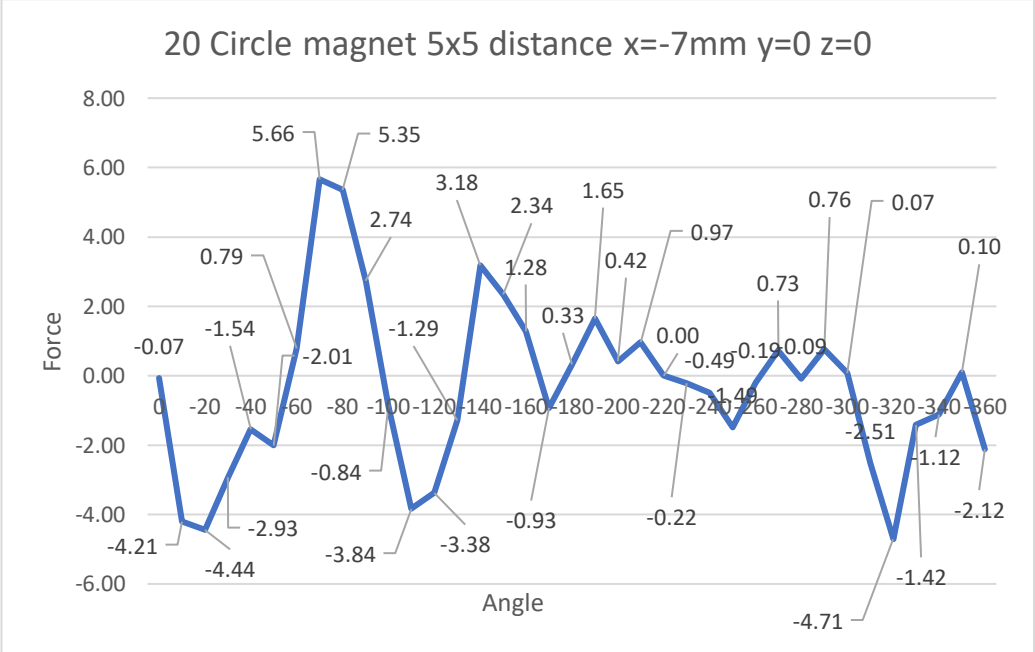

Figure 42 Force-angle graph of 20 circle magnet Position 1 x=-7mm y=0 z=0 (counter clockwise)

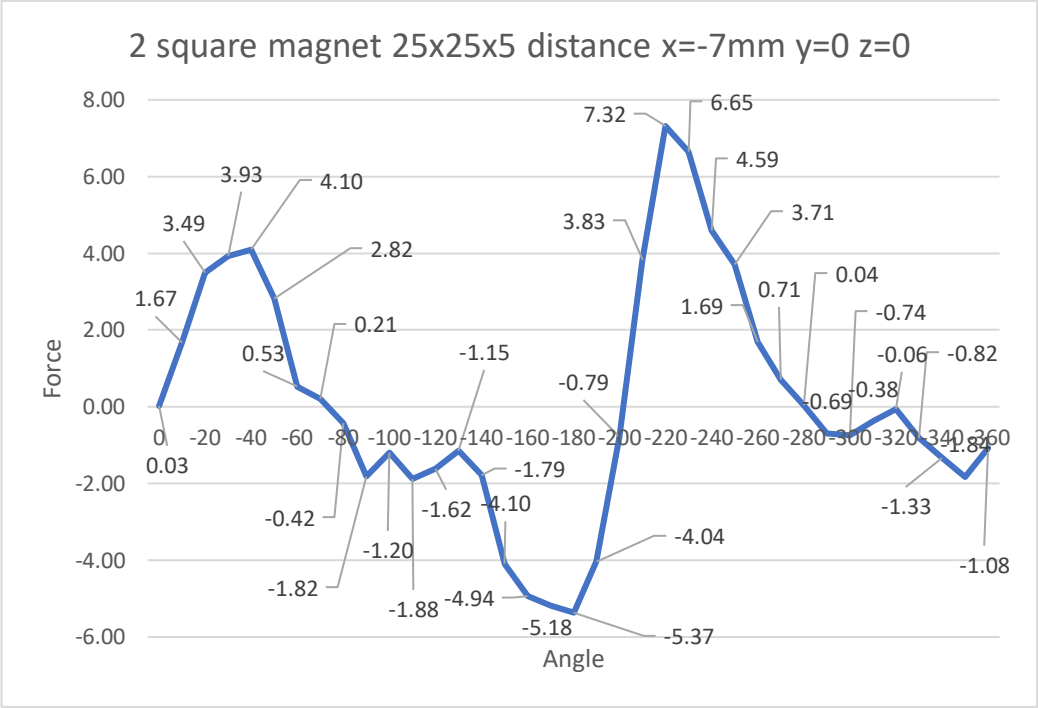

Figure 43 Force-angle graph of 2 square magnet Position 1 x=-7mm y=0 z=0 (counter clockwise)

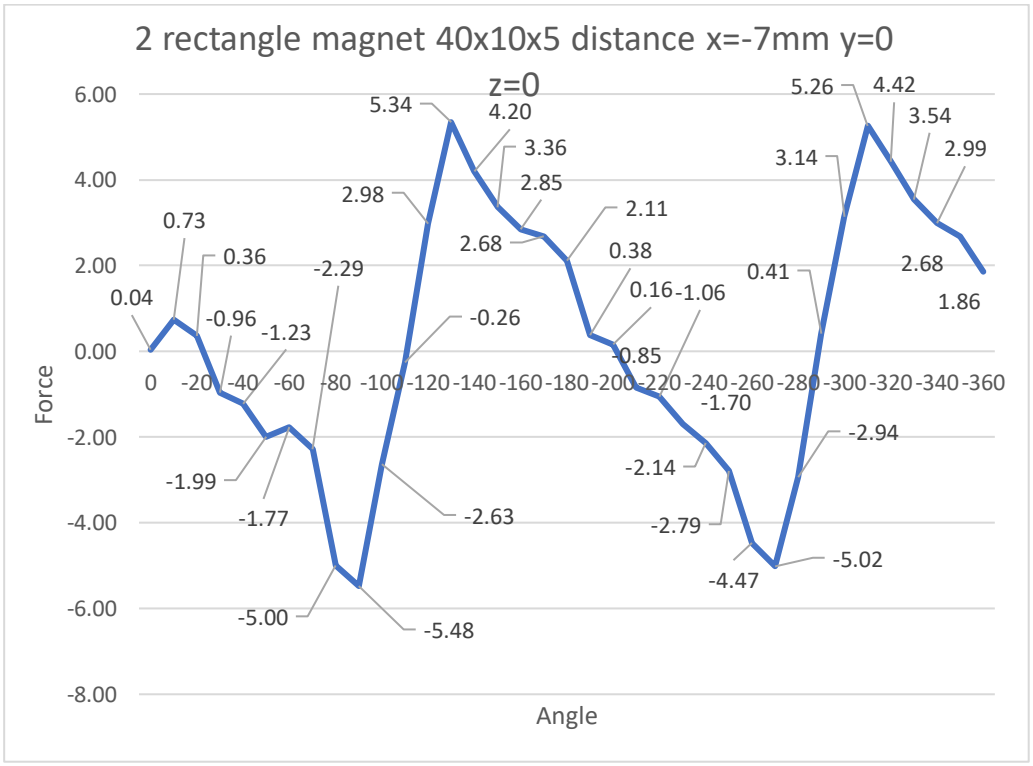

Figure 44 Force-angle graph of 2 rectangle magnet Position 1 x=-7mm y=0 z=0 (counter clockwise)

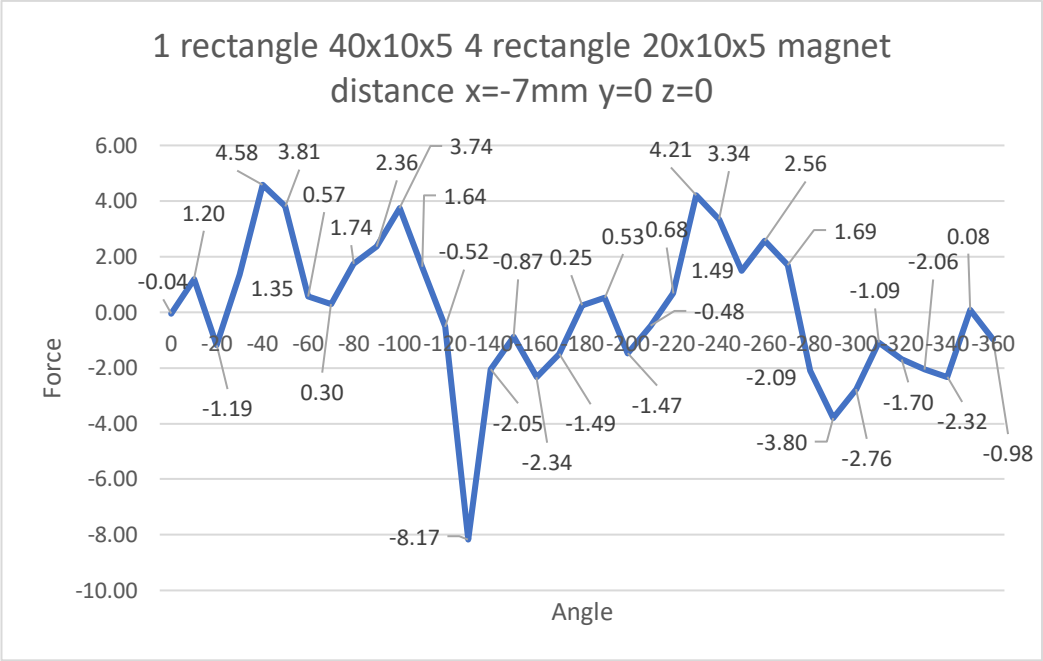

Figure 45 Force-angle graph of 5 rectangle magnet Position 1 x=-7mm y=0 z=0 (counter clockwise)

3.3 Position 2 x=-7mm y=+5 z=0 (clockwise)

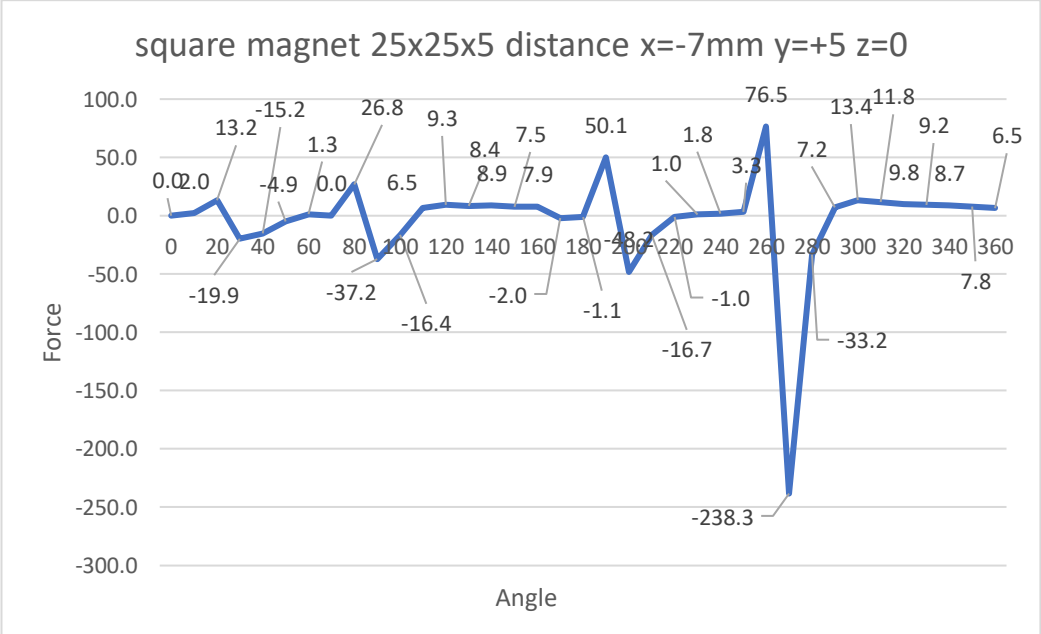

Figure 46 Force-angle graph of square magnet Position 2 x=-7mm y=+5 z=0 (clockwise)

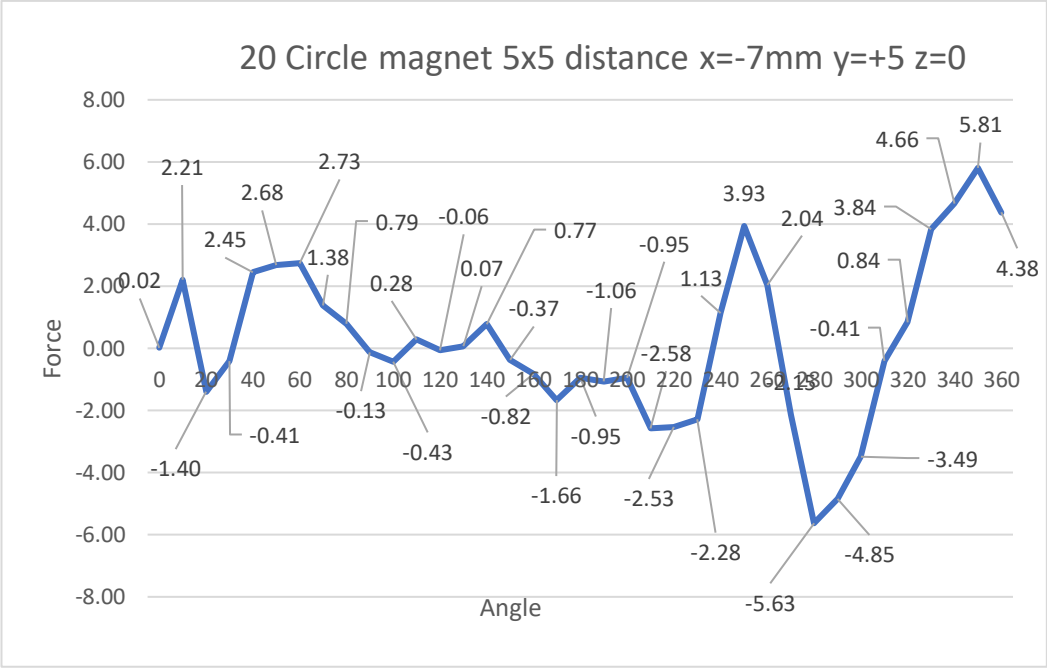

Figure 47 Force-angle graph of 20 circle magnet Position 2 x=-7mm y=+5 z=0 (clockwise)

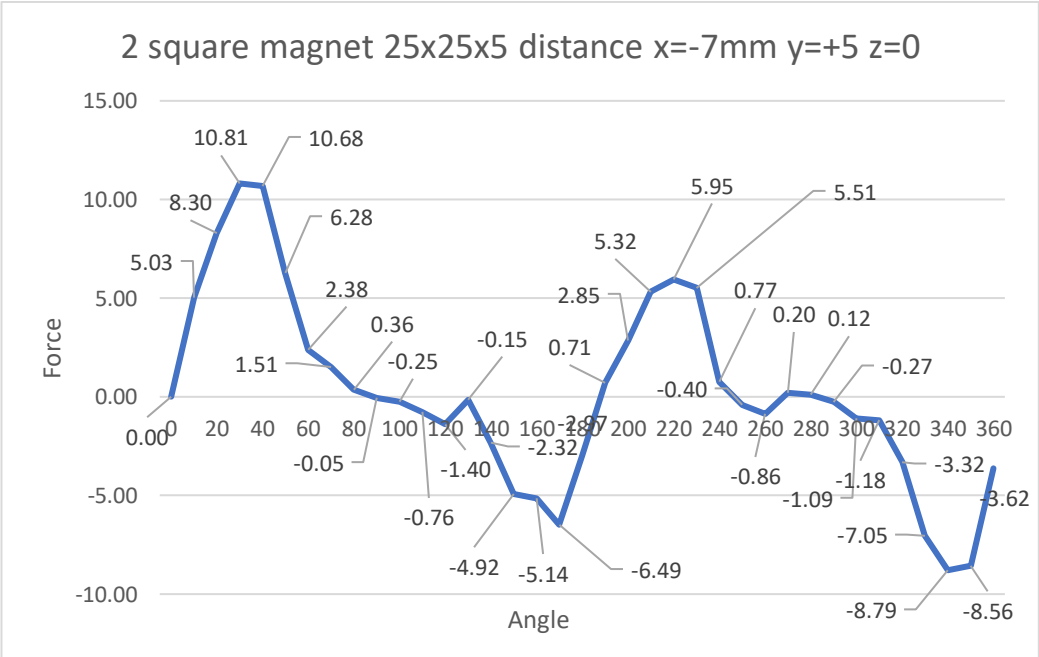

Figure 48 Force-angle graph of 2 square magnet Position 2 x=-7mm y=+5 z=0 (clockwise)

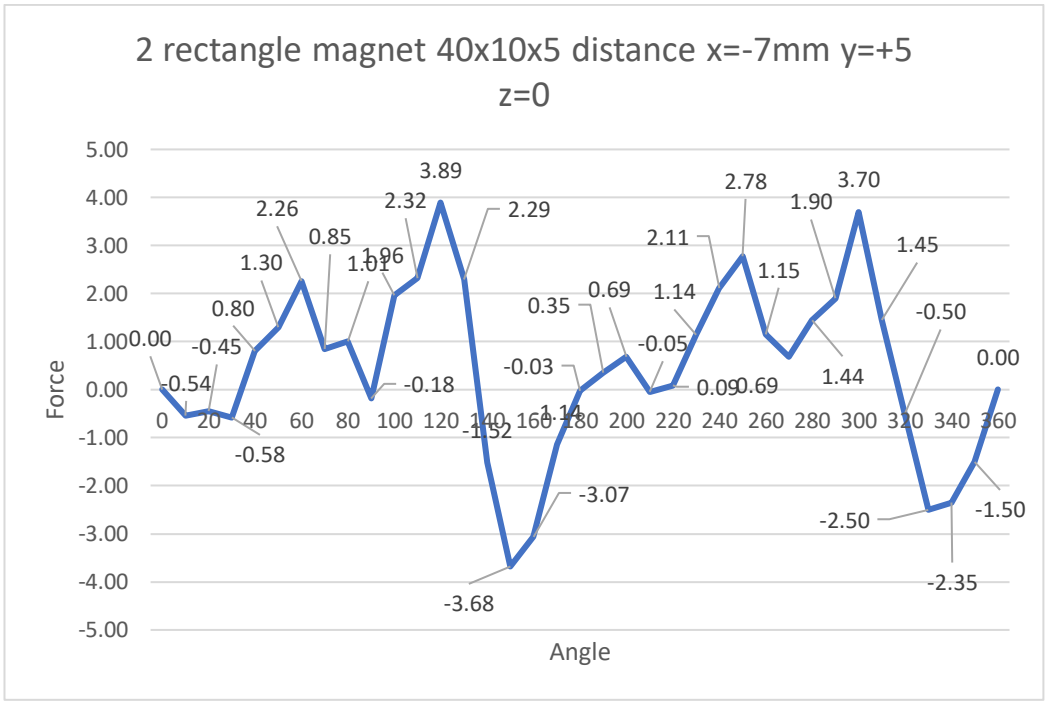

Figure 49 Force-angle graph of 2 rectangle magnet Position 2 x=-7mm y=+5 z=0 (clockwise)

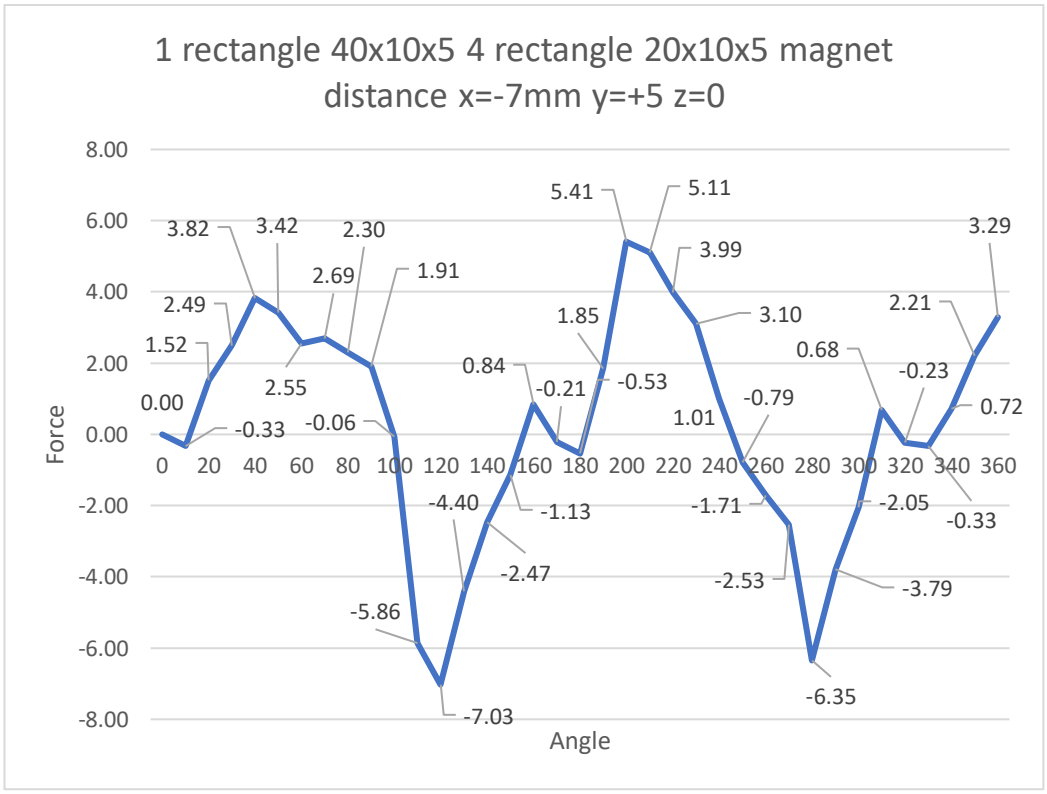

Figure 50 Force-angle graph of 5 rectangle magnet Position 2 x=-7mm y=+5 z=0 (clockwise)

3.4 Position 2 x=-7mm y=+5 z=0 (counter clockwise)

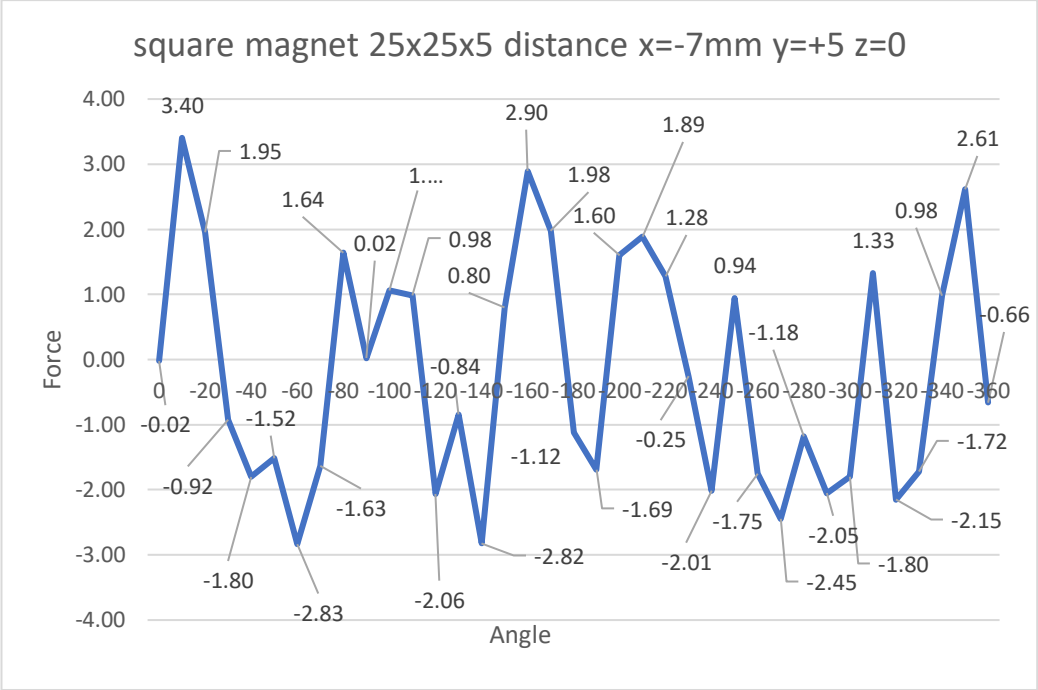

Figure 51 Force-angle graph of square magnet Position 2 x=-7mm y=+5 z=0 (counter clockwise)

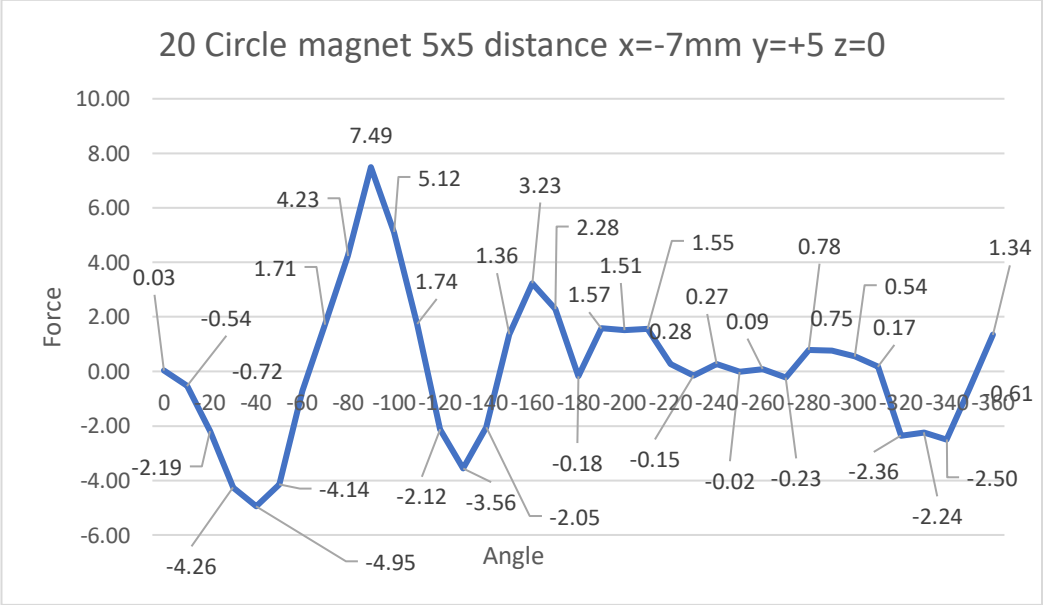

Figure 52 Force-angle graph of 20 circle magnet Position 2 x=-7mm y=+5 z=0 (counter clockwise)

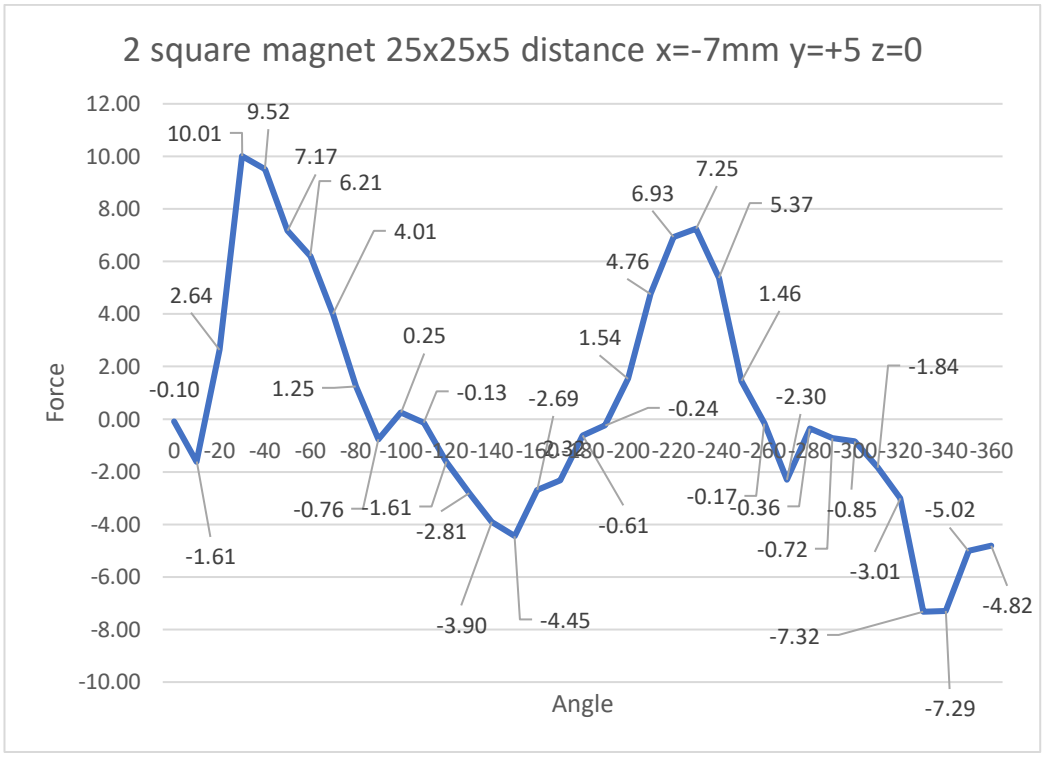

Figure 53 Force-angle graph of 2 square magnet Position 2 x=-7mm y=+5 z=0 (counter clockwise)

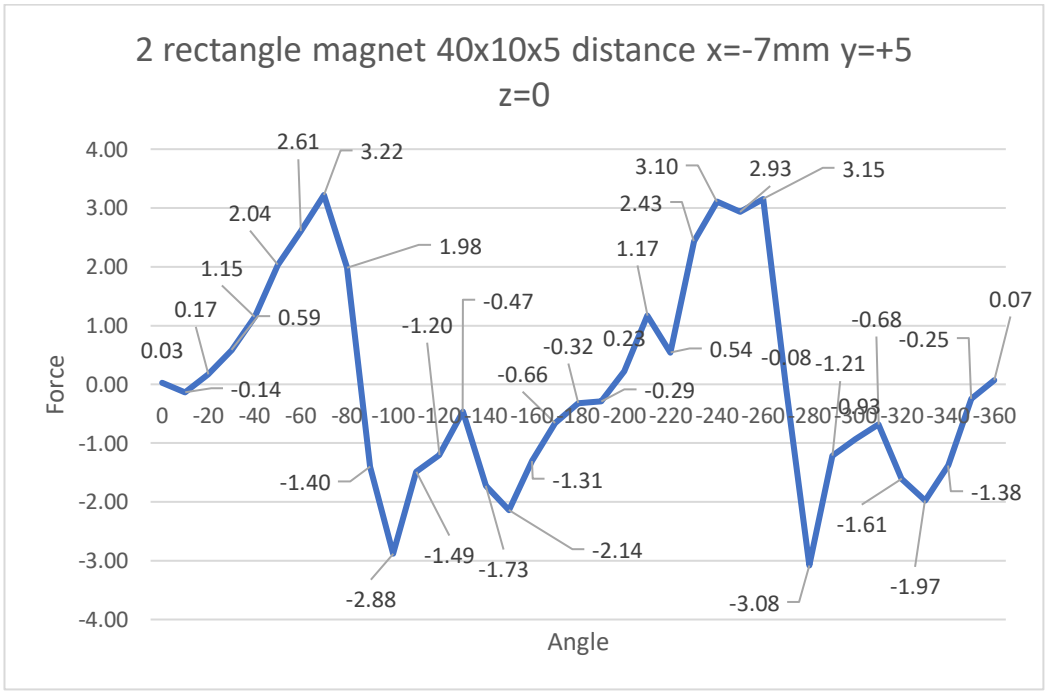

Figure 54 Force-angle graph of 2 rectangle magnet Position 2 x=-7mm y=+5 z=0 (counter clockwise)

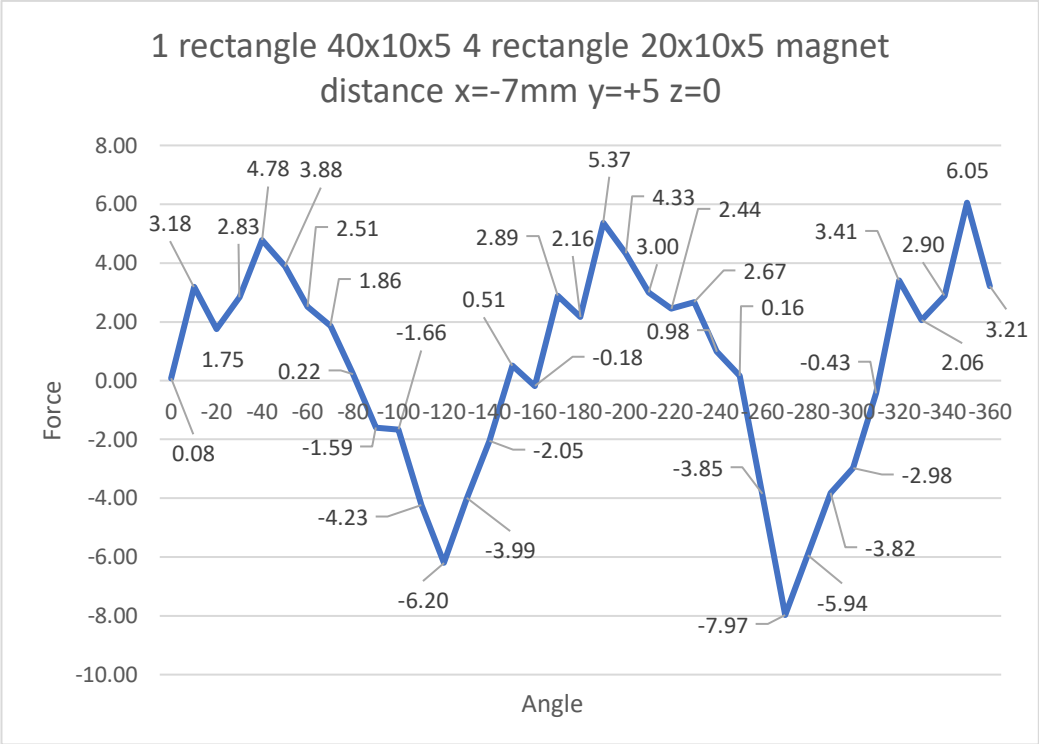

Figure 55 Force-angle graph of 5 rectangle magnet Position 2 x=-7mm y=+5 z=0 (counter clockwise)

3.5 Position 3 x=-7mm y=-5 z=0 (clockwise)

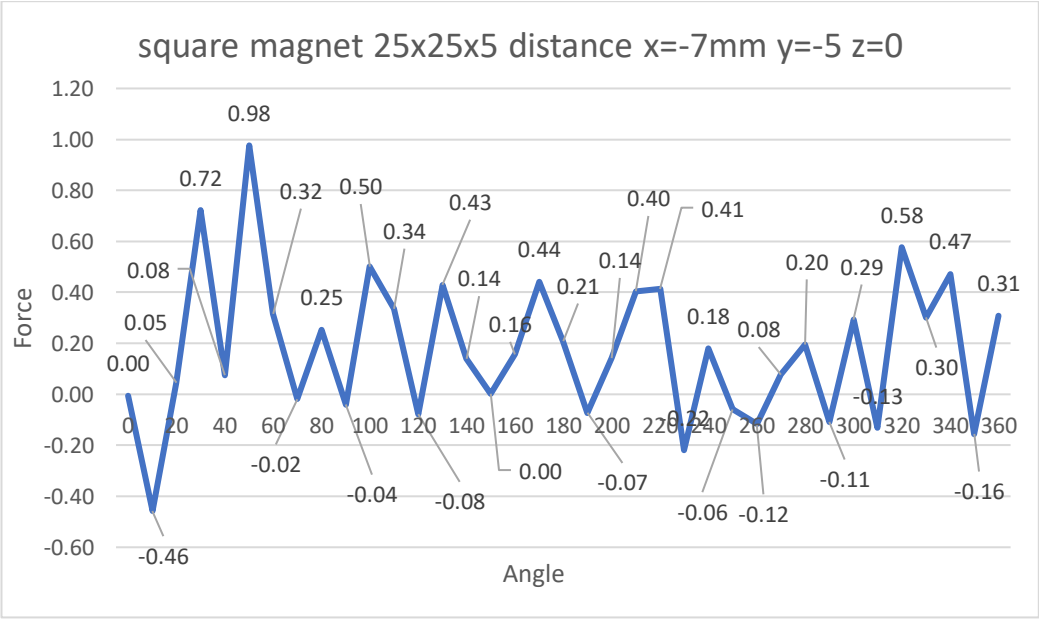

Figure 56 Force-angle graph of square magnet Position 3 x=-7mm y=-5 z=0 (clockwise)

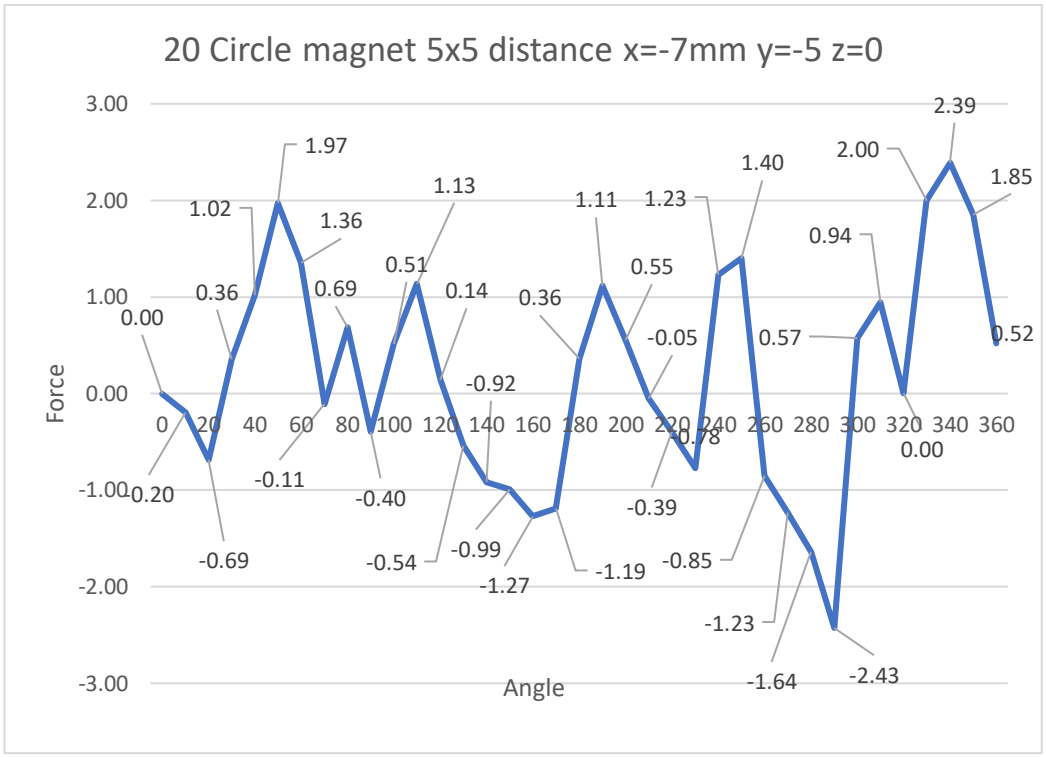

Figure 57 Force-angle graph of 20 circle magnet Position 3 x=-7mm y=-5 z=0 (clockwise)

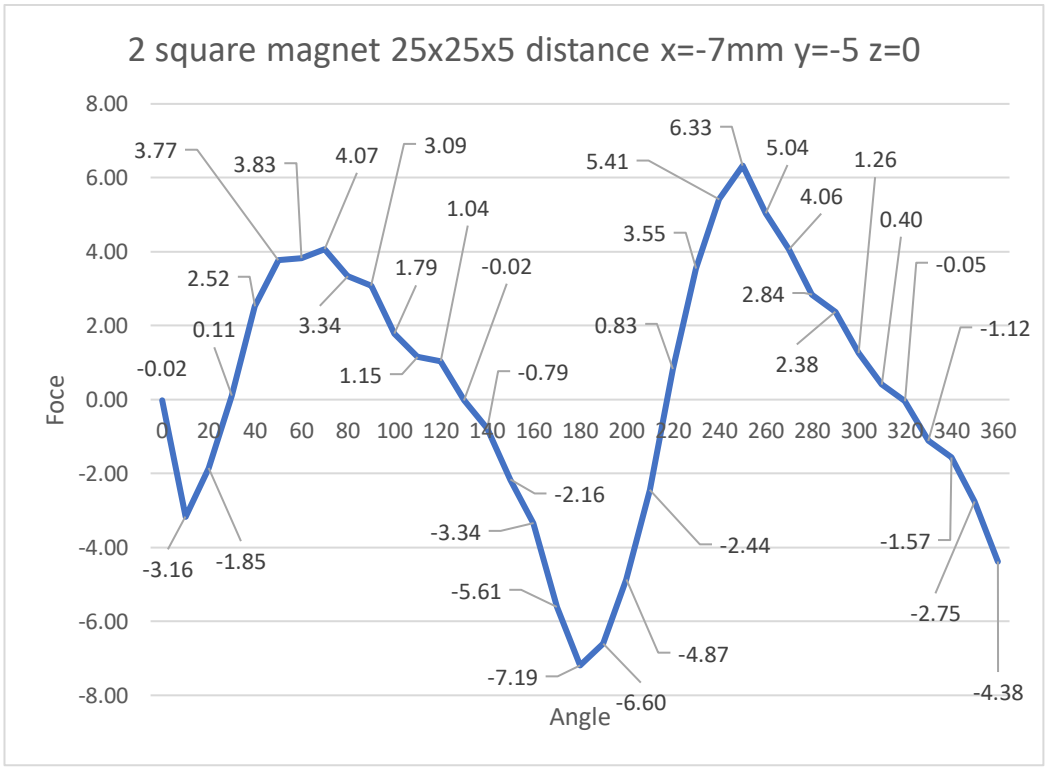

Figure 58 Force-angle graph of 2 square magnet Position 3 x=-7mm y=-5 z=0 (clockwise)

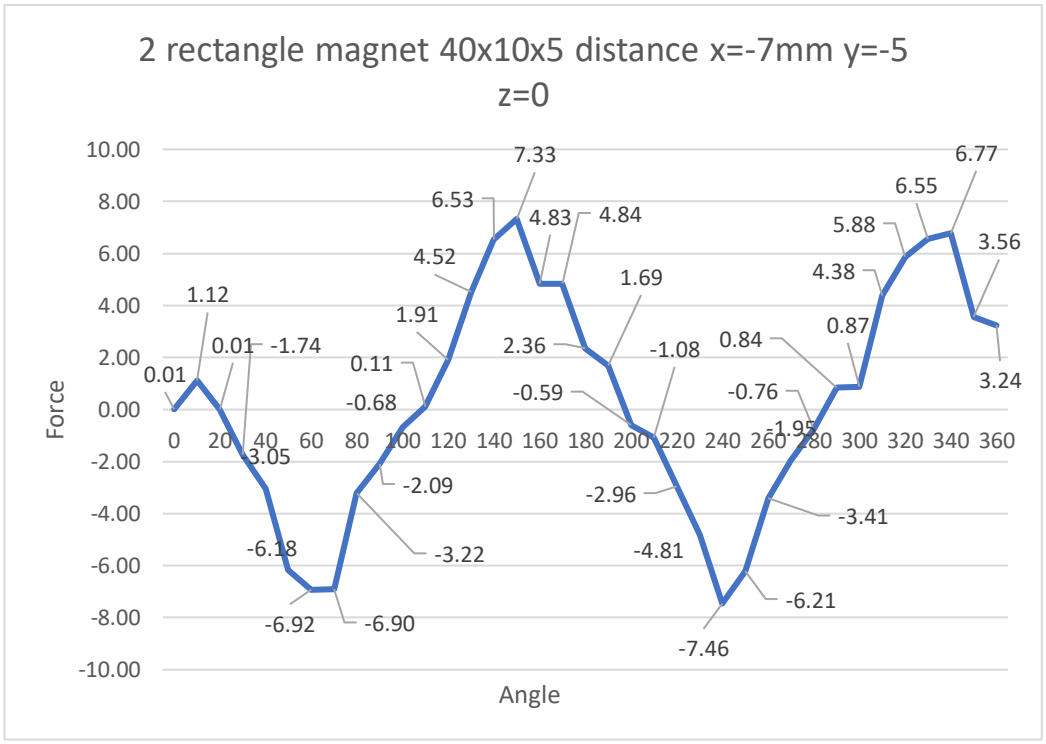

Figure 59 Force-angle graph of 2 rectangle magnet Position 3 x=-7mm y=-5 z=0 (clockwise)

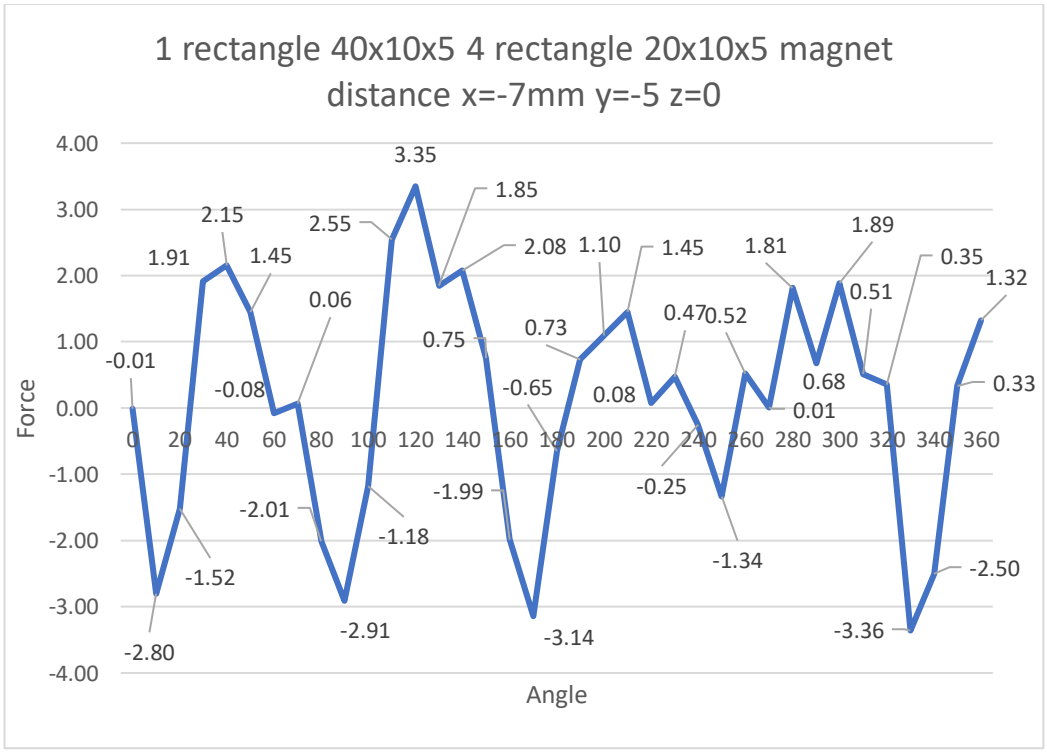

Figure 60 Force-angle graph of 5 rectangle magnet Position 3 x=-7mm y=-5 z=0 (clockwise)

3.6 Position 3 x=-7mm y=-5 z=0 (counter clockwise)

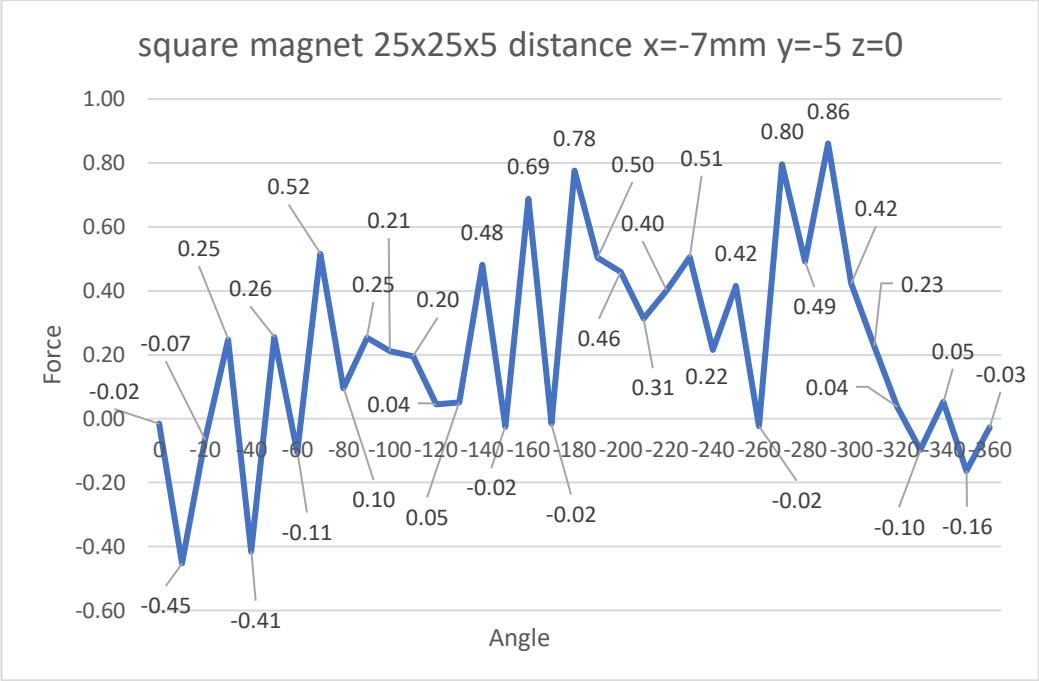

Figure 61 Force-angle graph of square magnet Position 3 x=-7mm y=-5 z=0 (counter clockwise)

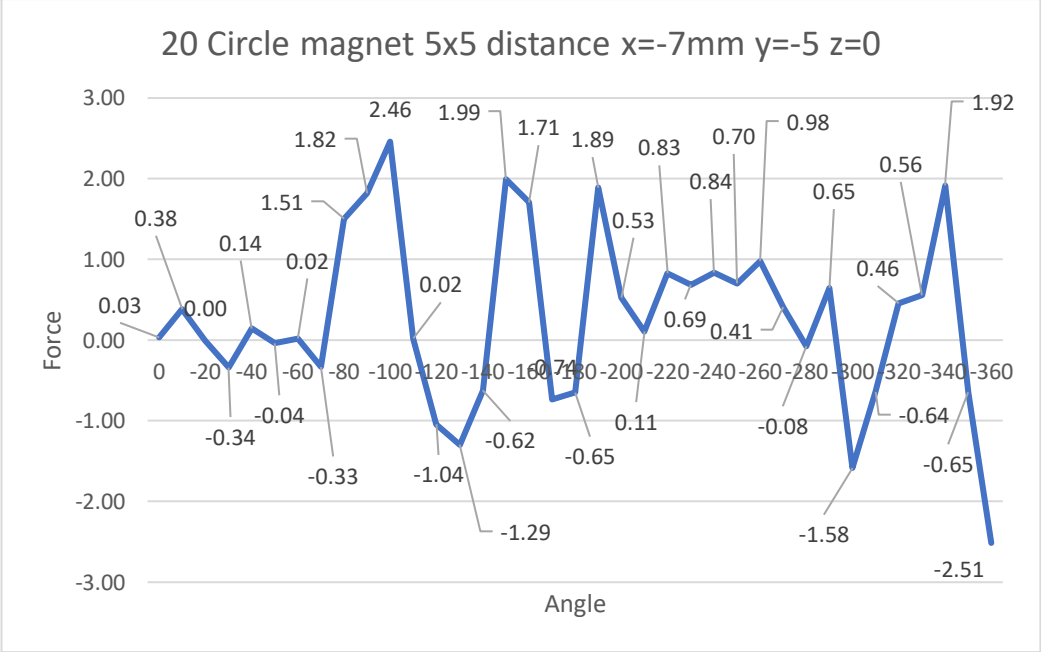

Figure 62 Force-angle graph of 20 circle magnet Position 3 x=-7mm y=-5 z=0 (counter clockwise)

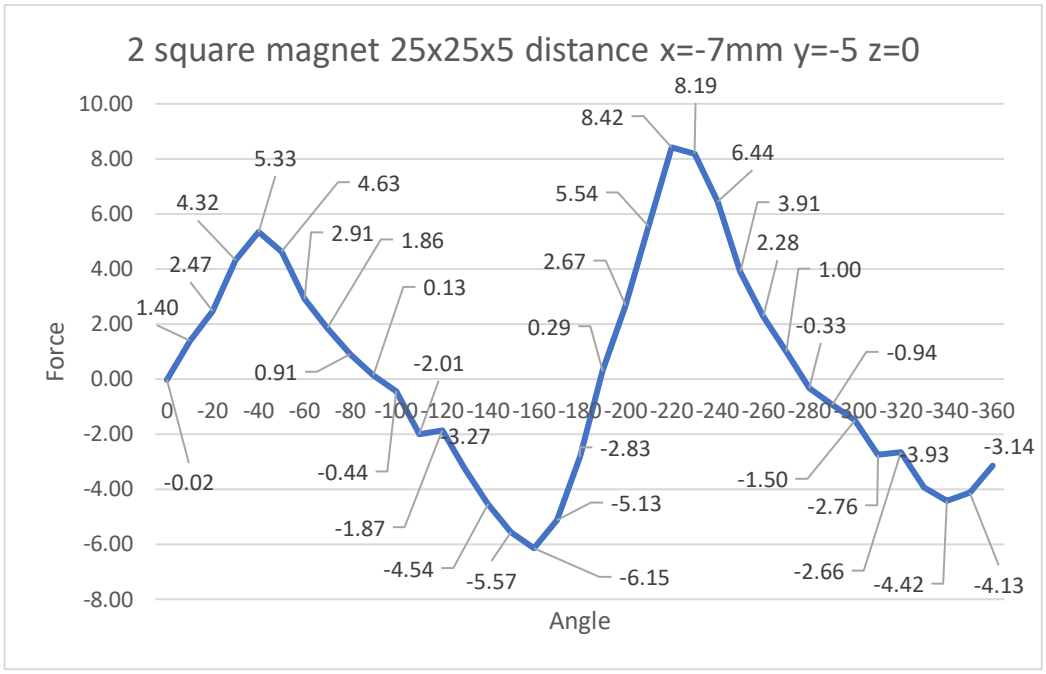

Figure 63 Force-angle graph of 2 square magnet Position 3 x=-7mm y=-5 z=0 (counter clockwise)

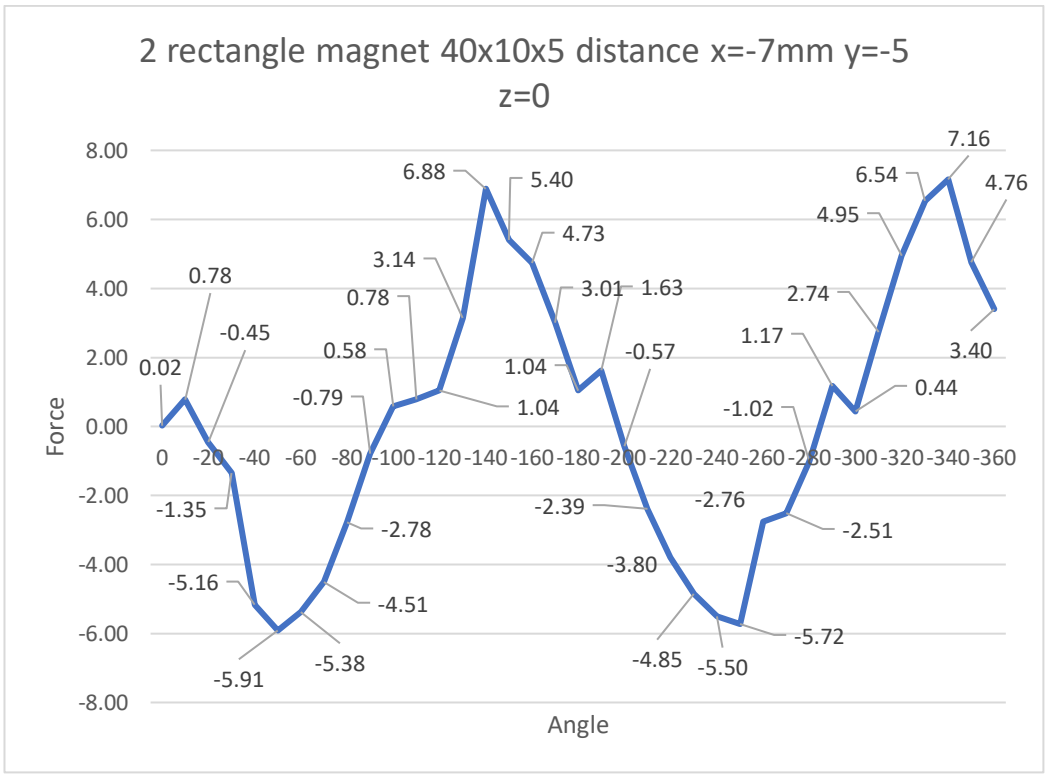

Figure 64 Force-angle graph of 2 rectangle magnet Position 3 x=-7mm y=-5 z=0 (counter clockwise)

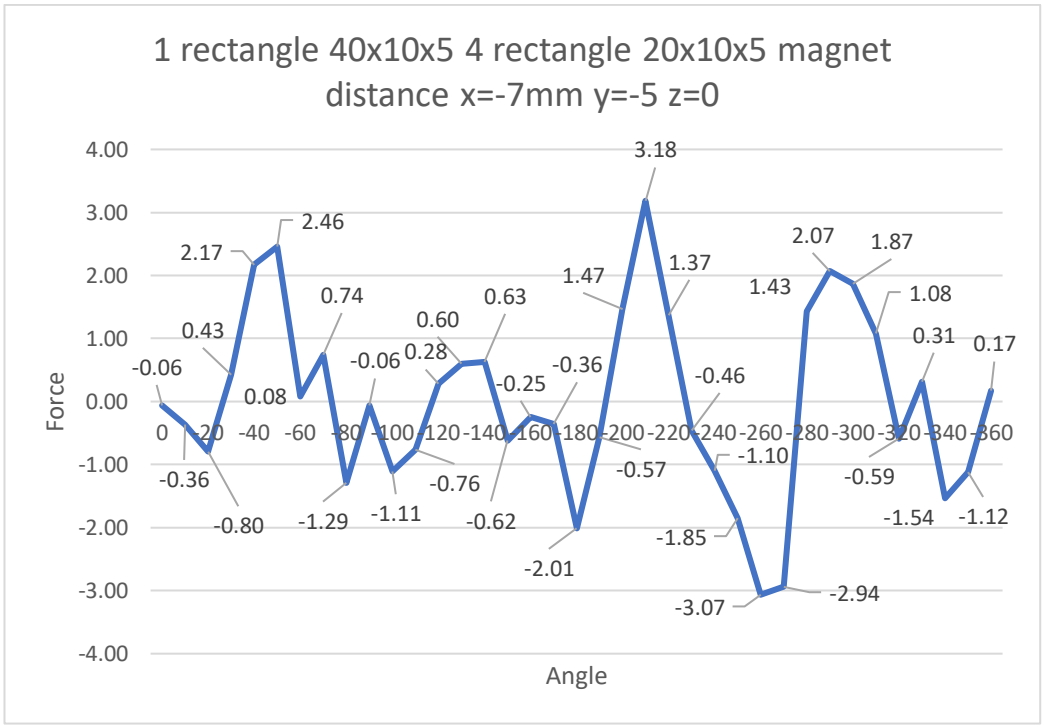

Figure 65 Force-angle graph of 5 rectangle magnet Position 3 x=-7mm y=-5 z=0 (counter clockwise)

3.7. Position 4 x=+7.5mm y=0 z=-42 (clockwise)

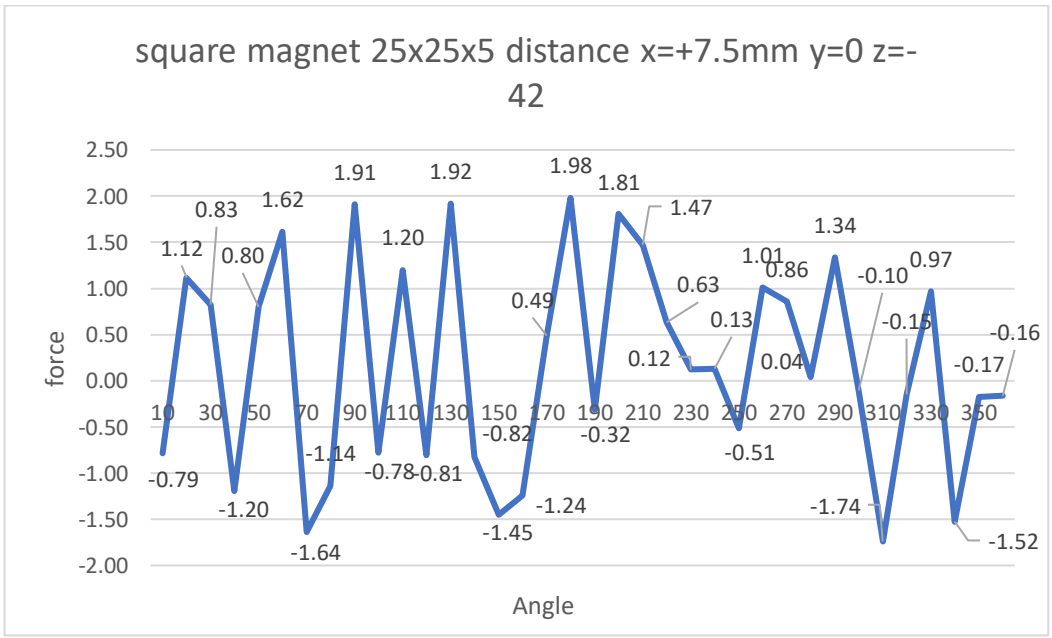

Figure 66 Force-angle graph of square magnet Position 4 x=+7.5mm y=0 z=-42 (clockwise)

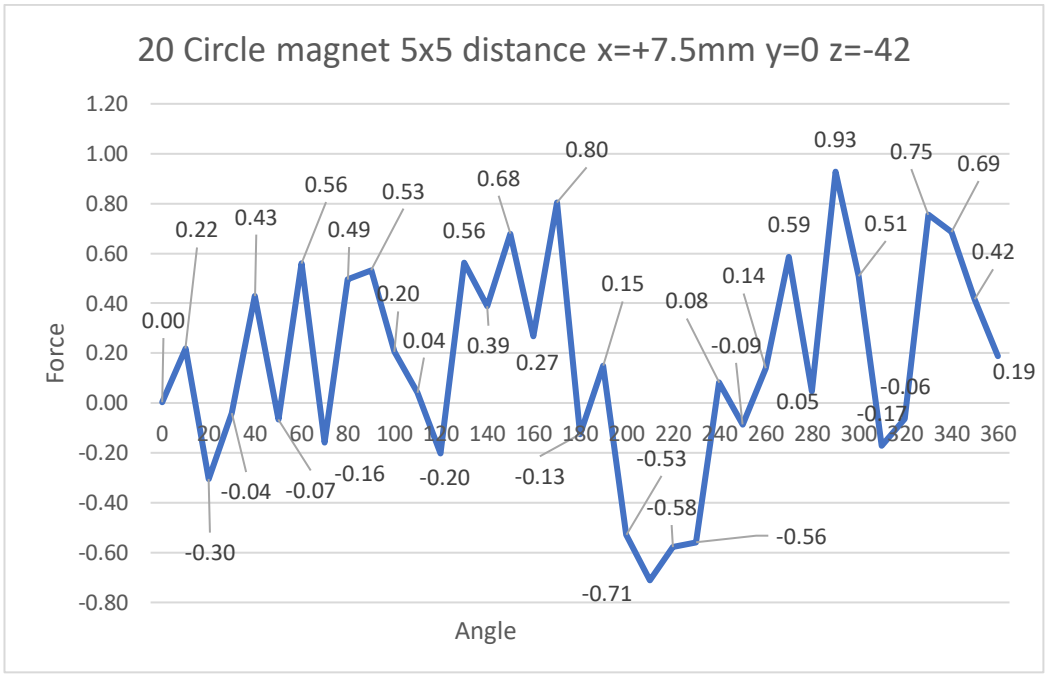

Figure 67 Force-angle graph of 20 circle magnet Position 4 x=+7.5mm y=0 z=-42 (clockwise)

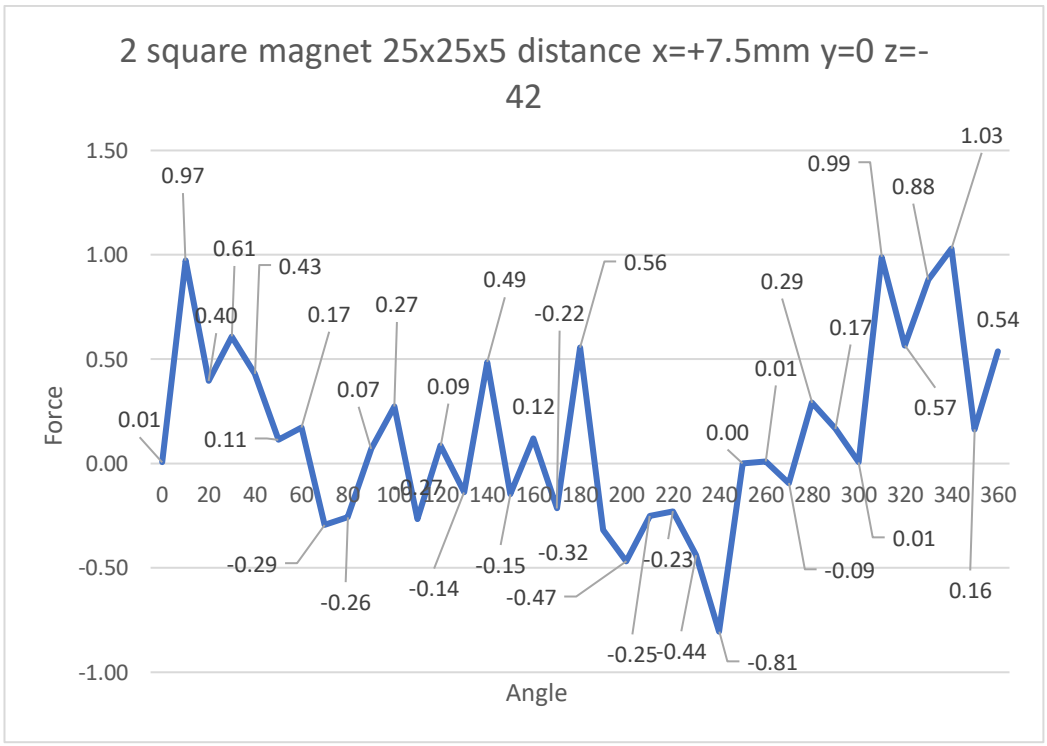

Figure 68 Force-angle graph of 2 square magnet Position 4 x=+7.5mm y=0 z=-42 (clockwise)

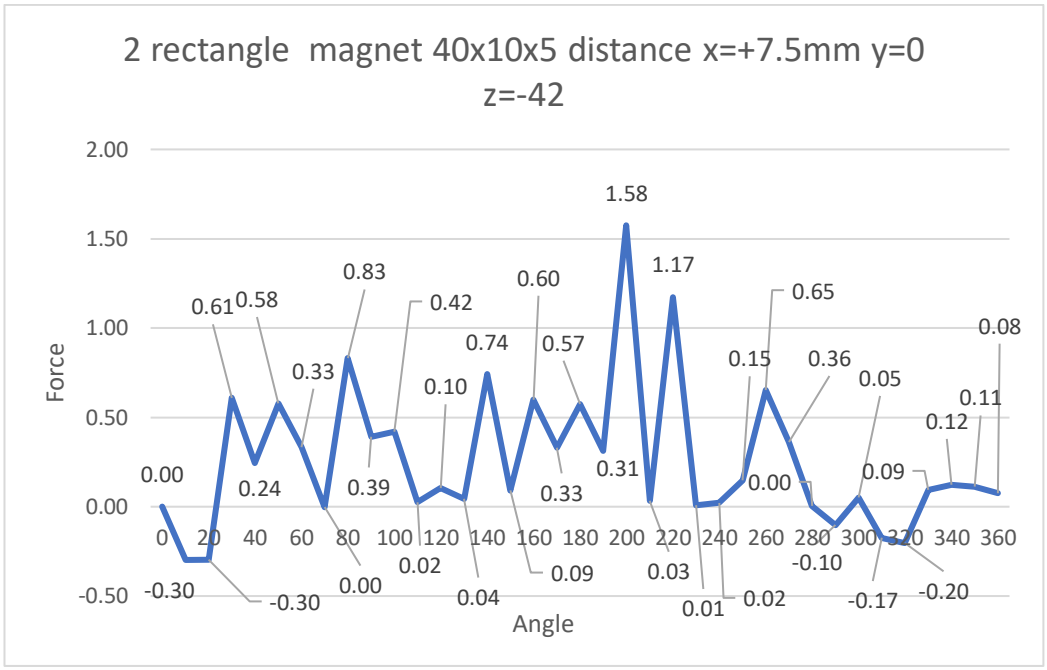

Figure 69 Force-angle graph of 2 rectangle magnet Position 4 x=+7.5mm y=0 z=-42 (clockwise)

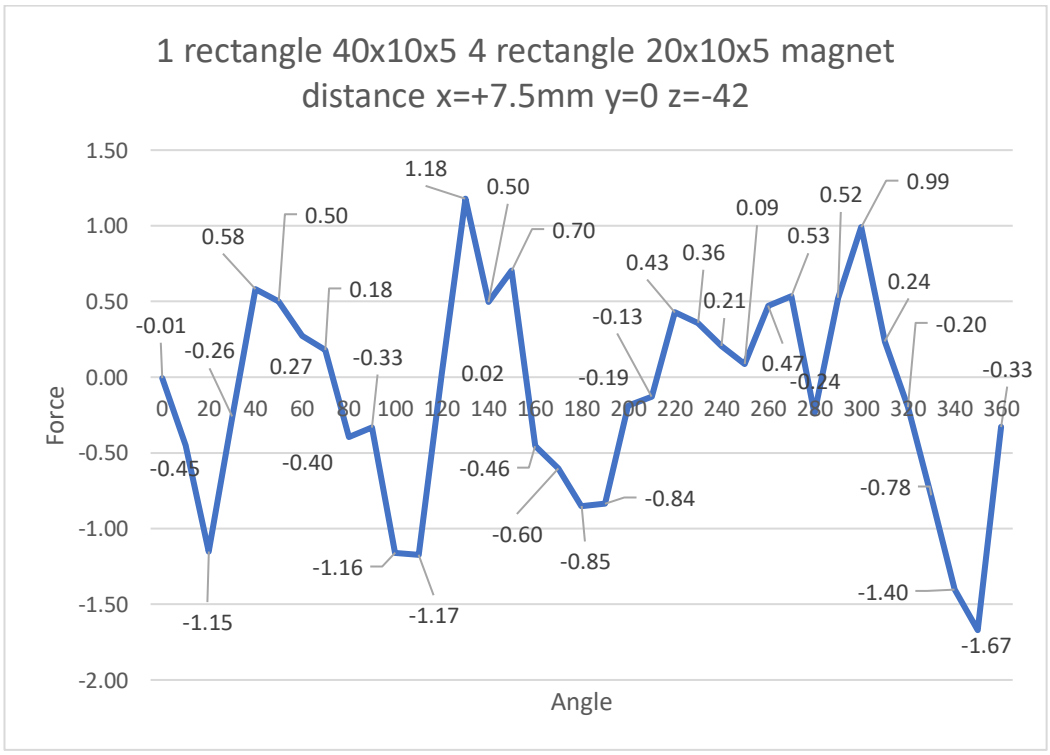

Figure 70 Force-angle graph of 5 rectangle magnet Position 4 x=+7.5mm y=0 z=-42 (clockwise)

3.8 Position 4 x=+7.5mm y=0 z=-42 (counter clockwise)

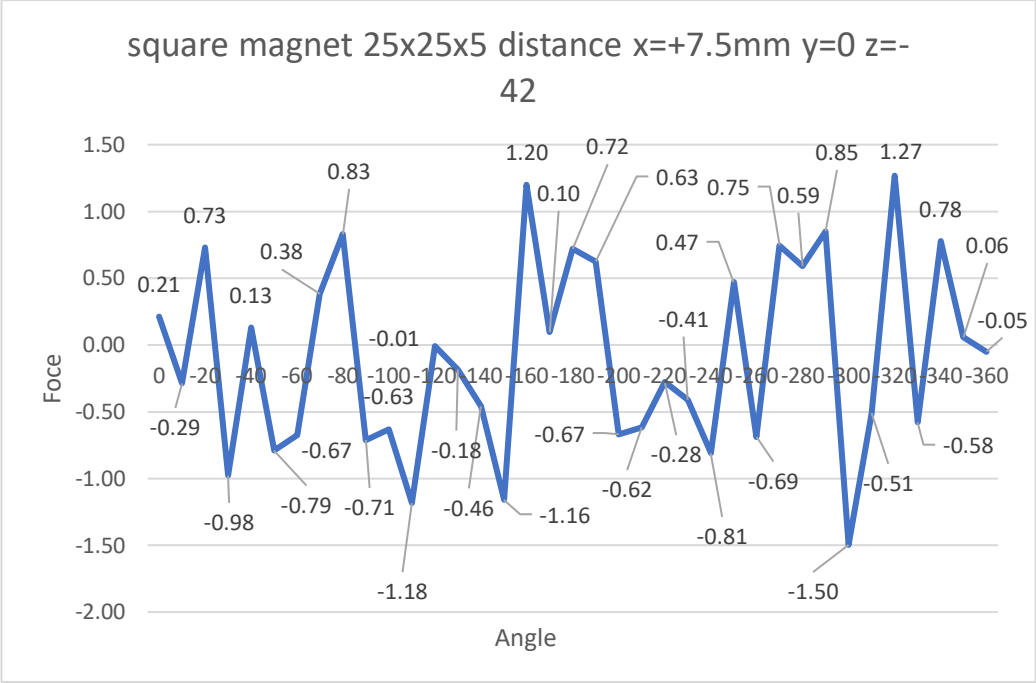

Figure 71 Force-angle graph of square magnet Position 4 x=+7.5mm y=0 z=-42 (counter clockwise)

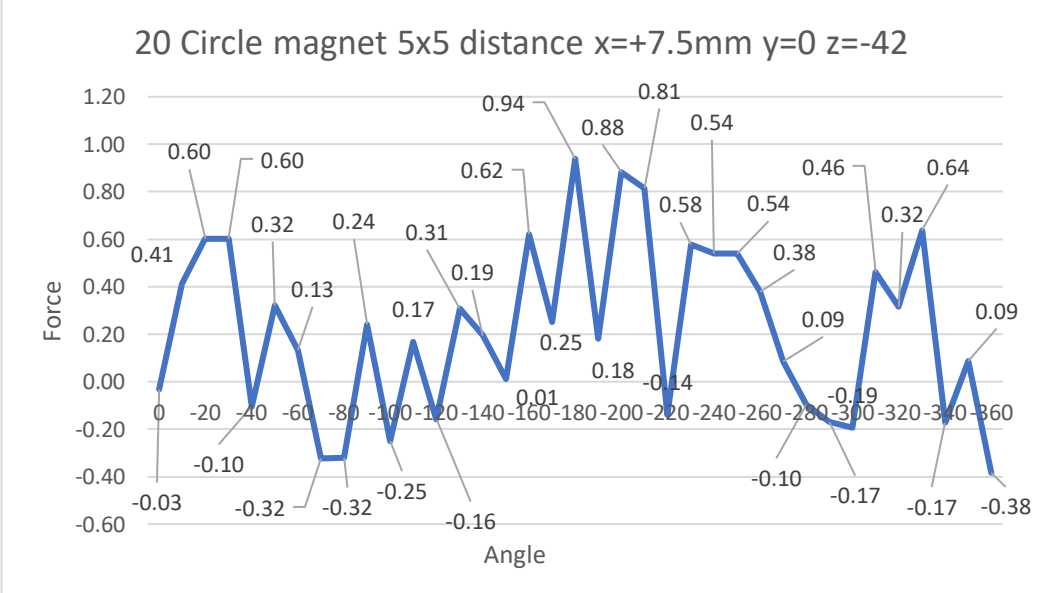

Figure 72 Force-angle graph of 20 circle magnet Position 4 x=+7.5mm y=0 z=-42 (counter clockwise)

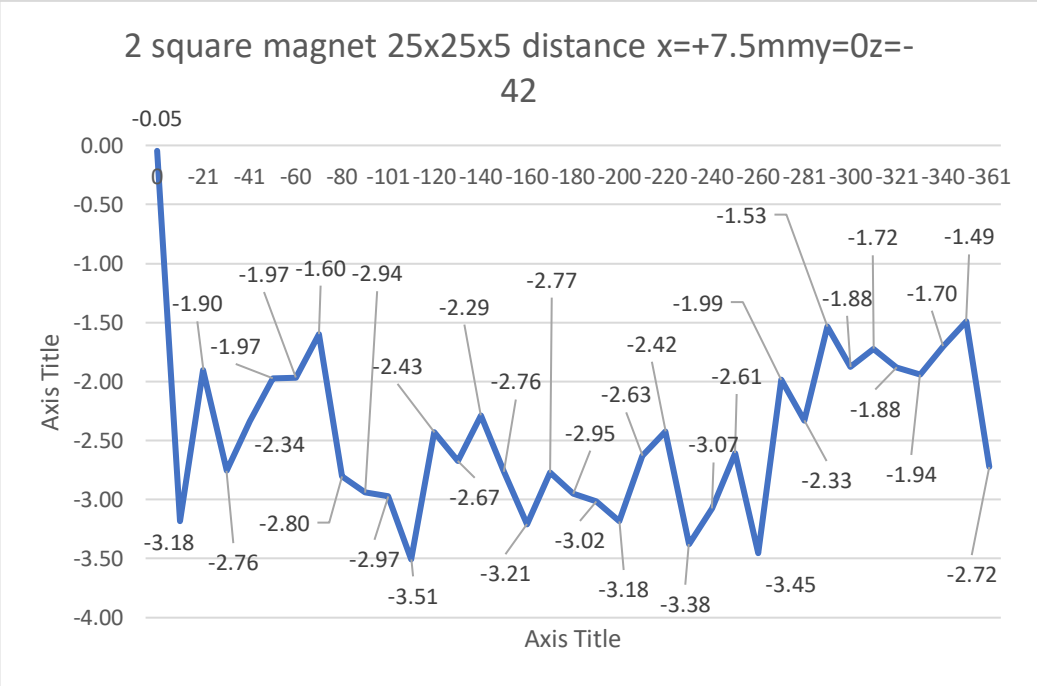

Figure 73 Force-angle graph of 2 square magnet Position 4 x=+7.5mm y=0 z=-42 (counter clockwise)

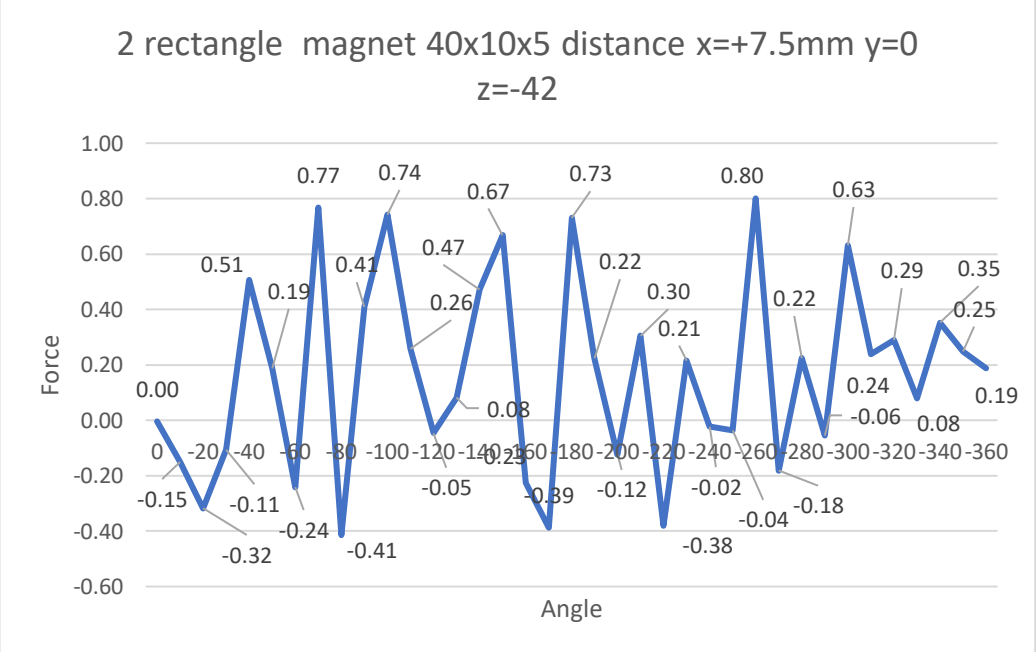

Figure 74 Force-angle graph of 2 rectangle magnet Position 4 x=+7.5mm y=0 z=-42 (counter clockwise)

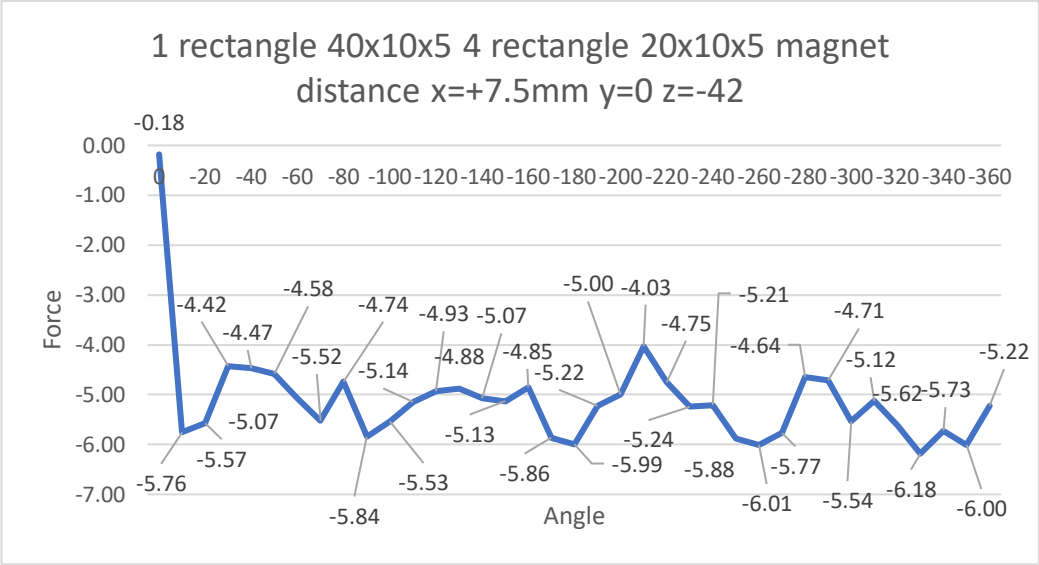

Figure 75 Force-angle graph of 5 rectangle magnet Position 4 x=+7.5mm y=0 z=-42 (counter clockwise)

All charts are given. When we examined the graphics, we obtained the most ideal results for us with the results in the second disc design. In Figure 38, 2 square magnets with the size of 25x25x2 were used. In terms of position, measurements were made at a distance of x=7 y=0 z=0. As a result, as seen in the graph, we observe that each 180-degree angle makes a force change. As a result of this, the changes in our magnets while rotating from s pole to n pole or from n pole to s pole have been clearly observed.

Another magnet geometry that we can evaluate the results in the best way is 2 magnet pairs in the size of 40x10x5. When Figure 39 is examined in detail, it is seen that each 90 degree angle increases and decreases. At the end of 180 degrees, the angle returns to the previous 180 degrees. This is due to the displacement of the s and n poles of the magnets every 180 degrees.

In the graphs we examined, these two magnet pairs (2 squares and two rectangles) rotate clockwise. The counter clockwise rotations of these two measurement results are given in figure 43 and figure 44. When we examine these two graphs, an increase and decrease is observed for every 180 degrees in counter clockwise rotations. In these counter clockwise rotations, we can establish the angle relationship between the magnet and the Magnetostrictive material. On the other hand, as a result of the experiments with square magnet and rectangular magnet, the force values of the square magnet were higher

than the rectangular magnet. The reason for this is that the square magnet produces more magnetic field than the rectangular magnet.

The results of 2 turns (720 degrees) of the stepper motor at 2 rectangular magnets 40x10x5 position 1 point are given in figure 76. In this graph, more clearly, the same result values and the same graphs are seen constantly when they complete every 360 degrees.

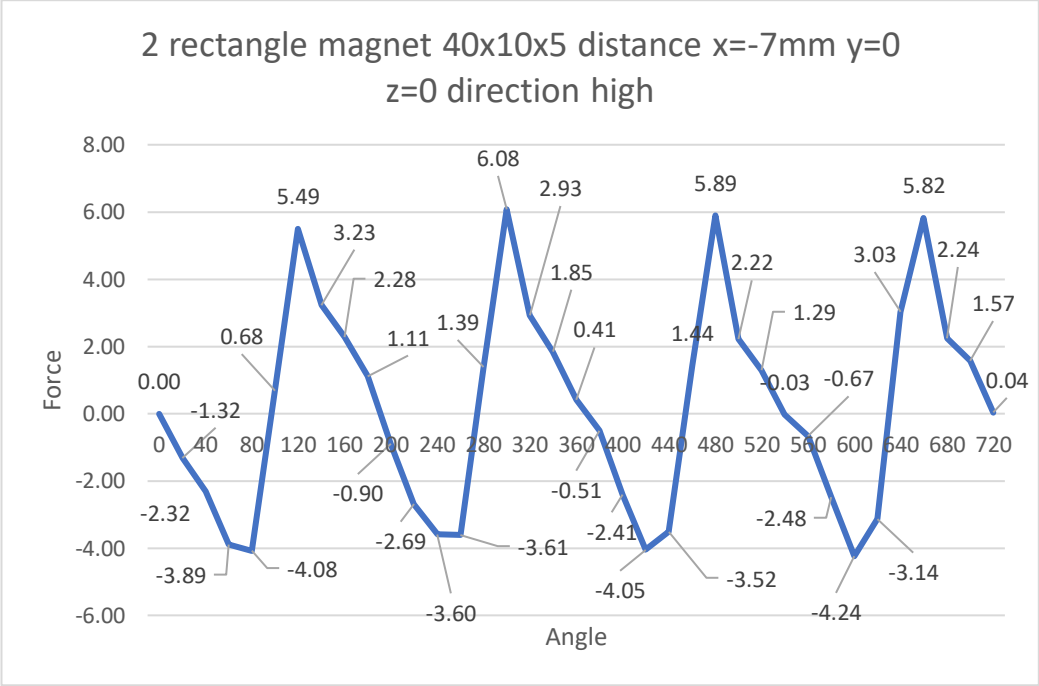

Figure 76 Force-angle graph of 2 rectangle magnet Position 1 x=-7mm y=0 z=0 (clockwise)

The results of 2 square magnets and 2 rectangular magnets are given in Figures 77 and 78. In these two different experiments, the S (south) poles of the square magnet face the right direction, while the N (north) poles of the rectangular magnet face the right direction. In these two graphs, an experimental result showed an increase in the same degree, while another test result showed a decrease. The reason for this is that the magnetic field is from the N pole to the S pole, so the values in these two graphs gave the opposite results.

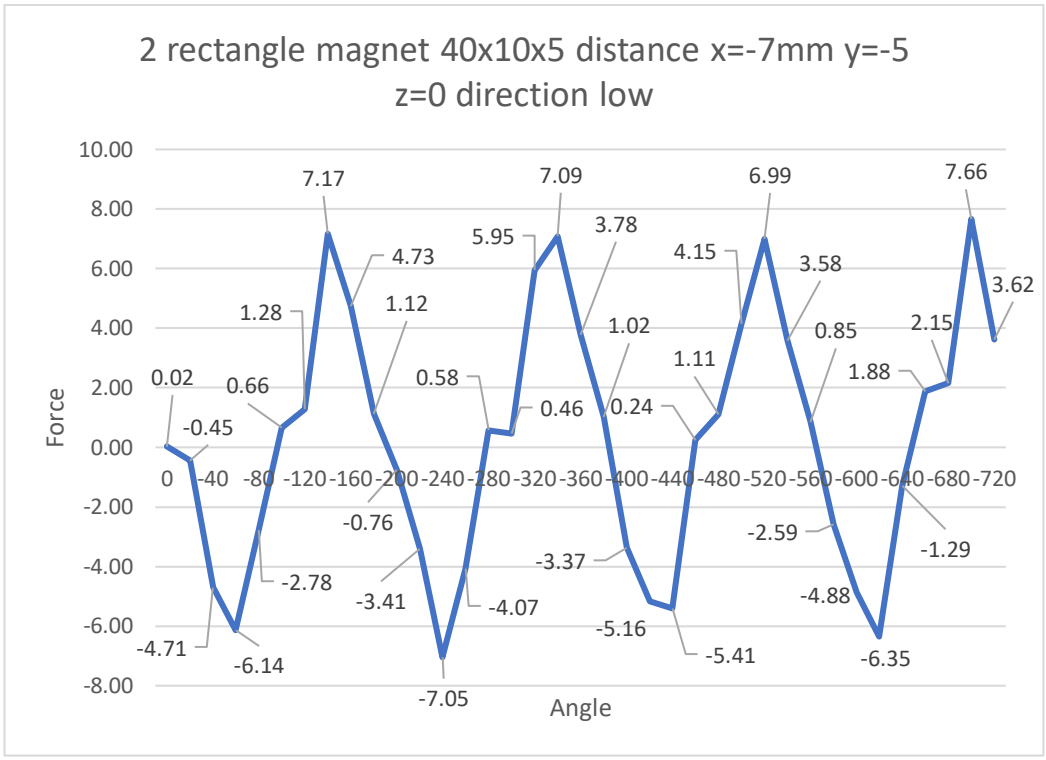

Figure 77 Force-angle graph of 2 rectangle magnet Position 3 x=-7mm y=-5 z=0 (counter clockwise)

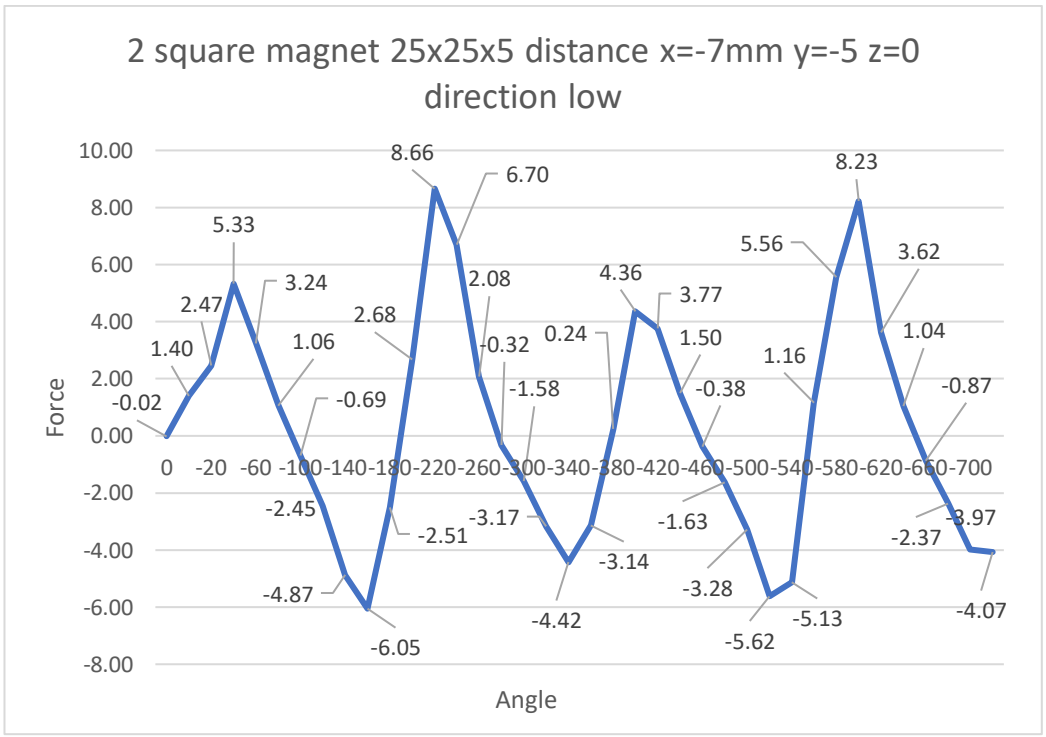

Figure 78 Force-angle graph of 2 square magnet Position 3 x=-7mm y=-5 z=0 (counter clockwise)

The graph created using all the data without applying any filters is given in figure 79. Likewise, the changes between the n and s poles are clearly observed in this graph.

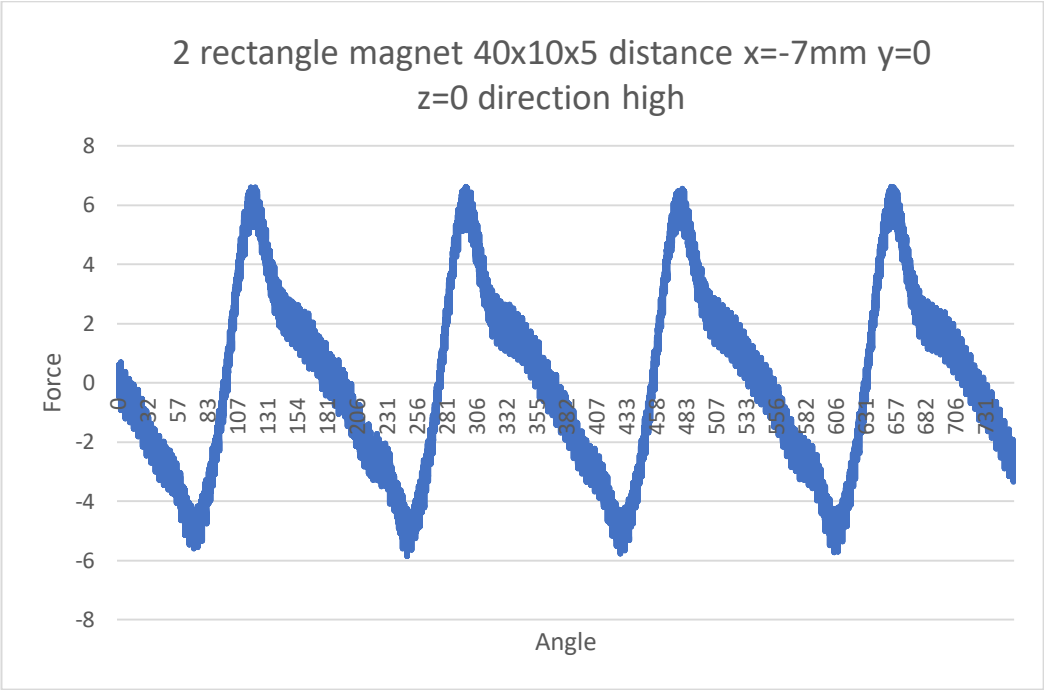

Figure 79 Graph created using all data.

4. CONCLUSIONS

In this thesis, measurements were made with magnets in different geometric shapes and at different distances. The purpose of these measurements is to analyse the magneto strictive materials and to find the angle relationship between the magnet and the material.

In order to make these measurements, the experimental setup was first prepared. We needed motion to be able to take measurements from different points. As a result, sigma profiles, tee nuts and fasteners were used. Nema 17 stepper motor actuator and Arduino were used for the rotation of our stepper motor. Rotary motion sensor was used for angle measurements and force sensor was used for force measurements.

In the measurement results, the most ideal angle information was obtained from 2 pieces of 25x25x5 square magnets and 2 pieces of 40x10x5 rectangular magnets. In these two magnets, results were obtained between negative force and positive force values at every 180 degrees. Since the magnets change their poles every 180 degrees, these results were taken and the angle relationship between the magnet and the magneto-constrictor material was found. However, the results were compared with the results obtained by the reverse rotation of the stepper motor, and the results of each angle change of the magnet were examined and interpreted in these graphs.

2 square magnets and 2 rectangular magnets were each mounted on the discs in opposite directions. In these two different experiments, the S (south) pole of the square magnet faces the right direction, while the N (north) pole of the rectangular magnet faces the right direction. In these two graphs, one of the experimental results increased to the same degree, while the other graph showed the same decrease. The reason for this is that the magnetic field is from the N pole to the S pole, so the values in these two graphs have opposite results.

5. References

[1] M. J. DAPINO, “MAGNETOSTRICTIVE MATERIALS,” 2009.

[2] H. a. W. HAKEN, “The physics of Atoms and Quanta,” 2000.

[3] E. KENDİR, “OPTİK LİF MANYETİK ALAN ALGILAYICISI TASARIMI VE MANYETİK,” 2011.

[4] S. A. N. A. Y. Cengiz Yuksel, “The use of neodymium magnets in healthcare and their effects on health,” 2018.

[5] Ç. İ. EKİM Burak, “STEP MOTORKONTROLÜ,” 2015.

[6] “STEP VE SERVO MOTORLAR,” 2011.

[7] 2022. [Online]. Available: https://www.dfrobot.com/.

[8] P. R. Kumar, “Position control of a Stepper Motor using LabView,” 2018.

[9] “Vernier,” 2022. [Online]. Available: https://www.vernier.com/.

[10] “Vernier,” 2022. [Online]. Available: https://www.vernier.com/.

[11] “PCB PIEZOTRONICS,” 2022. [Online]. Available: https://www.pcb.com/.

[12] “National Instruments,” 2022. [Online]. Available: https://www.ni.com/.

[13] B. Yang, “Non-Contact Translation-Rotation Sensor Using Combined,” 2012.

[14] “Doğuş kalıp,” 2022. [Online]. Available: https://www.doguskalip.com.tr/.

[15] “Direnç Net,” 2022. [Online]. Available: https://www.direnc.net/.

[16] B. d. Bakker, “TB6600 Stepper Motor Driver with Arduino Tutorial,” p. 6, 2019.

[17] “Elektromanyetik Dalgalar,” 2022. [Online]. Available: https://www.akrad.org.tr/.

6. APPENDIX

6.1 Arduino Data File of clockwise rotation

```
void setup() {
  pinMode(2, OUTPUT);
  pinMode(3, OUTPUT);
  digitalWrite(2, HIGH) ;

}
void loop() {
  digitalWrite(3, LOW);
  digitalWrite(3, HIGH);
  delayMicroseconds(100000) ;
}
```

6.2 Arduino Data File of Counterclockwise Rotation

```
void setup() {
  pinMode(2, OUTPUT);
  pinMode(3, OUTPUT);
  digitalWrite(2, LOW) ;

}
void loop() {
  digitalWrite(3, LOW);
  digitalWrite(3, HIGH);
  delayMicroseconds(100000) ;
}
```

6.3 TB6600 Stepper Motor Driver Specification

Input Current	0~5.0A
Output Current	0.5-4.0A
Power (MAX)	160W
Micro Step	1, 2/A, 2/B, 4, 8, 16, 32
Temperature	-10~45℃
Humidity	No Condensation
Weight	0.2 kg
Dimension	96*56*33 mm

INPUT & OUTPUT:

Signal Input:

PUL+ Pulse +

PUL- Pulse –

DIR+ Direction

+ DIR- Direction –

EN+ Off-line Control Enable +

EN- Off-line Control Enable –

Motor Machine Winding:

Motor Machine Winding:

A+ Stepper motor A+

A- Stepper motor A-

B+ Stepper motor B+

B- Stepper motor B-

Power Supply:

VCC VCC (DC9-42V)

GND GND

Micro Step Setting

The follow tablet shows the driver Micro step. You can set the motor microstepvia the first three DIP switch.

Step Angle = Motor Step Angle / Micro Step

E.g. An stepper motor with 1.8° step angle, the finial step angle under “Micro step 4” will be 1.8°/4=0.45°

Micro Step	Pulse/Rev	S1	S2	S3
NC	NC	ON	ON	ON
1	200	ON	ON	OFF
2/A	400	ON	OFF	ON
2/B	400	OFF	ON	ON
4	800	ON	OFF	OFF
8	1600	OFF	ON	OFF
16	3200	OFF	OFF	ON
32	6400	OFF	OFF	OFF

Current (A)	S4	S5	S6
0.5	ON	ON	ON
1.0	ON	OFF	ON
1.5	ON	ON	OFF
2.0	ON	OFF	OFF
2.5	OFF	ON	ON
2.8	OFF	OFF	ON
3.0	OFF	ON	OFF
3.5	OFF	OFF	OFF

Dimension (96*56*33)

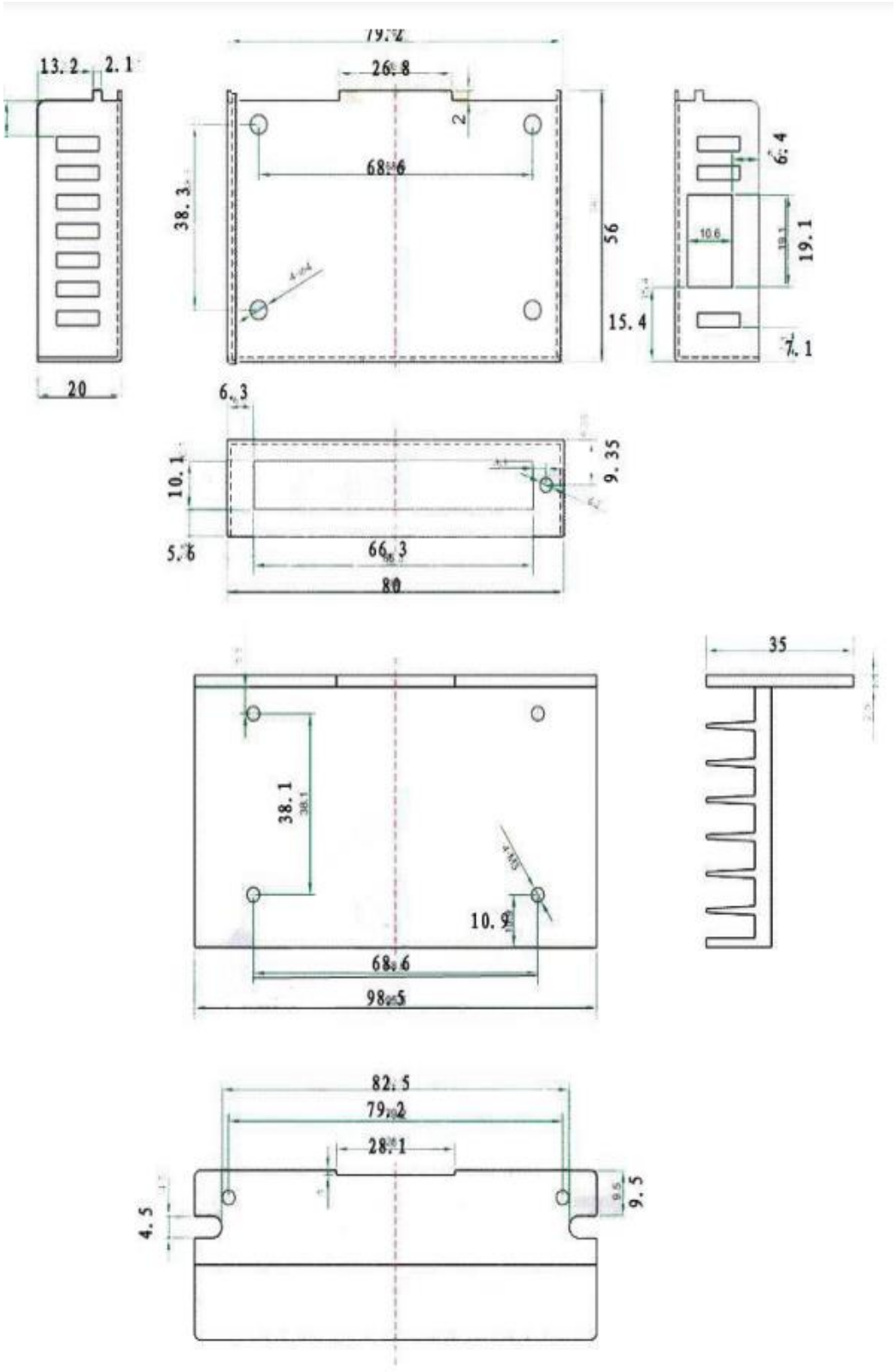
13.2
2.1
20
26.8
2
38.3
56
15.4
6.4
10.6
19.1
7.1
6.3
10.1
9.35
5.6
66.3
80
35
38.1
10.9
68.6
98.5
82.5
79.2
28.1
4.5
9.5

6.4 Vernier Rotary Motion Sensor Specification

Resolution	1° or 0.25° [1]
Optical Encoder	Bidirectional, quadrature encodeer, 360 cycle per revolution
Maximum Speed	30 rev/s at 1° resolution 7.5 rev/s at 0.25° resolution
3-step Pulley	10 mm, 29 mm and 48 mm groove diameter

Note: High resolution mode is also known as X4 mode. When active, the sensor has a 0.25 degree resolution and a limited maximum measurable rotational velocity.

How the Sensor Works

The Rotary Motion Sensor uses a quadrature optical (incremental type) encoder to measure the amount and direction of rotation. The encoder, which is attached to the rotating sensor shaft, consists of a coded pattern of opaque and transparent sectors. The quadrature encoder produces two pulse output patterns 90° apart in phase. The position of the shaft is determined by counting the pulses. The phase relationship between the output signals determines the direction of rotation.

Repair Information

If you have watched the related product video(s), followed the troubleshooting steps, and are still having trouble with your Rotary Motion Sensor, contact Vernier Technical Support at support@vernier.com or call 888-837-6437. Support specialists will work with you to determine if the unit needs to be sent in for repair. At that time, a Return Merchandise Authorization (RMA) number will be issued and instructions will be communicated on how to return the unit for repair.

Accessories

Item	Order Code
Rotary motion accessory kit	AK-RMV
Rotary motion motor kit	MK-RMV

6.5 Vernier SensorDAQ Specification

SensorDAQ Components

SensorDaq features four channels to connect Vernier sensors (three analog, one digital) as well as a screw connector providing two analog input (AI) channels, one analog output (AO) channel, four digital input/output (DIO) channels, and a 32-bit counter/timer (PFI).

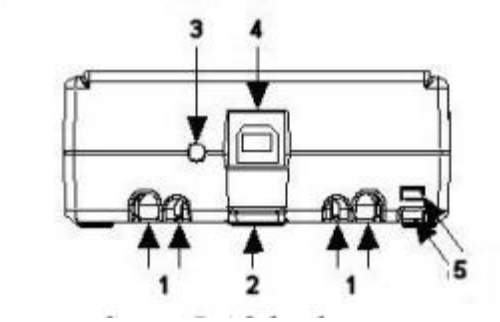

1. The USB Cable Strain Relief is used to ensure a secure USB connection.
2. Use the Mounting Slot and Panel Mount to mount SensorDAQ to an object.
3. The LED blinks when SensorDAQ has power and is recognized by the DAQmx driver.
4. The USB Port is for computer connection.
5. Use the Tie Wrap Point to lock down and secure the device.

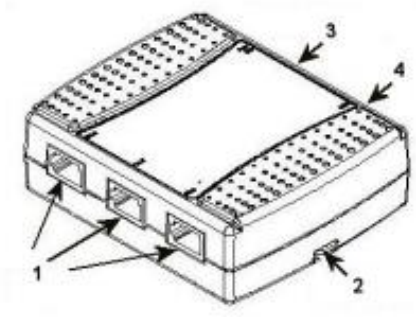

1. Ch.1–Ch.3 BTA (British Telecom Analog) channels for Vernier analog sensors. The Vernier voltage probe is an analog sensor.

2. Use the Mounting Slot and Panel Mount to mount SensorDAQ to an object.
3. The Screw Terminal Connector is available for customized input and output. The screw terminal can be removed after being wired for specific experiments. Replacement terminals are available from Vernier.
4. DIG BTD (British Telecom Digital) input/output channel for Vernier digital sensors.

Vernier Analog Sensors

Sensors can be divided into two basic types—analog and digital. Examples of analog sensors are Voltage, Temperature Probes, pH Sensors, Force Sensors, and Oxygen Gas Sensors. Up to three analog sensors can be connected to SensorDAQ at any time1. The channels for the analog sensors (Ch.1–Ch.3) are located on the left side. The analog ports accept British Telecom-style plugs with a right-hand connector.

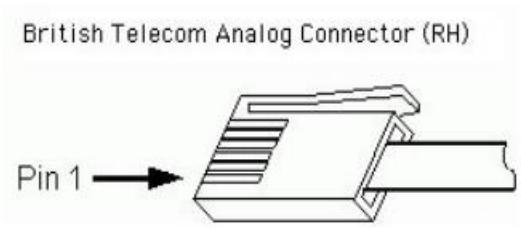

Pin 1 = Sensor output (+/-10V)
Pin 2 = GND
Pin 3 = Vres (resistance reference)
Pin 4 = AutoIDENT (used for auto-ID of most Vernier sensors)
Pin 5 = Power (+5VDC)
Pin 6 = Sensor output (0-5V)

Most sensors provided by Vernier are auto-ID sensors. When you plug an auto-ID sensor into SensorDAQ, the software will be able to identify it and set up the file accordingly. Auto-ID information includes default settings for data collection rate, length of collection, and calibration coefficients. Most Vernier analog sensors send a raw voltage signal in the range of 0-5V on pin 6. A few send a signal in the range of ±10V on Pin 1. The raw voltage signal is converted to proper units using the sensor's calibration coefficients. Most Vernier sensors that plug directly into SensorDAQ without an adapter are auto-ID. However, the SensorDAQ can read a 0-5V or ±10V signal from many types of sensors. To make the connection to SensorDAQ with a sensor without a BTA plug, use an adapter (www.vernier.com/adapters/), or a bare BTA cable (order code BB-BTA) wired to your custom sensor.

Vernier Digital Sensors

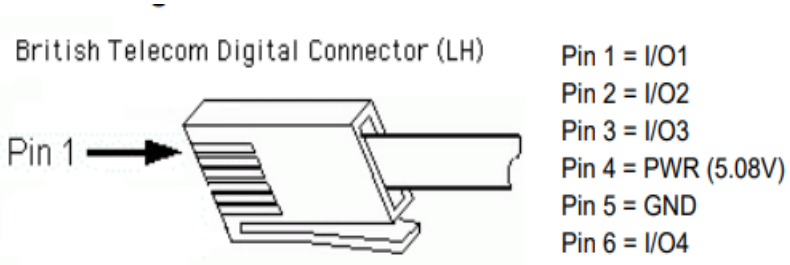

Examples of digital sensors are Motion Detectors, Photogates, and Rotary Motion Sensors. One digital sensor at a time can be connected to SensorDAQ. The digital channel (DIG), which accepts British Telecom-style plugs with a left-hand connector, is located on the opposite side of the analog channels. The SensorDAQ's DIG Channel also accepts a Vernier Digital Control Unit. This is a small box with a short cable that uses the DIG channel to provide output (up to 600 mA of current) for controlling electrical devices.

Screw Terminal

SensorDAQ screw terminal connectors can be used for input or output. When used for output, these connectors provide a limited current (see specs below); therefore, in some cases you will have to provide an external power source. The +5V terminal can be used as your voltage source. This source can only supply 200 mA maximum.

Terminal	Signal Name	Reference	Direction	Description
5,8,10	GND	-	-	Ground: Reference point for singleended AI measurements, bias current return point for differential mode measurements, AO voltages, digital signals at the I/O connector, +5 VDC supply, and the +2.5 VDC reference

11,12	AI<0.1>	Varies	Input	Analog Input Channels 0 and 1: For single-ended measurements, each signal is an analog input voltage channel. For differential measurements, AI 0 and AI 1 are the positive and negative inputs, respectfully, of differential analog input channel 0.
9	AO 0	GND	Output	Analog Output Channel 0: Supplies the voltage output of AO channel 0 from 0-5V with an output current drive value of 5 mA. The maximum update rate is 150 Hz, software timed.
1-4	P0.<0.3	GND	Input or Output	Digital I/O Signals: You can individually configure each signal as an input or output.
6	+5 V	GND	Output	+5 V Power Source: Provides +5 V power.
7	PFI 0	GND	Input	PFI 0: This pin is configurable as either a digital trigger, an event counter input, pulse generation output, or as a period, semi-period, two edge separation timer.

Analog Input Wiring

In the differential input setting, connect the the positive lead of the source to the AI(0) terminal, and the negative lead to the AI(1) terminal. The differential input mode allows the SensorDAQ to measure a voltage difference on these terminals up to +20V or –20V in the ±20V range; however, the maximum voltage on any one terminal cannot exceed ±10 V with respect to GND. In the referenced single-ended input mode setting, connect the positive lead of the source to either AI channel terminal, AI(0) or AI(1), and the ground or negative lead to the GND terminal.

Analog Output Wiring

The SensorDAQ has one AO channel that can generate an output from 0–5V. The AO has an output current drive value of 5 mA. The maximum update rate of the channel is 150 Hz, software timed. To connect loads to the SensorDAQ, connect the positive lead of the load to the A0 terminal, and connect the ground lead of the load to a GND terminal.

Digital I/O

In addition to supporting Vernier digital sensors, the SensorDAQ has four digital lines, P0., which comprise the DIO port. GND is the groundreference signal for the DIO port. The default configuration of the SensorDAQ DIO ports is open collector, allowing 5 V operation, with an onboard 4.7 kΩ pull-up resistor. An external, user-provided, pull-up resistor can be added to increase the source current drive up to 8.5 mA limit per line.

Counter/Timer

SensorDAQ has a counter/timer that can be configured for pulse output, timing input, event counting, or as a digital trigger.

6.6 Model 208C01 Force Sensor Specification

GENERAL PURPOSE – RADIAL

Model 208C01-C05 General Purpose Sensors are designed to measure compression and impact forces from a fraction of a lb(N) to 5,000 lbs (to 22.24 kN). Tension forces can be measured to 500 lbs (2.224 kN). Model 084A03, a supplied convex, stainless steel cap with integral 10-32 mounting stud, converts this tension/compression model to a sensor capable of impact measurements. Polyimide film tape covers the cap surface to reduce high frequency ringing associated with metal to-metal impacts.

GENERAL PURPOSE – AXIAL

Models 208A11-A15 Axial Sensors provide performance and specifications similar to the Model 208C Sensors. These sensors are designed primarily to measure compression and impact forces from a few pounds(N) to 5,000 lbs (to 22.24 kN). Tensile forces can be measured to 500 lbs (2.224 kN). The 10- 32 axial electrical connector orientation associated with these sensors makes them ideal for installations where radial space is restricted or where physical connector damage may occur due to the nature of

the specific application. The M7 x 0.75-6g mounting threads (all models) may be installed directly into a test structure so that the 10-32 electrical connector exits from the opposite side of the mounting fixture. This helps prevent potential damage during drop test applications. This version also uses the Model 084A03 cap for impact measurements.

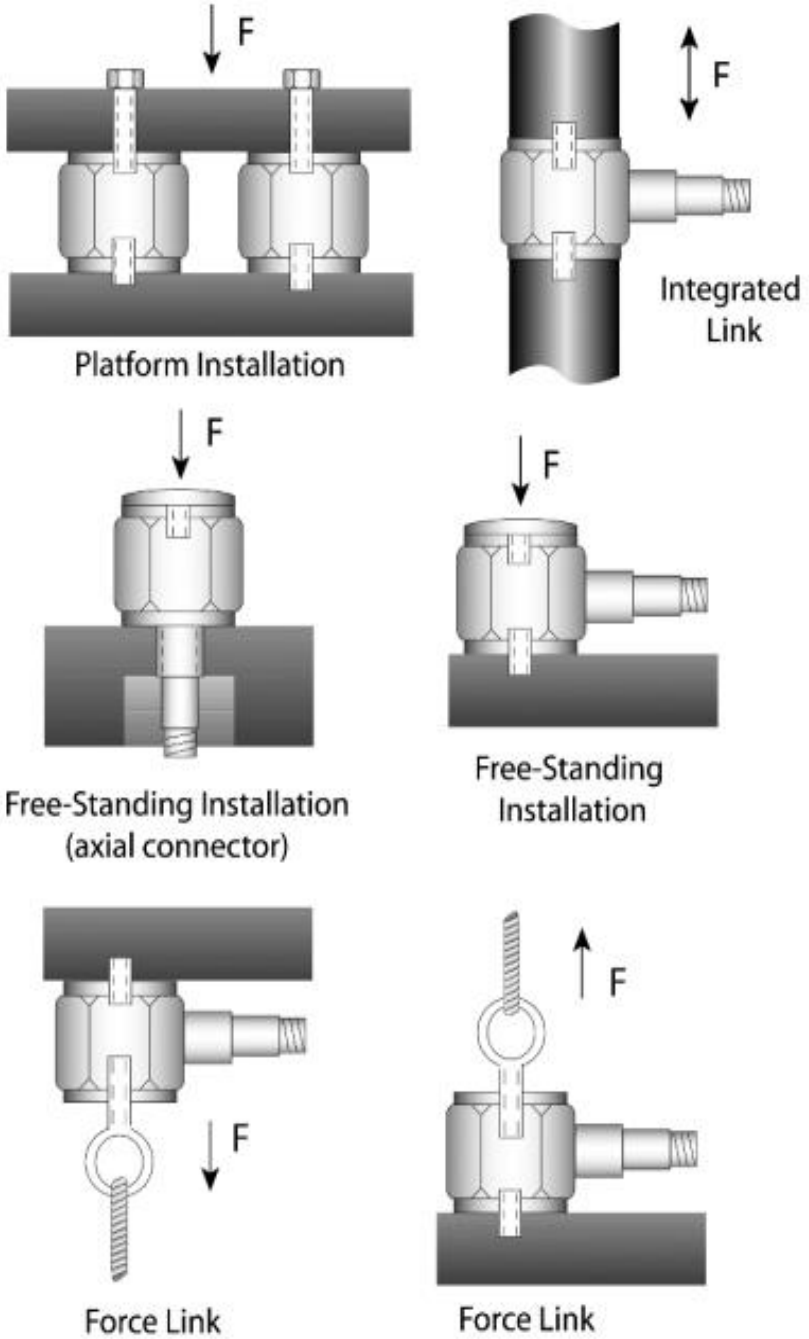

Force Sensor Preload Requirements

Force Ring Models	Preload (lbf)	Incremental Steps	Sensitivity (mV/lbf)	Step Increment (mV)
201B01	60	3	500	10,000
201B02	100	1	50	5,000
201B03	200	1	10	2,000
201B04	400	1	5	2,000
201B05	1,000	1	1	1,000
202B	2,000	1	0.5	1,000
203B	4,000	1	0.25	1,000
204C	8,000	1	0.12	960
205C	12,000	1	0.08	960
206C	16,000	1	0.06	960
207C	33,750	1	0.05	1,688
3-Component Models				
260A01	5,000	2	2.5	6,250
260A02	10,000	3	2.5	8,333
260A03	40,000	1	0.25	10,000

WORKING RANGE, PRELOAD, AND MAXIMUM LOAD

The Working Range is the ideal dynamic working load that may be applied to a sensor during operation. In most sensors, the product of the working range and the sensor sensitivity will provide a 5 Volt output, following the equation; 5Volts = range x sensitivity.

The Sensor Preload is the load applied to the sensor before the sensor is used in an operation. In ring and triax models, preload is essential to match PCB's calibrated sensitivity as well it assure sensor linearity at the lower measurement range.

The Maximum Load is the dynamic load that may be applied before the sensor approaches physical damage. In some sensors this value is a result of a mechanical limitation. In ICP® models this may be an electrical limitation (applying an excessive load under sudden dynamic condition outside the specified range may damage the internal electronic circuitry).

With most sensors, the specified dynamic working range and maximum compression is riding ON TOP OF the applied preload. As an example, triax force sensor Model 260A01 has a specified preload of 5000 lbs (22kN), a working range of 1000 lb (4500N), and a maximum compression range of 1320 lbs (6000 N). To provide the best linear response of the sensor, a 5000 lbs (22kN) preload should be loaded on it. From there one may take dynamic measurements through the entire 1000 lb (4500N) working range of the sensor. Dynamically one should not take measurements above 1320 lbs (6000) as this total load value approaches physical damage to the sensor.

APPLICATION OF A FORCE

For best results, the applied force should be distributed evenly over the contact surface of the sensor. Care should be taken to limit the bending moment induced into the sensor by edge loading or off-axis loading of the sensor. This is accomplished by applying a force to the sensor as close as possible to the center of the sensor. In the event sensor is to be installed to measure a unit under test with a much larger area than that of the sensing surface of sensor, such as a large metal plate, it may be necessary to use an arrangement of two to four sensors in a measuring platform. Independent sensor output can be monitored or the sensors can be connected electrically in parallel to measure the resulting summed forces when used in a multiple sensor type arrangement

POLARITY

Compressive forces upon an ICP□ force sensor produce a positive-going voltage output. Tensile forces produce a negative-going voltage output. Sensors with reversed polarity are available upon request.

LOW-FREQUENCY MONITORING

Force sensors used for applications in short term, steady state monitoring, such as sensor calibration, or short term, quasistatic testing should be powered by signal conditioners that operate in DC-coupled mode. PCB Series 482 and 484 Signal Conditioner operates in either AC or DC-coupled mode and may be supplied with gain features or a zero “clamped” output often necessary in repetitive, positive polarity pulse train applications.

CALIBRATION

A NIST (National Institute of Standards and Technology) traceable calibration graph is supplied with each force sensor certifying its voltage sensitivity (mV/lb). Calibration procedures follow accepted guidelines as recommended by ANSI (American National Standards Institute), ISA (Instrument Society of America), and ISO (International Organization for Standardization). These standards provide the establishment and management of complete calibration systems, thus controlling the accuracy of a sensor's specifications by controlling measuring and test equipment accuracy. PCB is A2LA accredited for technical competence in the field of calibration, meeting the requirements of ISO/IEC 17025-1999 and ANSI/NCSL 2540-1-1994.

TROUBLESHOOTING

When a PCB signal conditioner with any of the following indicators are used, turn the power on and observe the voltmeter (or LED's) on the front panel.

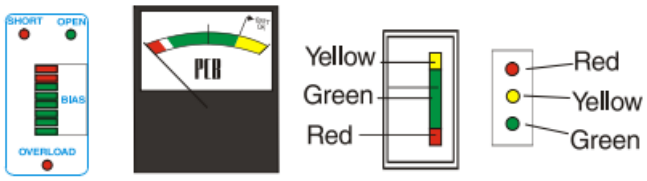

NORMAL OPERATION

INDICATOR	DVM READING	OPERATION
GREEN (Mid-Scale)	8 to 14 V	Proper range for most ICP sensors.
GREEN (Low End)	3 to 7 V	Proper range for low bias ICP sensors.
GREEN (High End)	15 to 17 V	Proper range for high bias ICP sensors.
RED	0 Volts	Short in the sensor, cable, or connections.
YELLOW	24 to 28 V	Open circuit in the sensor, cable, or connections. (Excitation voltage is being monitored.)

Output voltage moves from YELLOW to GREEN slowly until charging is complete. AC coupled signal conditioners require sufficient time to charge the internal coupling capacitor. Allow signal conditioner to charge for five (5) discharge time constants for stable operation. In most cases, this is just a few seconds.

Model Number	ICP® FORCE SENSOR	Revision: K
208C01		ECN #: 45224

Performance	**ENGLISH**	**SI**	
Sensitivity(± 15 %)	500 mV/lb	112,410 mV/kN	
Measurement Range(Compression)	10 lb	0.04448 kN	
Measurement Range(Tension)	10 lb	0.04448 kN	
Maximum Static Force(Compression)	60 lb	0.27 kN	
Maximum Static Force(Tension)	60 lb	0.27 kN	
Broadband Resolution(1 to 10,000 Hz)	0.0001 lb-rms	0.00045 N-rms	[2]
Low Frequency Response(-5 %)	0.01 Hz	0.01 Hz	[3]
Upper Frequency Limit	36,000 Hz	36,000 Hz	[4]
Non-Linearity	≤ 1 % FS	≤ 1 % FS	[5]
Environmental			
Temperature Range	-65 to +250 °F	-54 to +121 °C	
Temperature Coefficient of Sensitivity	≤ 0.05 %/°F	≤ 0.09 %/°C	
Electrical			
Discharge Time Constant(at room temp)	≥ 50 sec	≥ 50 sec	
Excitation Voltage	18 to 30 VDC	18 to 30 VDC	
Constant Current Excitation	2 to 20 mA	2 to 20 mA	
Output Impedance	≤ 100 Ohm	≤ 100 Ohm	
Output Bias Voltage	8 to 12 VDC	8 to 12 VDC	[1]
Spectral Noise(1 Hz)	0.0000126 lb/√Hz	0.0000562 N/√Hz	[2]
Spectral Noise(10 Hz)	0.0000042 lb/√Hz	0.0000189 N√Hz	[2]
Spectral Noise(100 Hz)	0.0000015 lb/√Hz	0.0000067 N/√Hz	[2]
Spectral Noise(1000 Hz)	0.0000005 lb/√Hz	0.0000023 N/√Hz	[2]
Output Polarity(Compression)	Positive	Positive	
Physical			
Stiffness	6 lb/µin	1.05 kN/µm	[2]
Size (Hex x Height x Sensing Surface)	0.625 in x 0.625 in x 0.500 in	15.88 mm x 15.88 mm x 12.7 mm	
Weight	0.80 oz	22.7 gm	
Housing Material	Stainless Steel	Stainless Steel	
Sealing	Hermetic	Hermetic	
Electrical Connector	10-32 Coaxial Jack	10-32 Coaxial Jack	
Electrical Connection Position	Side	Side	
Mounting Thread	10-32 Female	10-32 Female	

CE[6]

All specifications are at room temperature unless otherwise specified.
In the interest of constant product improvement, we reserve the right to change specifications without notice.
ICP® is a registered trademark of PCB Group, Inc.

OPTIONAL VERSIONS

Optional versions have identical specifications and accessories as listed for the standard model except where noted below. More than one option may be used.

N - Negative Output Polarity

Output Polarity(Compression)	Negative	Negative

W - Water Resistant Cable

NOTES:
[1]Sensor contains protected electronics which may cause long "turn-on" times.
[2]Typical.
[3]Calculated from discharge time constant.
[4]Estimated using rigid body dynamics calculations.
[5]Zero-based, least-squares, straight line method.
[6]See PCB Declaration of Conformance PS023 for details.

SUPPLIED ACCESSORIES:
Model 080A81 Thread Locker (1)
Model 081B05 Mounting Stud (10-32 to 10-32) (2)
Model 084A03 Impact Cap (1)
Model M081A62 Mounting stud, 10-32 to M6 x 1, BeCu with shoulder (2)

Entered: LK	Engineer: MJK	Sales: KWW	Approved: APB	Spec Number:
Date: 3/29/2016	Date: 3/29/2016	Date: 3/29/2016	Date: 3/29/2016	**8625**

PCB PIEZOTRONICS
3425 Walden Avenue, Depew, NY 14043
Phone: 716-684-0001
Fax: 716-684-0987
E-Mail: info@pcb.com

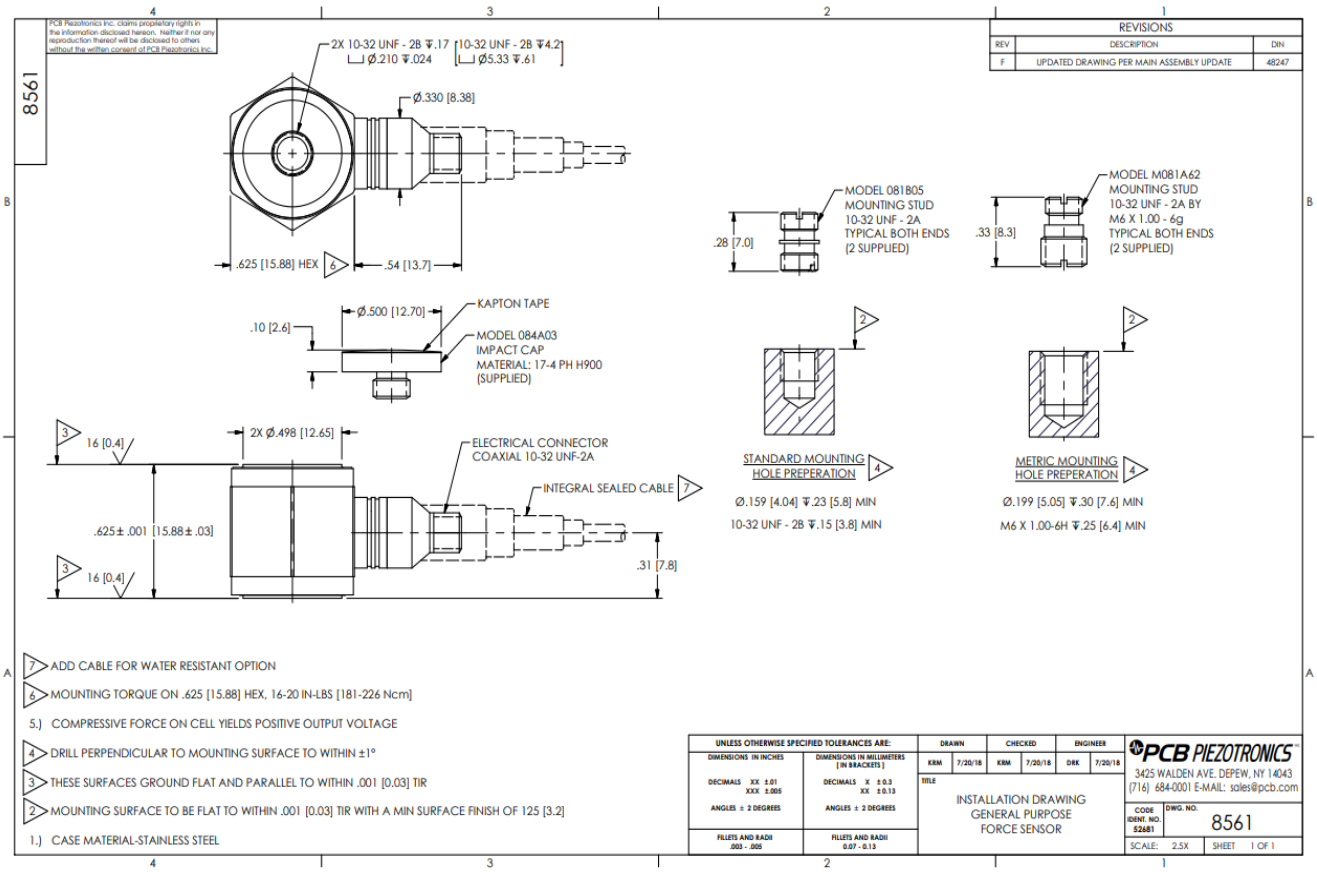

6.7 NI 9234 Module Specification

The following specifications are typical for the range –40 to 70 °C unless otherwise noted.

Input Characteristics

Number of channels.....4

Analog input channels ADC resolution.....24 bits

Type of ADC.....Delta-Sigma (with analog prefiltering)

Sampling mode .....Simultaneous

Type of TEDS supported .....IEEE 1451.4 TEDS Class I Internal master timebase (fM)

Frequency .....13.1072 MHz

Accuracy.....±50 ppm max

Data rate range (fs) using internal master timebase

Minimum.....1.652 kS/s

Maximum .....51.2 kS/s

Data rate range (fs) using external master timebase

Minimum.....0.391 kS/s

Maximum .....52.734 kS/s

Data rates1 (fs)..... $\frac{F_m+256}{n}$, n = 1, 2, …, 31

Input coupling.....AC/DC (software-selectable)

AC cutoff frequency

–3 dB .....0.5 Hz

–0.1 dB.....4.6 Hz max

AC cutoff frequency response

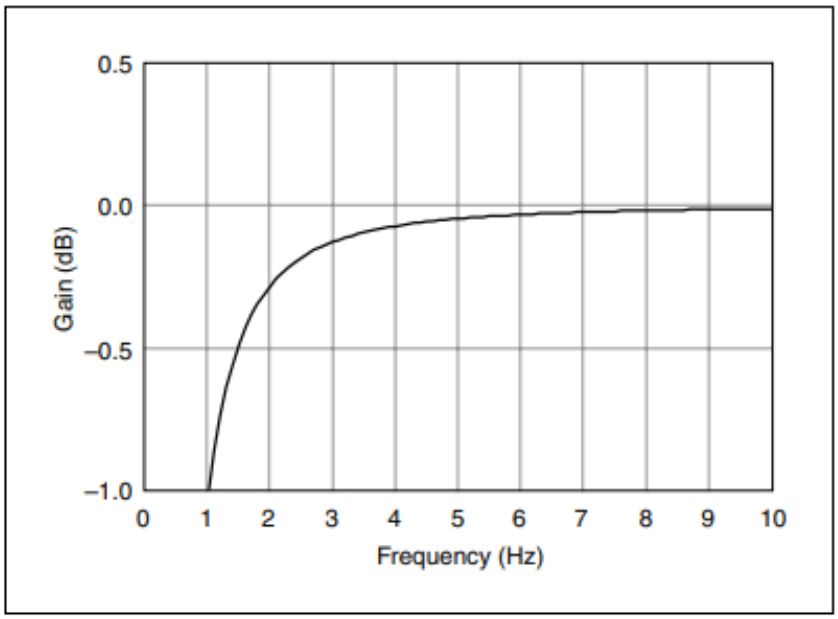

Input range.....±5 V

AC voltage full-scale range

Minimum.....±5 Vpk

Typical.....±5.1 Vpk

Maximum .....±5.2 Vpk

Common-mode voltage range

(AI– to earth ground).....±2 V max

IEPE excitation current (software-selectable on/off)

Minimum.....2.0 mA

Typical.....2.1 mA

Power-on glitch.....90 µA for 10 µs

IEPE compliance voltage.....19 V max

If you are using an IEPE sensor, use the following equation to make sure your configuration meets the IEPE compliance voltage range.

(Vcommon-mode + Vbias ± Vfull-scale) must be 0 to 19

Overvoltage protection (with respect to chassis ground)

For a signal source connected

to AI+ and AI– .....±30 V

For a low-impedance source connected to AI+ and AI– .....–6 to 30 V.

Input delay .....38.4/ fs + 3.2 µs

Accuracy

Measurement Conditions	Percent of Reading (Gain Error)	Percent of Range* (Offset Error)
Calibrated max (–40 to 70 °C)	0.34%, ±0.03 dB	±0.14%, 7.1 mV
Calibrated typ (25 °C ±5 °C)	0.05%, ±0.005 dB	±0.006%, 0.3 mV
Uncalibrated max (–40 to 70 °C)	1.9%, ±0.16 dB	±0.27%, 13.9 mV
Uncalibrated typ (25 °C ±5 °C)	0.48%, ±0.04 dB	±0.04%, 2.3 mV
* Range = 5.1 V_{pk}		

Gain drift

Typical.....0.14 mdB/°C (16 ppm/°C)

Maximum .....0.45 mdB/°C (52 ppm/°C)

Offset drift

Typical.....19.2 µV/°C

Maximum .....118 µV/°C

Channel-to-channel matching

Gain

Typical.....0.01 dB

Maximum.....0.04 dB

Phase (fin in kHz).....fin · 0.045° + 0.04 max

Passband

Frequency .....0.45 · fs

Flatness (fs = 51.2 kS/s).....±40 mdB (pk-to-pk max)

Phase nonlinearity

(fs = 51.2 kS/s) .....±0.45° max

Stopband

Frequency .....0.55 · fs

Rejection.....100 dB

Alias-free bandwidth .....0.45 · f

Oversample rate .....64 · fs

Crosstalk (1 kHz).....–110 dB

CMRR (fin ≤ 1 kHz)

Minimum.....40 dB

Typical.....47 dB

SFDR (fin = 1 kHz, –60 dBFS).....120 dB

Idle channel noise and noise density

Idle Channel	51.2 kS/s	25.6 kS/s	2.048 kS/s
Noise	97 dBFS	99 dBFS	103 dBFS
	50 μV_{rms}	40 μV_{rms}	25 μV_{rms}
Noise density	310 nV/√Hz	350 nV/√Hz	780 nV/√Hz

Input impedance

Differential .....305 kΩ

AI– (shield) to chassis ground.....50 Ω

Total harmonic distortion (THD)

Input Amplitude	1 kHz	8 kHz
–1 dBFS	–95 dB	–87 dB
–20 dBFS	–95 dB	–80 dB

Intermodulation distortion (–1 dBFS)

DIN 250 Hz/8 kHz

4:1 amplitude ratio .....–80 dB

CCIF 11 kHz/12 kHz

1:1 amplitude ratio .....–93 dB